

UC Davis

UC Davis Electronic Theses and Dissertations

Title

Microencapsulation of bioactives by in situ complex coacervation during spray drying

Permalink

<https://escholarship.org/uc/item/96f530mr>

Author

Tang, Yuting

Publication Date

2022

Peer reviewed|Thesis/dissertation

Microencapsulation of Bioactives by in situ Complex Coacervation during Spray Drying

By

YUTING TANG
DISSERTATION

Submitted in partial satisfaction of the requirements for the degree of

DOCTOR OF PHILOSOPHY

in

Biological Systems Engineering

in the

OFFICE OF GRADUATE STUDIES

of the

UNIVERSITY OF CALIFORNIA

DAVIS

Approved:

Tina Jeoh, Chair

Bryan M. Jenkins

D. Ken Giles

Committee in Charge

2022

Copyright © 2022 by

Yuting Tang

Table of Contents

Table of Contents	ii
List of Figures.....	v
List of Tables	viii
Supplementary Figures and Tables.....	ix
Abstract.....	x
Acknowledgements	xiii
Chapter 1 Introduction	1
1.1 Overview.....	1
1.2 Research goal	3
1.3 Literature review	4
1.3.1 Microencapsulation.....	4
1.3.2 Complex coacervation	6
1.3.3 Spray drying.....	9
1.3.4 In situ complex coacervation during spray drying (CoCo process).....	10
1.3.5 Bioactives encapsulation.....	17
1.3.6 Summary	20
1.3.7 References.....	20
Chapter 2 Industrially scalable complex coacervation process to microencapsulate food ingredients	26
2.1 Abstract	26
2.2 Industrial relevance	26
2.3 Introduction.....	27
2.4 Materials and methods	30
2.4.1 Materials	30
2.4.2 Methods.....	31
2.5 Results and discussion	36
2.5.1 In situ complex coacervation during spray drying (the ‘CoCo process’)	36
2.5.2 The extent of complex coacervation in CoCo particles	37
2.5.3 Volatile retention of D-limonene in L-CoCo microcapsules during spray-drying and subsequent storage	39
2.5.4 The influence of the emulsifying process on volatile retention of D-limonene in L-CoCo microcapsules	41
2.5.5 Size and morphology of the CoCo microparticles.....	43
2.5.6 Opportunities to further optimize and more broadly apply the CoCo process	45
2.6 Conclusions.....	47
2.7 Abbreviations used.....	47
2.8 References.....	47
Chapter 3 Volatile retention and enteric release of D-limonene by encapsulation in complex coacervated powder formed by spray drying.....	51
3.1 Abstract	51
3.2 Introduction.....	51

3.3	Materials and methods	54
3.3.1	Materials	54
3.3.2	Methods.....	54
3.4	Results.....	61
3.4.1	D-limonene loaded CoCo powders prepared by spray drying.....	61
3.4.2	Volatile retention of D-limonene in CoCo microcapsules during spray drying	63
3.4.3	Volatile retention of D-limonene in CoCo microcapsules during storage.....	65
3.4.4	The potential for enteric release of D-limonene from CoCo powders.....	66
3.4.5	The ECC as a measure of barrier properties	68
3.5	Discussion	71
3.5.1	The effect of the ECC on volatile retention and controlled release of D-limonene .	71
3.5.2	Modulating the ECC by formulation	74
3.6	Conclusions.....	76
3.7	Abbreviations.....	76
3.8	Supplemental information.....	76
3.9	References.....	77
Chapter 4 The effect of ethylcellulose on retention and release of D-limonene encapsulated by complex coacervated microcapsules formed by spray drying.....		80
4.1	Abstract.....	80
4.2	Introduction.....	80
4.3	Materials and methods	82
4.3.1	Materials	82
4.3.2	Methods.....	83
4.4	Results and discussion	87
4.4.1	Volatile retention of D-limonene in CoCo microcapsules after spray drying	87
4.4.2	Retention and oxidation of D-limonene in CoCo microcapsules during storage	92
4.4.3	Controlled release of D-limonene from CoCo microcapsules in aqueous media.....	96
4.4.4	SEM and particle size of CoCo microcapsules.....	99
4.5	Conclusions.....	101
4.6	Abbreviations.....	102
4.7	Supplementary information	103
4.8	References.....	104
Chapter 5 Enteric release of therapeutic peptides encapsulated by complex coacervated microcapsules formed by spray drying.....		106
5.1	Abstract.....	106
5.2	Introduction.....	106
5.3	Materials and methods	110
5.3.1	Materials	110
5.3.2	Methods.....	111
5.4	Results.....	117
5.4.1	2h release profile of peptides from CoCo microcapsules in aqueous media	117
5.4.2	20h release profile of peptides from CoCo microcapsules in aqueous media	120
5.4.3	SEM of the peptides loaded CoCo microcapsules.....	122
5.4.4	Particle size of the peptides loaded CoCo microcapsules.....	124
5.4.5	Powder yield and peptide loading of CoCo microcapsules	125
5.5	Discussion.....	127

5.5.1	Peptide differences lead to various release profile of peptides from microcapsules in aqueous media.....	127
5.5.2	The influence of latex polymer on release profile of peptides from microcapsules in aqueous media.....	128
5.6	Conclusions.....	130
5.7	Abbreviations.....	131
5.8	Supplementary information	131
5.9	References.....	132
Chapter 6 Microencapsulation of bromelain by industrially scalable complex coacervation process.....		135
6.1	Introduction.....	135
6.2	Materials and methods	136
6.2.1	Materials	136
6.2.2	Methods.....	137
6.3	Results and discussion	140
6.3.1	pI of protein in pineapple extract powder	140
6.3.2	The protein content in pineapple extract powder.....	141
6.3.3	Percent of coacervated protein of the total protein in the CoCo powder.....	141
6.3.4	Bromelain activity recovery of CoCo microcapsules after spray drying.....	142
6.4	Conclusions.....	144
6.5	Supplementary information	144
6.6	References.....	144
Chapter 7 Conclusions and future work.....		146
7.1	Summary.....	146
7.2	Future work.....	147
7.2.1	Physicochemical and structural properties of the CoCo matrix.....	147
7.2.2	Influence of formation and process parameters on barrier properties of CoCo microcapsules.....	149
7.2.3	Modeling the kinetic release of bioactive compound	150
7.3	Conclusions.....	150

List of Figures

Figure 1–1. Schematic of conventional complex coacervation.	2
Figure 1–2. The novel process of in situ complex coacervation during spray drying.	3
Figure 2–1. Schematic representation of the in situ complex coacervation during spray drying process (the ‘CoCo process’).	29
Figure 2–2. Insoluble gelatin or alginate (%) in spray dried powder formed with the formulations in Table 2–1 when suspended in water (Formulation 1: with non-volatile NaOH, Formulation 2: with volatile NH ₄ OH, Formulation 3: with Succinic acid and volatile NH ₄ OH; all formulations contained the same ratios of alginate and gelatin as detailed in the methods section).	38
Figure 2–3. SEM images showing the external structures of CoCo particles (a~c) and L-CoCo particles (d,e). (a) Particles formulated with NaOH; (b) particles formulated with NH ₄ OH; (c) particles formulated with combination of NH ₄ OH and succinic acid; (d) L-CoCo particles with high volatile retention; (e) U-L-CoCo particles with low volatile retention. The scale bars represent 5 μm.	43
Figure 2–4. Particle size distributions of spray dried CoCo microcapsules measured in isopropanol.	45
Figure 3–1. A schematic representation of the process to encapsulate D-limonene in complex coacervated (CoCo) powder by spray-drying.	56
Figure 3–2. Volume weighted particle size distributions of spray dried CoCo powders dispersed in isopropanol. The formulations for the samples are given in Table 3–1.	62
Figure 3–3. a: Volatile retention of D-limonene in CoCo microcapsules after spray drying; b: D-limonene content in CoCo microcapsules formed by spray drying using formulations; c: Volatile retention of D-limonene in CoCo microcapsule after 4 months storage; d: The D-limonene loaded CoCo powders stored in sealed vials after 4 months. At each level of succinic acid, the powder in vial from left to right was generated from formulation with gelatin concentration of 1%, 2.5% and 4% respectively. Each vial is labeled with percent of D-limonene loss after 4 months storage. Means with same letters do not differ statistically by Tukey's test ($\alpha = 0.05$).	65
Figure 3–4. Release of D-limonene from CoCo microcapsules after 2 h. D-limonene release in water (pH 5.8, room temperature) (a), SGF (pH 1.8, 37 °C) (b) and SIF (pH 7.4, 37 °C) (c) was assessed by dispersing powders in each fluid and incubating with end-over-end rotation for 2 h. Means with same letters do not differ statistically by Tukey's test ($\alpha = 0.05$).	67
Figure 3–5. a: Coacervated gelatin; b: coacervated alginate; and c: the ECC in CoCo powders. Means with same letters do not differ statistically by Tukey's test ($\alpha = 0.05$).	69
Figure 3–6. The relationship between the ECC and the release of D-limonene in: a: water, and b: SGF. Lines are drawn to guide the eye.	70
Figure 3–7. a: Undissolved alginate, undissolved gelatin and undissolved matrix polymers (alginate+gelatin) from the 4G0.75S CoCo sample in various aqueous media. b: The relationship between ECC and the release of D-limonene in aqueous media from the 4G0.75S CoCo sample (Table 3–1).	71
Figure 4–1. Schematic representation of the formation of CoCo powder with/without latex and its following release.	82

Figure 4–2. The storage conditions for shelf-life study of D-limonene CoCo microcapsules with/without ethylcellulose.....	86
Figure 4–3. a: Volatile retention of D-limonene in the CoCo microcapsules during spray drying; b: Emulsion size of D-limonene in the CoCo feed with different concentration of ethylcellulose.....	88
Figure 4–4. The volatile retention of D-limonene in microcapsules generated from different formulation during spray drying and the emulsion size in the feed: L gelatin: 2.5% gelatin, 0.5% alginate and 1% succinic acid, 25% D-limonene based on dry inlet feed (w/w) where D-limonene emulsion was prepared with a 0.2 D-limonene to gelatin ratio (w/w); H gelatin: 2.5% gelatin, 0.5% alginate and 0.75% succinic acid, 25% D-limonene based on dry inlet feed (w/w) where D-limonene emulsion was prepared with a 1.2 D-limonene to gelatin ratio (w/w).....	90
Figure 4–5. The volatile retention of D-limonene in the CoCo microcapsules formulated with different emulsifier during spray drying and the emulsion size for each formulation. The detailed formulation was shown in supplementary information Table 4-1.....	91
Figure 4–6. The volatile retention of D-limonene (a-c) and the surface D-limonene content (a'-c') in microcapsules stored at different storage conditions: CoCo (a and a'), low-EC CoCo (b and b'), and high-EC Coco (c and c') microcapsules.....	94
Figure 4–7. The appearance of D-limonene loaded CoCo powders stored at different conditions after 1 week.....	95
Figure 4–8. The formation of carvone (a and b) and limonene oxide (c and d) in D-limonene loaded microcapsules with/without ethylcellulose stored at 10% RH condition (a and c) and 30% RH (ambient condition) (b and d). The formation of carvone and limonene oxide in microcapsules stored at 75% RH condition was not shown because it was below the detection limits.....	96
Figure 4–9. The kinetics release of D-limonene from the CoCo microcapsules with/without ethylcellulose in water (a), SGF (b) and SIF (c).....	98
Figure 4–10. The size distribution of D-limonene loaded CoCo microcapsules with/without ethylcellulose.....	100
Figure 4–11. The SEM of microcapsules: CoCo (a), low-EC CoCo (b) and high-EC CoCo (c).....	101
Figure 5–1. 2 h (a, b, c, d, e) and 20h (f, g, h, j, k) release profile of peptides from CoCo microcapsules with latex polymer and the CoCo microcapsules: semaglutide (a, f); liraglutide (b, g); GLP-1 (c, h); gonadorelin acetate (Gona) (d, j); oxytocin acetate (e, k). Ethylcellulose (EC), polyvinyl acetate phthalate (PVAP), cellulose acetate phthalate (CAP), methacrylic acid copolymer (MAC).....	119
Figure 5–2. Recovery of liraglutide in different media after 20h incubation (Water and PB 8.5 at room temperature; SGF and SIF at 37°C).....	122
Figure 5–3. SEM of peptides loaded CoCo powders with/without the latex polymer where the Latex polymer is labelled: semaglutide (a); liraglutide (b); GLP-1(c); gonadorelin acetate (d); oxytocin acetate (e).....	123
Figure 5–4. Particle size distribution of peptide-loaded CoCo microcapsules with/without the latex polymer: semaglutide (a); liraglutide (b); GLP-1(c); gonadorelin acetate (d); oxytocin acetate (e).....	125

Figure 5–5. Structure of peptides: semaglutide (a); liraglutide (b); GLP-1 (c); gonadorelin acetate (d); oxytocin acetate (e). The positively and negatively charged groups are indicated by orange and blue circles, respectively. The bolded circles indicate charged ends. 129

Figure 6–1. Titration curve of 0.2% (w/v) pineapple extract solution (a); First derivative of the titration curve of 0.2% (w/v) pineapple extract solution (b)..... 140

Figure 6–2. Bromelain activity recovery of the 0.75A-CoCo and 1A-CoCo powders dispersed in water with/without pH adjustment. Error bars represent standard deviation of triplicates. 143

List of Tables

Table 2–1. Formulations used in the formation of CoCo particles by spray drying. Means with same subscript letters do not differ statistically by Tukey’s test ($\alpha = 0.05$). Each sample was measured in triplicate.	32
Table 2–2. Volatile retention of L-CoCo during spray drying and storage. Means with same subscript letters in the same column do not differ statistically by Tukey’s test, where $\alpha=0.05$. Each sample was measured in triplicate.	40
Table 3–1. Inlet formulations used in the formation of D-limonene-loaded CoCo microcapsules by spray drying.	55
Table 3–2. Surface D-limonene content, water activity and pH of CoCo powders. Means with same letters do not differ statistically by Tukey's test ($\alpha = 0.05$).	63
Table 4–1. Formulations to form D-limonene-loaded CoCo powders with or without ethylcellulose.	84
Table 5–1. Formulations used in the formation of peptide loaded CoCo powders by spray drying.	113
Table 5–2. Peptide loading and powder yield of the CoCo microcapsules with/without the latex polymer.	126
Table 6–1. Formulations used in the formation of bromelain CoCo microcapsules.....	138
Table 6–2. Percent of coacervated protein in bromelain-CoCo powders on a mass basis. Each sample was measured in triplicate.	142
Table 6–3. Bromelain activity recovery of bromelain CoCo powders after spray drying.	143

Supplementary Figures and Tables

Supplementary Figure 3–1. The volatile retention of limonene in CoCo powder during spray drying and after 75 days storage and the ECC of D-limonene microcapsules formed with different concentration of acid, 2.5% gelatin and 0.5% alginate. The volatile retention of limonene after storage from powder formulated with 1.5% succinic acid was not measured (a); The pH of 1% (w/v) D-limonene microcapsules formed with different concentration of acid (b).	77
Supplementary Figure 4–1. SEM of the CoCo microcapsules formed with different emulsifier: WPI (a), SPI (b), gelatin (c), casein (d) and Tween 85 (e).	103
Supplementary Figure 6–1. Absorbance of pineapple extract powder (a); Standard curve for Bio-Rad Protein microplate standard assay, bovine serum albumin (BSA) (b). Error bars represent standard deviation of triplicates.	144
Supplementary Table 3–1. Particle size of CoCo powders (μm).	77
Supplementary Table 4–1. Formulations used in the formation of D-limonene-loaded CoCo microcapsules using different emulsifier by spray drying.	104
Supplementary Table 5–1. Particle size of peptide loaded CoCo microcapsules with/without the latex polymer.	131

Abstract

Complex coacervation is a phase separation of a mixture into two immiscible liquid phases mainly due to electrostatic interactions between two oppositely charged polymers. Microencapsulation by complex coacervation, though highly effective and achievable at the bench-scale, is challenging to scale-up because of the complexity and high-cost of the process. Thus, I developed a novel complex coacervation process (herein referred to as the ‘CoCo process’) that combines the coacervation, shell hardening and drying steps into one step by spray drying. During spray drying, the base vaporizes upon atomization, lowering the pH of the atomized droplets and inducing the two oppositely charged polymers to associate by complex coacervation. Rapid moisture removal force tightens associations between the polymers, leading to formation of water-insoluble microcapsules that are collected at the outlet of the spray dryer. The CoCo process overcomes the commercialization barrier and appears as a promising technique to encapsulate various cargo for a wide range of applications. This work investigated how to control the barrier properties of matrix microcapsules formed by the CoCo process to stabilize the bioactive components and control the release of the bioactive components for various applications.

First, as a proof concept, the potential of the CoCo process to encapsulate volatile oil was investigated by encapsulating D-limonene using gelatin and alginate as matrix building components, and succinic acid and a volatile base in the formulations to modulate the pH. Here I defined a metric termed as the extent of complex coacervation (ECC) to assess the extent to which all polymers within the particles participate in complex coacervation and it was defined as the fraction of polymers that do not solubilize from the CoCo particles when the spray dried powders are suspended in water. Insoluble CoCo particles were produced without chemical cross-linking,

with extent of complex coacervation of $75 \pm 6\%$ for D-limonene loaded CoCo particles with $82.7 \pm 3.6\%$ of D-limonene retained during spray drying (Chapter 2).

Second, to understand how to control the barrier properties of the matrix, I investigated how the formulation variables including succinic acid and gelatin content influenced the extent of complex coacervation and how the extent was related to the barrier properties of the CoCo matrix to protect D-limonene from volatilization in dry powders and control the release of D-limonene in aqueous environments. The CoCo powders formulated with 4% gelatin, 0.5% alginate, either 0.5% or 0.75% succinic acid demonstrated enteric release of D-limonene with $18.0 \pm 3.9\% \sim 26.3 \pm 6.4\%$ of D-limonene release in simulated gastric fluid (SGF) and $58.2 \pm 6.4\% \sim 71.3 \pm 3.4\%$ of D-limonene release in simulated intestinal fluid (SIF) and $7.2 \pm 1.0 \sim 7.7 \pm 0.5\%$ of D-limonene release in water. The matrix also provided robust protection for volatile compounds during spray drying, where $\sim 78\%$ D-limonene was retained and followed by 2-8% loss during subsequent 4-month storage at room temperature. This study demonstrated controlling barrier properties of gelatin-alginate CoCo powders using the novel CoCo process. For controlling the release of cargo in aqueous media, the extent of complex coacervation was important, where the higher extents of complex coacervation were achieved by increasing the gelatin concentration (increasing gelatin to alginate ratio) in the formulation. For retaining the cargo during spray drying and subsequent storage, controlling the extent of complex coacervation was not important (Chapter 3).

Third, the latex polymer was added to the CoCo formulation to investigate how the incorporation of the polymer in the CoCo microcapsules influenced the barrier properties of the CoCo matrix. The effect of the latex polymer in the CoCo microcapsules was cargo-related. The CoCo microcapsules amended with a latex polymer-ethylcellulose were markedly less efficient at retaining D-limonene during spray drying. The volatile retention of D-limonene was 19.7% in the

microcapsules with 0.25 parts ethylcellulose and 1 part CoCo polymers, compared to 77.7% of D-limonene retention in the CoCo microcapsules. The ethylcellulose in CoCo microcapsules also accelerated the release of D-limonene from 9.4% to 25.2% in water in 2 h and from 14.1% to 25.2% in SGF in 30 min and slowed the initial release of D-limonene from 58.4% to 35.7% in SIF in 5 min (Chapter 4).

The CoCo process was used for peptide encapsulation to facilitate oral delivery of therapeutic peptides. Five peptides - semaglutide, liraglutide, GLP-1, gonadorelin acetate, oxytocin acetate were used as model peptides. Promising enteric release of semaglutide and liraglutide was achieved with 0.25 parts latex polymers (e.g. ethylcellulose and polyvinyl acetate phthalate)-1.0 part CoCo polymers. Only $12.3 \pm 0.7\%$ of semaglutide and $24.0 \pm 0.5\%$ of liraglutide was released in SGF in 2h, while more than 88% of peptides was released in SIF. Peptides with more charges and side chains could enable more interactions between peptides and the matrix, leading to better protection for peptide in SGF (Chapter 5).

Finally, the CoCo process was used to encapsulate bromelain, an enzyme mixture extracted from stems and fruits of the pineapple plant, and to explore the capability of the CoCo process to maintain the proteolytic activity of bromelain. Bromelain was not only the cargo but also incorporated as the wall material. Full bromelain activity recovery in bromelain CoCo powder was achieved using the CoCo process with approximately 40% protein coacervated with alginate (Chapter 6).

Overall, the work demonstrated the potential of the CoCo process to microencapsulate different types of cargos and how the formulation development overcame the challenges related to the application of bioactive compounds.

Acknowledgements

Pursing PhD degree is a big decision I have made in my life, and I could not go this far without those who have supported me.

First and foremost, I am extremely grateful to Dr. Tina Jeoh for being my mentor and role model. Tina is an outstanding professor with exceptional abilities and masterful knowledge. With her expertise and leadership, Tina has helped me grow as a scientist by providing me invaluable mentorship, immeasurable support, and guidance. Tina has also helped me realize the significance and the value of my PhD work and inspired me to be a good scientist. Thank you for complimenting and celebrating my every small progress and success. Thank you for being patient with me and encouraging me to go through the difficult times during my PhD study. I am very grateful to join Tina's lab and I feel so fortunate to have Tina as my mentor and have the chance to learn from her.

I would also like to extend my deepest gratitude to Dr. Herbert Scher. With his expertise and extensive experience, Herb has provided me tremendous support to my research work, including patent application, research ideas, technical details, connecting with industry etc. His passion toward science and helping students is such a gift that influences me a lot. I am very grateful to work with Herb and thank you for all the encouragement and support and it means a lot to me.

It has been a pleasure working with present and former members of Jeoh Lab-Scott Strobel, Dana Wong, Jenn Nill, Akshata Mudinoor, Ryan Kawakita, Wayne Wu, Kevin Hudnall, Calvin Yee, Ben Arbaugh, Alex Hitomi, Lauren Lynn, Lucy Knowles, Hayeon Park, Bradley Soares, Sandra Pena. Thank you for your help in the lab and building such a supportive learning environment. Thank you for being friends who made my graduate study filled with wonderful moments. I especially want to thank Scott who has helped me a lot by providing valuable

suggestions, thoughtful discussions, and lab mentorship. I would also like to thank Ben and Hayeon who have helped me with my research project.

I would like to thank Dr. Bryan Jenkins, who served on both my qualifying examination and dissertation committees. Thank you for providing me critical feedback to help me grow. I would also like to thank Dr. D. Ken Giles for serving on my dissertation committee. Thank you for spending time to listen to my research and the feedback. Thank you both for reading my dissertation. In addition, I'd like to thank Dr. Nitin Nitin, Dr. Ruihong Zhang, Dr. Gail Bornhorst and Dr. Bruce German for serving on my qualifying examination committee.

I would like to thank Professor Jennifer Mullin to have me as a TA in her class. Professor Mullin is such a caring and inspiring professor. She has helped me develop and improve my teaching and communication skills.

I would like to thank our intellectual property officer Eugene Sisman and his colleagues for helping us with IP protection and licensing. I would also like to thank our industry collaborators-Timothy Childs and Van Duesterberg from Treasure8 and Jinling Chen, Liang Mao and Santipharp Panmai from Wuxi STA for supporting us to explore industry applications of our technology.

I gratefully acknowledge Andrew Thron from Advanced Materials Characterization and Testing Laboratory (AMCaT) and Marshall van Zijll from Keck Spectral Imaging Facility for training and assistance on SEM.

Many thanks to all the BAE staff who have helped me and all my friends at the BAE department and outside the BAE department.

I want to thank my partner Yifan to be at my side. I really appreciate everything you have done for me and the good and bad time that we have been through together. Thank you for making me smile, putting up with my mood swings, cheering me up and being my best friend.

Last, I want to thank my Mom and Dad, my Grandma and Grandpa, my sister and all of my family for your constant love and support that I will never take for granted. I am extremely grateful to grow up in a family full of love and thank you for being my heroes, protecting me and guiding me to be a good person, accepting me with my defects, supporting my dreams and always being there for me. I would not be here without your support and sacrifices. Grandma, you are the best grandma I could ask for. Spending time with you is unforgettable and the sweetest memories in my life that I cherish forever. Thank you for taking care of me, everything you have taught me, everything you have done for our family, your infinite love and support. I love you so much and I will miss you forever. Thank you so much!

Chapter 1 Introduction

1.1 Overview

Microencapsulation facilitates successful incorporation of bioactive compounds in many industries such as food, pharmaceutical, cosmetics, agriculture and functional materials. As the application of bioactive compounds is usually limited by their susceptibility to external environment, microencapsulation can provide a protective barrier, desirable release profile and make them compatible with different mediums. Complex coacervation is a particularly promising microencapsulation system. It is a phase separation of the mixture into two immiscible phases that occurs mainly through electrostatic interactions between two oppositely charged polymers (e.g. proteins and anionic polysaccharides). Microencapsulation by complex coacervation is of high interest in many industrial sectors because of high payloads achievable and controlled release possibilities. However, its application has so far been limited. The complicated and high-cost conventional multistep process consisting of emulsification, coacervation, shell hardening and drying remains an obstacle for commercialization as shown in **Figure 1–1**. The control of polymer interactions remains challenging. Additionally, crosslinking using toxic agents such as formaldehyde or glutaraldehyde is necessary to stabilize polymer associations, which is especially incompatible with food systems. For microcapsules formed by complex coacervation to be commercially viable and more broadly applicable, an industrially scalable process that eliminates these toxic crosslinking agents is needed.

Here I co-invented an industrially scalable microencapsulation process by *in situ* complex coacervation during spray drying (**Figure 1–2**). This novel process uses a low-cost spray drying process to form complex coacervation microcapsules. A volatile base is used to increase the pH of the spray drying feed solution to the point where both polymers are negatively charged and

therefore unassociated. Upon atomization at the spray dryer nozzle, the volatile base vaporizes, lowers the pH in the droplets below the isoelectric point of one of the two polymers, and allows oppositely charged polymers to associate by complex coacervation. As the droplets travel through the evaporation chamber, rapid moisture removal force tightens associations between the polymers, leading to formation of complex coacervated microcapsules that are collected at the outlet of the spray dryer. Results showed that water-insoluble complex coacervation microcapsules formed by this process did not require additional crosslinking. Matrix microcapsules are formed in this process instead of the core-shell microcapsules formed from the conventional complex coacervation process. As a novel process, little is known about how to control the ability of novel matrix microcapsules to stabilize the bioactive components and control the release of the bioactive components for various applications.

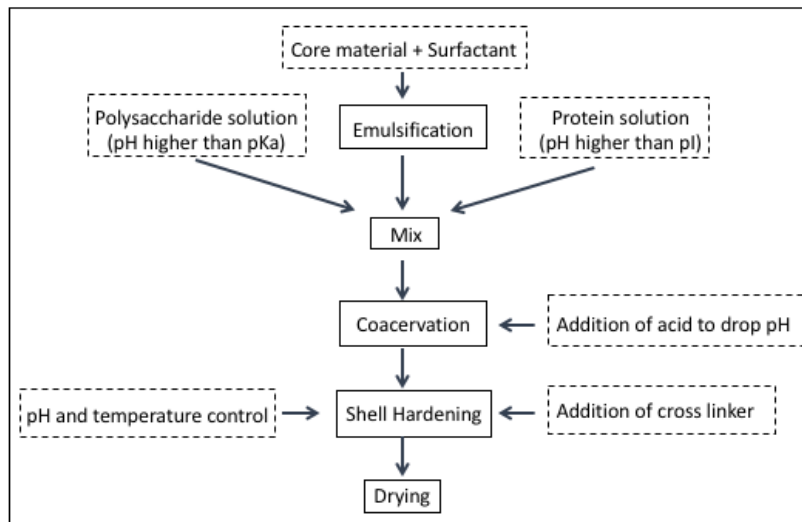


Figure 1–1. Schematic of conventional complex coacervation.

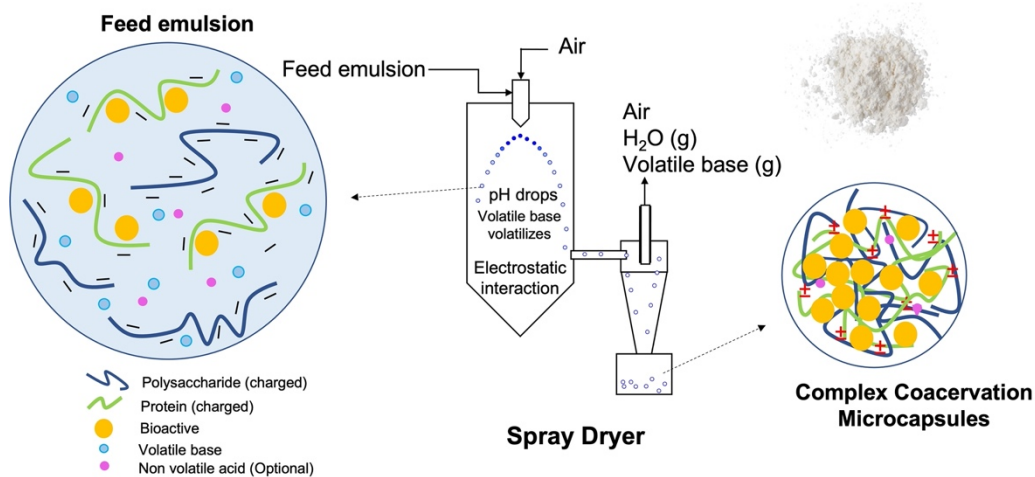


Figure 1–2. The novel process of *in situ* complex coacervation during spray drying.

1.2 Research goal

The goal of this research was to understand how to apply a novel industrially scalable complex coacervation process to provide protection and control release of cargo for food and medical application. I hypothesized that the physicochemical properties of the complex coacervated matrix can be tuned by formulation variables to influence the barrier properties related to functional attributes for targeted applications. This work explored the utilization of the CoCo process to encapsulate different types of cargos, including volatile oil – D-limonene, a model cargo for hydrophobic bioactive compounds, peptides - semaglutide, liraglutide, GLP-1, gonadorelin acetate, oxytocin acetate, simulating a hydrophilic small molecule drug, and enzyme - bromelain serving not only as a hydrophilic cargo but also wall material. The central theme of the work was to investigate how the formulation variables impacted the functional characteristics relevant to each application. Thus, the specific objectives of the project were to:

1. To investigate the potential of the novel CoCo process to protect volatile oil during spray drying and during storage (Chapter 2).

2. To explore how formulation variables including acid and protein content influence the extent of complex coacervation and how the extent of complex coacervation impacts the retention of volatile oil during spray drying and storage and release in aqueous environments (Chapter 3).

3. To investigate how the incorporation of latex polymer to the CoCo matrix influences the retention of volatile oil during spray drying and storage and release in aqueous environments (Chapter 4).

4. To investigate how the incorporation of latex polymer to the CoCo matrix controls the release of peptides in aqueous environments (Chapter 5).

5. To demonstrate how microencapsulation of enzyme in place of a matrix protein using the CoCo process maintains the enzyme activity (Chapter 6).

1.3 Literature review

1.3.1 Microencapsulation

Microencapsulation is a technique by which core compounds are surrounded by a shell wall or entrapped in a matrix formed by wall materials. Different types of microcapsule include core shell, matrix, irregular, multicore, multiwall and assembly of microcapsules (Bakry et al., 2016). Core compound, wall materials and microencapsulation technique are three key factors when designing the microencapsulation system. Core compounds are usually value-added products. Carotenoids, vitamins, enzymes, essential oils, fatty acids, phenolic compounds, proteins, organic acids and mixtures of bioactives are examples of microencapsulated core compounds in the food industry (Dias et al., 2015). Wall materials and microencapsulation techniques determine the quality and application of microcapsule including its shape, size, shelf life and bioactivity etc.

Briefly, microencapsulation is a process to create a physical barrier for core compounds to protect them from external environment and maintain their biological, functional, and physicochemical characteristics.

By providing a physical barrier, microencapsulation can bring numerous benefits into different industries. It can protect the core compounds from external environment such as oxygen, light, heat etc. through limiting or preventing interactions between external environment and core compounds. For example, encapsulation of essential oils can reduce the loss of the volatile compounds by decreasing the rate of evaporation and increase its shelf life. It can also modify the color, shape, volume, apparent density, reactivity of a core compound to expand its application. In addition, it maintains the biological and functional characteristics of core compounds and provides controlled release behavior. The release mechanism of core components from wall materials can be classified into diffusion, erosion, swelling and burst (Martins et al., 2014; Prajapati et al., 2015). By providing a physical barrier, it also improves the handling properties of sticky materials (Carvalho et al., 2016; Gharsallaoui et al., 2007).

Different techniques can be used to obtain desirable microcapsules. Proper process selection depends on the application of a designed microcapsule. The techniques of microencapsulation can be classified into three groups: physical techniques that rely on physical changes such as spray drying, lyophilization, fluidized bed coating; chemical techniques that involve chemical changes such as complex coacervation, interfacial polymerization, solvent evaporation; and physicochemical process that fall in between physical and chemical categories (Arenas-Jal et al., 2020).

1.3.2 Complex coacervation

1.3.2.1 The conventional process of complex coacervation

Coacervation, one of the microencapsulation techniques, is a phase separation of a mixture into two immiscible liquid phases. The word coacervation derives from the *latin* verb “coacervate” which means “crowd together” (Bungenberg De Jong & Kruyt, 1929). Complex coacervation is mainly due to electrostatic interactions between two oppositely charged polymers. The electrostatically bound polymers result in concentrating in liquid droplets, releasing the counterions and water to contribute to the entropy gain in the system. The system is separated into two phases: one phase rich in polyelectrolytes and the other containing mainly solvent (Weinbreck et al., 2003). This phenomenon was first studied by Tiebackx et al. in 1911, but the term ‘complex coacervation’ was first introduced in 1929 by Bungenberg de Jong and Kruyt based on their study on gum arabic and gelatin (Bungenberg De Jong & Kruyt, 1929). Since then, complex coacervation has been studied extensively. Proteins and polysaccharides are most widely used wall materials in complex coacervation (de Kruif et al., 2004; Christophe Schmitt & Turgeon, 2011; Yan & Zhang, 2014).

Complex coacervation offers numerous possibilities for microencapsulation of various bioactives in many industrial sectors. The first commercial application of complex coacervation was to produce microcapsules for carbonless copy paper developed by Barrett K. Green who worked for the National Cash Register Co. in the early 1950’s. The resulting Patent (US 2800457) was issued on July 23, 1957. It turned out to be a very successful product. Nowadays, complex coacervation is used in many industrial sectors such as food, pharmaceutical, cosmetic, agriculture, fragrance, textile etc. (Martins et al., 2014; Xiao et al., 2014). The protection of encapsulated bioactive compounds during processing, storage or other circumstances and the controlled release

of encapsulated bioactive compounds under certain environmental triggers offered by complex coacervation make it highly useful in the food industry. Besides that, complex coacervates exhibit novel rheological properties, gelling abilities, foaming ability and emulsifying abilities that are different from the individual constituting polymer (Braga & Cunha, 2004; Christophe Schmitt & Turgeon, 2011; Turgeon et al., 2007; Wang et al., 2007).

1.3.2.2 Applications of complex coacervation

Complex coacervation has been applied in different fields. Studies have reviewed the bioactive components being encapsulated by complex coacervation (Eghbal & Choudhary, 2018), including casein hydrolysate, sweet orange oil, propolis, lycopene, ascorbic acid, aspartame, tuna oil and probiotic *Lactobacillus casei* 431, astaxanthin, antioxidant extract, algal oil etc. In the food and nutraceutical industries, complex coacervation offers many benefits: allowing easier incorporation into different food products, preserving the bioactivity over the shelf life, providing effective delivery by controlled release and masking unpleasant taste or odor of some compounds. For example, complex coacervation reduces hygroscopicity and bitter taste of casein hydrolysate and increases the stability of ascorbic acid. It can also provide protection for components sensitive in stomach such as flavonoid, carotenoid during digestion (Rodríguez-Roque et al., 2013; Tarko et al., 2013). For compounds such as omega-3 fatty acid and vitamin E that are believed to be most absorbable in the intestine, complex coacervation can provide desirable release in the intestine to empower the bioactive accessibility of bioactive compound (Somchue et al., 2009). In the pharmaceutical industry, effective drug delivery through complex coacervation is achievable with low release in gastric fluid and prolonged release in intestinal fluid (Saravanan & Rao, 2010). Complex coacervation is also useful in the agricultural industry by promoting plant growth and

health through encapsulation of insect sex pheromones and microbes. For example, microencapsulation of insect sex pheromones provides controlled release under controlled temperature and relative humidity to disrupt insect production, functioning as environmentally friendly pesticides in agriculture (Gu et al., 2010). The neem seed oil microcapsules by complex coacervation were used for insecticidal preparation (Devi & Maji, 2011). Microencapsulation of biofertilizer improves the viability of microorganisms during storage and field application (John et al., 2011). In the textile industry, complex coacervation can be used for aromatherapy textiles or antibacterial clothes to deal with infection-induced skin diseases (J. Liu et al., 2013). In the cosmetic industry, microencapsulation of essential oils and antioxidants are applied to increase the shelf life and preserve bioactivities of components (Carvalho et al., 2016).

1.3.2.3 Limitations and challenges of complex coacervation

The process of complex coacervation usually consists of emulsification, coacervation and shell hardening process (**Figure 1–1**). The hardening process is necessary to stabilize the shell wall, but it is time consuming and energy demanding. There are three types of cross linkers for the hardening process: traditional chemical aldehyde cross linker such as formaldehyde or glutaraldehyde, natural cross linker such as genipin or enzyme cross linker such as transglutaminase (Dong et al., 2011; Saravanan & Rao, 2010; Z. Yang et al., 2014). No matter what type of cross linker is used, cross linking requires precise adjustment of pH and/or temperature and typically takes a few hours to complete (Dong et al., 2011; Saravanan & Rao, 2010; Z. Yang et al., 2014).

There are many drawbacks that hinder the commercial application of complex coacervation. The multistep process remains an obstacle for industrially scalable production. The electrostatic

interaction between polymers is not easy to control (deposition of complex coacervate onto droplet surfaces in the step where pH is adjusted to induce complex coacervation does not always take place). The addition of toxic crosslinking agent such as formaldehyde or glutaraldehyde limits its applicability, especially in food systems.

1.3.3 *Spray drying*

Spray drying is a process of transforming the feed from a fluid state into a dried particulate form by spraying the feed into a hot drying medium. Spray drying has been widely used for drying food ingredients, pharmaceuticals, and other substances. Besides as a drying process, spray drying has also been widely used as a microencapsulation method (I Ré, 1998). Food ingredients such as flavors, lipids and carotenoids have been encapsulated in wall materials through spray drying for decades (Gharsallaoui et al., 2007). Carbohydrates such as starch, gums, cyclodextrins, alginate and chitosan and proteins such as milk protein, soy protein are commonly used wall materials in spray-drying microencapsulation of food oils and flavors as reviewed by Jafari *et al.* (Jafari et al., 2008).

Spray drying offers many advantages, making it the most important techniques for microencapsulation of bioactive ingredients (Gharsallaoui et al., 2007; Patel et al., 2009): (1) it is one simple and easy scalable operation; (2) it can be designed to meet with various capacity required; (3) it is a low cost, continuous and fast process; (4) it can be used for both heat sensitive and heat resistance products; (5) there are many choices of wall materials that are suitable for spray drying.

1.3.4 In situ complex coacervation during spray drying (CoCo process)

1.3.4.1 Introduction of CoCo process

I recently developed a novel process of in situ complex coacervation during spray drying (Tang et al., 2021). The novel process is illustrated in Figure 1–2. Spray drying is a low-cost technology that is the most commonly used technology for microencapsulation (Gouin, 2004; Soottitantawat, Takayama, et al., 2005). The method utilizes a polysaccharide and a protein with an isoelectric point (pI) higher than the acid dissociation constant (pKa) of the polysaccharide. The spray dry feed consists of the protein, polysaccharide and an emulsion with cargo. A volatile base such as ammonium hydroxide is used to raise the pH of the spray dry feed emulsion to the point where the pH is higher than the pKa of polysaccharide and pI of protein. At a pH higher than the pI of the protein, both the carboxyl and amine groups in the protein are deprotonated such that the protein carries a net negative charge. At a pH higher than the pKa of polysaccharide, the carboxyl group in polysaccharide is mostly deprotonated such that the polysaccharide also carries a negative charge. Thus, phase separation is prevented in the spray dry feed emulsion. Upon atomization at the spray dry nozzle, the volatile base vaporizes and lowers the pH in the droplets, the amine groups in the protein will be protonated. When the pH is at the pI of the protein, the protein carries no net charge. When the pH drops lower than the pI, the protein carries a net positive charge. As pH is higher than pKa of polysaccharide, carboxyl groups in polysaccharide remains mostly deprotonated and negatively charged. Deprotonated carboxyl group in polysaccharide (negatively charged sites) and protonated amine groups in protein (positively charged sites) will interact with each other to induce complex coacervation. Simultaneously, rapid moisture removal exerts hydrostatic forces that tighten associations between the polymers, leading to the formation of dry, insoluble matrix microcapsules without the use of cross linker.

1.3.4.2 Advantages of the CoCo process

The novelty and advantages of the process are summarized as follows: (1) electrostatic interactions between polymers coupled with hydrostatic forces resulting from simultaneous drying forms insoluble microcapsules; (2) elimination of cross linker makes it broadly applicable in different industries; (3) matrix microcapsules are formed instead of core-shell microcapsules from conventional complex coacervation; (4) consolidation of multiple steps to form complex coacervation microcapsules makes it industrially scalable; (5) this is a high throughput production of microcapsules with narrow distribution of sizes and uniform properties; (6) encapsulated cargo has pH responsive release profile based on the selection of polymers.

1.3.4.3 Factors affecting complex coacervation

The interaction of two ionic polymers to form complex coacervates can be influenced by many factors. First, the interaction of two ionic polymers to form complex coacervates is associated with polymer properties such as the molecular weight, charge density and structure (Schmitt & Turgeon, 2011). Second, once the pair of polymers is selected, the concentration of each polymer and their ratio are influential to modulate the degree of complex coacervation by regulating the overall charge density of polysaccharide and protein. Third, electrostatic interaction is the dominant interaction for complex coacervation. The interaction is highly dependent on the individual charge density of the polymer, which is highly influenced by the solution pH. The pH appears to be the significant factor not only by influencing charge density of the polymer but also by inducing structural transition of the polymer (Mekhloufi et al., 2005; Y. Yang et al., 2012). Studies have shown that proteins can go through conformational transition at low pH, which contributes to the

size and morphology of complex coacervates (Lv et al., 2013). The pH effect on complex coacervation have been studied extensively. In aqueous environments, researchers have proposed four phase separation boundary pH: pH_c where soluble complexes forms, pH_{ϕ_1} where phase separation takes place, pH_{opt} where optimal complex coacervation occurs, and pH_{ϕ_2} where precipitate happens due to the protonation of polysaccharide (Weinbreck et al., 2003). The phase boundary pH varies in different systems. In the CoCo process, the type of the acid and its concentration in the feed influence complex coacervation. Besides that, the starting pH of the feed regulated by the addition of ammonium hydroxide may affect the protein structure thus complex coacervation (Gioffrè et al., 2012).

The spray drying operation parameters including the inlet air temperature, aspirator airflow rate, feed flow rate and nozzle pressure affect the drying process and the drying process is associated with the formation of complex coacervates. Loss of ammonia associated with the drying process affects the extent of pH lowering and the pH during spray drying is expected to reach the point below the pI of protein to maximize the positive charge density. The charge on polysaccharide remains negative and hence electrostatic attractions are induced. In addition, the greater the water loss during spray drying, the smaller the spacing between the oppositely charged polymer molecules and hence the stronger the electrostatic attractive forces. The hydrostatic forces come into play as the polymer intermolecular spacing is reduced. Hence the extent of pH lowering, and the extent of water loss could determine the insolubility of the complex coacervate polymers (the extent of complex coacervation). The hypothesis here is that these forces are strong enough such that a chemical cross linker is not necessary to achieve complete insolubility. Inlet air temperature is associated with dryer evaporative capacity and thermal efficiency. It affects the wet-bulb temperature of the surrounding hot air, the cooling process of the atomized feed droplets to

the wet-bulb temperature, the volatilization of ammonia, and the overall drying process. Aspirator airflow rate is related to the amount of heated drying air entering the spray chamber and it affects the drying process and separation of particles in the cyclone. Feed flow rate affects the outlet temperature and particle size. Nozzle pressure affects the atomized droplet size, the shape of the spray in the evaporation chamber (spray angle) thus the following drying process.

1.3.4.4 CoCo matrix formed by gelatin and alginate

Proteins and polysaccharides are classic wall materials to form complex coacervates. In this study, alginate and gelatin are selected as the polysaccharide and protein pair for the CoCo process considering the polymer's availability, safety, biodegradability, physicochemical properties including solubility, viscosity, emulsifying ability, charge density etc. Alginate and gelatin have been widely used in microencapsulation as reported (e.g. encapsulate drug, olive oil etc.) (Devi et al., 2012; Saravanan & Rao, 2010).

Gelatin is commonly used in the food industry. It is obtained from the hydrolysis of collagen extracted from skin, white connective tissue, and bones of animals. Collagen has a triple-helix structure stabilized by intra and inter-chain hydrogen bonds. Collagen fibril with recurring triple helix is composed of tropocollagen. Tropocollagen (Mr 300,000) is composed of three identical chains or two same chains and one different chain, about 300 nm long and only 1.5 nm thick. Tropocollagens are staggered longitudinally and bilaterally by inter- and intra-molecular crosslinks into microfibrils (Bhattacharjee & Bansal, 2005; Gorgieva & Kokol, 2011). Gelatin has both cationic and anionic groups along with hydrophobic groups. The cationic property of gelatin is due to lysine and arginine residues. The anionic property of gelatin is due to aspartic and glutamic acid residues. The hydrophobic groups are leucine, isoleucine, methionine and valine

(Elzoghby, 2013). The structure of gelatin with a high degree of complexity is influenced by many factors. There are three possible structure states of gelatin: a) amorphous coils; b) triple helixes and coils; c) bundles of triple helixes and coils. Unlike its parental structure with triple helix, many studies have shown that gelatin may lose its secondary and tertiary structure during hydrolysis, existing as random coils (Usha & Ramasami, 2004). When the pH is higher than gelatin's pI, gelatin is an "anionic" polymer with a large amount of -COO- groups. Gelatin molecule stretches due to electrostatic repulsion and the dispersion of the gelatin becomes better as the viscosity of the solution increases (Zhang et al., 2010). Gelatin is biocompatible, biodegradable, edible and soluble at the body temperature. The remarkable properties of gelatin are its thermally reversible gelling ability, emulsifying capacity and high crosslinking activity (H. Y. Liu et al., 2008; Meng & Cloutier, 2014; Zhou et al., 2006). These characteristics make it a popular ingredient in food and a promising candidate for a microencapsulation wall material. Moreover, gelatin has a very good film-forming property during spray drying, which implied the rapid formation of a dense film and a good protection of core ingredient during spray drying (Matsuno & Adachi, 1993).

As a linear polysaccharide derived from algae cell wall, alginate is also a widely used microencapsulation material due to its biocompatibility, biodegradability and nontoxicity (de Oliveira et al., 2014). It consists of alternating blocks of 1–4 linked α -L-guluronic and β -D-mannuronic acid residues and has the ability to cross link with divalent ions such as calcium to induce gel formation (George & Abraham, 2006; Gombotz & Wee, 2012). The geometries of the G-block regions, M-block regions, and alternating regions are substantially different due to the shapes of monomers and the way the monomer links. Specifically, the G-blocks are buckled while the M-blocks have a shape referred to as an extended ribbon. G-block regions and M-block regions are interspersed with alternating regions. Molecular length per mannuronic and guluronic acid

residue in an alginate molecule in aqueous solutions have been estimated and root mean square end-to-end distance of alginate with average molecular weight of 28200 and high G/M ratio (G/M=1.8) was calculated by 48nm (Kawai et al., 1992). The molecular weights of commercially available sodium alginates range between 32,000 and 400,000 g/mol (Lee & Mooney, 2012). The ratio of G/M of the alginate with molecular weight of 172,800±458 used in this work was up to 2.8 and size of alginate is expected to be larger than gelatin (Jeoh et al., 2021). The charge density of this linear chain polymer makes it a very promising matrix building polymer.

1.3.4.5 Understanding how to control the barrier properties of the CoCo microcapsules

The barrier properties of complex coacervated (CoCo) powder are crucial to its application in various industries. For example, for microencapsulation of volatile cargo like limonene in the food industry, the barrier properties of microcapsules to protect the cargo loss during spray drying and storage play an important role to facilitate its incorporation into other food products with long shelf life. For cargo that is prone to oxidation such as omega-3 fatty acid, the major challenge is to create a protective layer/matrix with good oxygen barrier properties. For component like carotenoid that needs enteric release to maintain or enhance its bioactivity during digestion, protective matrix should have tunable barrier properties corresponding to the aqueous environment, thus offering desirable release rate at targeted locations.

In conventional complex coacervation, barrier properties of complex coacervated microcapsules are linked to the interactions between polymers. Measure of coacervation yield, zeta potential and turbidity are commonly used to evaluate the interactions between polymers and thus determine the optimal pH and biopolymer ratio for the formation of complex coacervates (Mendanha et al., 2009; Yan & Zhang, 2014). The optimum coacervation parameters for maximum

coacervation yield vary from sets of polymers, as each set of polymers may have its specific pH and polymers ratio. Coacervation yield is the ratio of total polymers involved in complex coacervation to the total polymers added into the system. However, it does not reveal the ratio of each polymer involved in complex coacervation to the polymer added into the system. Many studies first determined the optimum complex coacervation parameters by maximizing the coacervation yield and then investigated the barrier properties of microcapsules prepared under optimum condition, based on the assumption that the higher coacervation yield would contribute to better barrier properties of the microcapsules. The other ways to evaluate the interaction between polymers are measuring the turbidity of polymer mixture and zeta potential. The optimum parameters are determined as highest turbidity of the mixture reaches where the intensity of electrostatic attraction between polymers is the highest. Studies have shown that the optimum parameters from turbidity turned out to be a matchable response of the coacervation yield (Lv et al., 2012; Timilsena et al., 2016). This is not surprised as the turbidity of the mixture is related to the ratio of polymers interacted. However, turbidity measurement requires good distribution of the coacervates in the continuous phase. Last, measuring zeta potential can identify the pH range that the polymers interact with each other. When the intensity of electrostatic attraction between polymers reaches the highest, the sum of the zeta potential of the polymers reaches the electrical equivalence pH. One study showed that the optimum parameters from zeta potential turned out to be a matchable response of the coacervation yield (Timilsena et al., 2016), while the other study has shown the optimum parameters from zeta potential measurement was different from that from turbidity measurement (Lv et al., 2012).

These methods are assessing complex coacervation in a liquid media, not of dried powder dispersed into media. In the CoCo process where drying and pH adjustment occur simultaneously

and rapidly, the extent to which the polymers coacervated is assessed by resuspending in liquid media and encouraging non-coacervated polymers to dissolve out. It contributes to understanding how the formation of complex coacervates in the CoCo process affects the barrier properties of the microcapsules.

1.3.5 Bioactives encapsulation

1.3.5.1 D-limonene encapsulation

In this research, D-limonene was selected as the model volatile oil cargo. Abundant in nature, D-limonene accounts for more than 90% citrus peel oil and is a valuable renewable byproduct in the citrus industry (Ciriminna et al., 2014). As a monocyclic monoterpene, D-limonene has a pleasant citrus-like smell and has many bioactivities such as antifungal, bacteriostatic and bactericidal properties, making it appealing in many industries. D-limonene has been used in various areas such as food packaging, alternative biosolvent, cosmetic products, soaps, household cleaning products, medical care, pest control, food industry etc. (Arrieta et al., 2014; Espina et al., 2013; Miller et al., 2011; Virot et al., 2008). In the food industry, D-limonene is used in many food products such as chewing gum, citrus juices, vegetables, herbs, candy and drinks. It has been used as a flavoring agent in some food products such as fruit beverages and ice cream and supplement for immunity, digestion and detox. Moreover, it has the potential to be a food preservative as it exhibits antifungal, bacteriostatic and bactericidal properties (Espina et al., 2013).

Microencapsulation of D-limonene can overcome the challenge of D-limonene application due to its volatility and instability. Microencapsulation of D-limonene is usually done by spray drying using polysaccharides such as maltodextrin, HI-CAP 100, gum arabic as wall material (Jafari et al., 2007; Soottitantawat, Bigeard, et al., 2005). Efforts have also been explored to

encapsulate flavor compounds through complex coacervation to improve the stability against environmental stresses such as heat. Examples include sweet orange oil encapsulated in coacervated soybean protein isolate and gum arabic, flavor oil encapsulated in coacervated gelatin and gum arabic, vanilla oil encapsulated in coacervated chitosan and gum arabic, and jasmine essential oil encapsulated in coacervated gelatin and gum arabic (Jun-xia et al., 2011; Lv et al., 2014; Z. Yang et al., 2014; Yeo et al., 2005). Controlled release of flavors in water/water bath was investigated in complex coacervated microcapsules (Dong et al., 2011; Lv et al., 2014).

1.3.5.2 Peptide encapsulation

In the pharmaceutical industry, oral delivery of peptide that has therapeutical benefits is especially desirable due to dosing convenience, patient acceptance, potential shorter treatment period and low cost. However, the oral delivery of peptide faces substantial challenges that are related to the normal physiological roles of gastrointestinal tracts (Drucker, 2020; McClements, 2018). Peptides are susceptible to denaturation, aggregation or hydrolysis in the stomach. Gastrointestinal tracts have a set of cellular and mucus barriers, restricting the passage of peptide (Drucker, 2020). Different strategies have been explored including permeation enhancer, modulating of pH, direct enzyme inhibition, peptide cyclization, mucus-penetrating agents, as well as cell penetrating peptides etc. (Drucker, 2020). Microencapsulation of peptide is another strategy to facilitate the oral delivery by protecting peptides in the stomach. The carrier materials used for peptide encapsulation are typically polysaccharides and protein based carriers (Mohan et al., 2015).

1.3.5.3 Enzyme encapsulation

Proteolytic enzymes (also termed proteases) can be found in all living organisms and are capable of hydrolyzing peptide bonds in proteins. Proteolytic enzymes have been extensively applied in several sectors of industry including the application in the life sciences, food and pharmaceutical (da Silva, 2017; Mótyán et al., 2013). Bromelain is a common available protease derived from pineapple and it has been widely used in several areas such as medicine, health, food and cosmetics. However, the bromelain proteolytic activity is susceptible to stress conditions such as heat, high acidity, gastric protease. The operational, storage and application conditions can diminish its activity, therefore limiting its health benefits and its application. Different strategies have been explored to maintain bromelain activity for its application (Ataide et al., 2018). Methods such as enzyme chemical modifications, protein engineering techniques, use of compatible osmolytes have been used to increase the enzyme activity. The use of nanoparticles that encapsulate bromelain in inorganic compounds such as silica, synthetic polymers such as polyacrylic acid and natural polymers such as chitosan aims for the development of targeted delivery for pharmaceutical uses. Different methods such as ionotropic gelatin, double emulsion-solvent evaporation can be employed to produce the bromelain nanoparticles/microcapsules. However, studies have also shown that the encapsulation process resulted in bromelain activity loss (e.g. 76% of activity remained in polyacrylic acid nanoparticles) depending on the process (Wei et al., 2017). In this study, the CoCo process was used to encapsulate bromelain in place of a protein as one of matrix building blocks. The bromelain proteolytic activity was measured by EnzChek™ Protease assay and the success of maintaining bromelain proteolytic activity in the CoCo microcapsules was a good start to investigate how the encapsulated bromelain reacts in stress conditions related to its application.

1.3.6 Summary

Microencapsulation of bioactive components facilitates their application in various industries by allowing easier incorporation into products, preserving bioactivities over the shelf life and providing effective delivery. Complex coacervation is one of the microencapsulation techniques and particularly effective to accomplish these goals. However, the application of complex coacervation in industry faces obstacles as it is a complicated and expensive process which is not easy for scaling up and there is unmet need for an effective and inexpensive delivery matrix for the application of bioactive component for various industries. Thus, an effective and industrially scalable complex coacervation process (CoCo process) by spray drying was developed to address the barrier to commercialization. The CoCo process can enable high microencapsulation efficacy, promote health benefits for consumers, increase profitability for manufacturer and help the environment by reducing energy use.

The literature review summarized the factors affecting complex coacervation for desirable barrier properties. As a novel process, little is known about how to control the barrier properties of novel matrix microcapsules. The following chapters investigate the relationships between formulation variables, physiochemical properties of CoCo matrix (e.g. the interaction between polymers) and the barrier properties of the CoCo microcapsules in order to advance the application of the CoCo process in food and pharmaceutical industries.

1.3.7 References

- Arenas-Jal, M., Suñé-Negre, J. M., & García-Montoya, E. (2020). An overview of microencapsulation in the food industry: opportunities, challenges, and innovations. *European Food Research and Technology*, 246(7), 1371–1382. <https://doi.org/10.1007/s00217-020-03496-x>
- Arrieta, M. P., López, J., Hernández, A., & Rayón, E. (2014). Ternary PLA–PHB–Limonene

- blends intended for biodegradable food packaging applications. *European Polymer Journal*, 50, 255–270. <https://doi.org/https://doi.org/10.1016/j.eurpolymj.2013.11.009>
- Ataide, J. A., Gérios, E. F., Mazzola, P. G., & Souto, E. B. (2018). Bromelain-loaded nanoparticles: A comprehensive review of the state of the art. *Advances in Colloid and Interface Science*, 254, 48–55. <https://doi.org/https://doi.org/10.1016/j.cis.2018.03.006>
- Bakry, A. M., Abbas, S., Ali, B., Majeed, H., Abouelwafa, M. Y., Mousa, A., & Liang, L. (2016). Microencapsulation of Oils: A Comprehensive Review of Benefits, Techniques, and Applications. *Comprehensive Reviews in Food Science and Food Safety*, 15(1), 143–182.
- Bhattacharjee, A., & Bansal, M. (2005). Collagen Structure: The Madras Triple Helix and the Current Scenario. *IUBMB Life*, 57(3), 161–172. <https://doi.org/https://doi.org/10.1080/15216540500090710>
- Braga, A. L. M., & Cunha, R. L. (2004). The effects of xanthan conformation and sucrose concentration on the rheological properties of acidified sodium caseinate–xanthan gels. *Food Hydrocolloids*, 18(6), 977–986. <https://doi.org/https://doi.org/10.1016/j.foodhyd.2004.04.002>
- Bungenberg De Jong, H. G., & Kruyt, H. R. (1929). Coacervation (partial miscibility in colloid systems). *Proc. K. Ned. Akad. Wet.*, 32, 849–856.
- Carvalho, I. T., Estevinho, B. N., & Santos, L. (2016). Application of microencapsulated essential oils in cosmetic and personal healthcare products – a review. *International Journal of Cosmetic Science*, 38(2), 109–119. <https://doi.org/10.1111/ics.12232>
- Ciriminna, R., Lomeli-Rodriguez, M., Demma Carà, P., Lopez-Sanchez, J. A., & Pagliaro, M. (2014). Limonene: a versatile chemical of the bioeconomy. *Chemical Communications*, 50(97), 15288–15296. <https://doi.org/10.1039/C4CC06147K>
- da Silva, R. R. (2017). Bacterial and Fungal Proteolytic Enzymes: Production, Catalysis and Potential Applications. *Applied Biochemistry and Biotechnology*, 183(1), 1–19. <https://doi.org/10.1007/s12010-017-2427-2>
- de Kruijff, C. G., Weinbreck, F., & de Vries, R. (2004). Complex coacervation of proteins and anionic polysaccharides. *Current Opinion in Colloid & Interface Science*, 9(5), 340–349. <https://doi.org/https://doi.org/10.1016/j.cocis.2004.09.006>
- de Oliveira, E. F., Paula, H. C. B., & de Paula, R. C. M. (2014). Alginate/cashew gum nanoparticles for essential oil encapsulation. *Colloids and Surfaces B: Biointerfaces*, 113, 146–151.
- Devi, N., Hazarika, D., Deka, C., & Kakati, D. K. (2012). Study of Complex Coacervation of Gelatin A and Sodium Alginate for Microencapsulation of Olive Oil. *Journal of Macromolecular Science, Part A*, 49(11), 936–945. <https://doi.org/10.1080/10601325.2012.722854>
- Devi, N., & Maji, T. K. (2011). Study of Complex Coacervation of Gelatin A with Sodium Carboxymethyl Cellulose: Microencapsulation of Neem (*Azadirachta indica* A. Juss.) Seed Oil (NSO). *International Journal of Polymeric Materials and Polymeric Biomaterials*, 60(13), 1091–1105. <https://doi.org/10.1080/00914037.2011.553851>
- Dias, M. I., Ferreira, I. C. F. R., & Barreiro, M. F. (2015). Microencapsulation of bioactives for food applications. *Food & Function*, 6(4), 1035–1052.
- Dong, Z., Ma, Y., Hayat, K., Jia, C., Xia, S., & Zhang, X. (2011). Morphology and release profile of microcapsules encapsulating peppermint oil by complex coacervation. *Journal of Food Engineering*, 104(3), 455–460. <https://doi.org/https://doi.org/10.1016/j.jfoodeng.2011.01.011>
- Drucker, D. J. (2020). Advances in oral peptide therapeutics. *Nature Reviews Drug Discovery*,

- 19(4), 277–289. <https://doi.org/10.1038/s41573-019-0053-0>
- Eghbal, N., & Choudhary, R. (2018). Complex coacervation: Encapsulation and controlled release of active agents in food systems. *LWT*, *90*, 254–264. <https://doi.org/https://doi.org/10.1016/j.lwt.2017.12.036>
- Elzoghby, A. O. (2013). Gelatin-based nanoparticles as drug and gene delivery systems: Reviewing three decades of research. *Journal of Controlled Release*, *172*(3), 1075–1091. <https://doi.org/https://doi.org/10.1016/j.jconrel.2013.09.019>
- Espina, L., Gelaw, T. K., de Lamo-Castellví, S., Pagán, R., & García-Gonzalo, D. (2013). Mechanism of Bacterial Inactivation by (+)-Limonene and Its Potential Use in Food Preservation Combined Processes. *PLOS ONE*, *8*(2), e56769. <https://doi.org/10.1371/journal.pone.0056769>
- George, M., & Abraham, T. E. (2006). Polyionic hydrocolloids for the intestinal delivery of protein drugs: Alginate and chitosan — a review. *Journal of Controlled Release*, *114*(1), 1–14. <https://doi.org/https://doi.org/10.1016/j.jconrel.2006.04.017>
- Gharsallaoui, A., Roudaut, G., Chambin, O., Voilley, A., & Saurel, R. (2007). Applications of spray-drying in microencapsulation of food ingredients: An overview. *Food Research International*, *40*(9), 1107–1121. <https://doi.org/http://dx.doi.org/10.1016/j.foodres.2007.07.004>
- Gioffrè, M., Torricelli, P., Panzavolta, S., Rubini, K., & Bigi, A. (2012). Role of pH on stability and mechanical properties of gelatin films. *Journal of Bioactive and Compatible Polymers*, *27*(1), 67–77. <https://doi.org/10.1177/0883911511431484>
- Gombotz, W. R., & Wee, S. F. (2012). Protein release from alginate matrices. *Advanced Drug Delivery Reviews*, *64*, 194–205. <https://doi.org/https://doi.org/10.1016/j.addr.2012.09.007>
- Gorgieva, S., & Kokol, V. (2011). Collagen- vs. Gelatine-Based Biomaterials and Their Biocompatibility: Review and Perspectives. In *Biomaterials: Applications for Nanomedicine* (pp. 18–52). IntechOpen. <https://doi.org/10.5772/24118>
- Gouin, S. (2004). Microencapsulation: industrial appraisal of existing technologies and trends. *Trends in Food Science & Technology*, *15*(7), 330–347. <https://doi.org/https://doi.org/10.1016/j.tifs.2003.10.005>
- Gu, X.-L., Zhu, X., Kong, X.-Z., & Tan, Y. (2010). Comparisons of simple and complex coacervations for preparation of sprayable insect sex pheromone microcapsules and release control of the encapsulated pheromone molecule. *Journal of Microencapsulation*, *27*(4), 355–364. <https://doi.org/10.3109/02652040903221532>
- I Ré, M. (1998). MICROENCAPSULATION BY SPRAY DRYING. *Drying Technology*, *16*(6), 1195–1236. <https://doi.org/10.1080/07373939808917460>
- Jafari, S. M., Assadpoor, E., He, Y., & Bhandari, B. (2008). Encapsulation efficiency of food flavours and oils during spray drying. *Drying Technology*, *26*(7), 816–835.
- Jafari, S. M., He, Y., & Bhandari, B. (2007). Encapsulation of Nanoparticles of d-Limonene by Spray Drying: Role of Emulsifiers and Emulsifying Techniques. *Drying Technology*, *25*(6), 1069–1079. <https://doi.org/10.1080/07373930701396758>
- Jeoh, T., Wong, D. E., Strobel, S. A., Hudnall, K., Pereira, N. R., Williams, K. A., Arbaugh, B. M., Cunniffe, J. C., & Scher, H. B. (2021). How alginate properties influence in situ internal gelation in crosslinked alginate microcapsules (CLAMs) formed by spray drying. *PLOS ONE*, *16*(2), e0247171. <https://doi.org/10.1371/journal.pone.0247171>
- John, R. P., Tyagi, R. D., Brar, S. K., Surampalli, R. Y., & Prévost, D. (2011). Bio-encapsulation of microbial cells for targeted agricultural delivery. *Critical Reviews in Biotechnology*, *31*(3),

- 211–226. <https://doi.org/10.3109/07388551.2010.513327>
- Jun-xia, X., Hai-yan, Y., & Jian, Y. (2011). Microencapsulation of sweet orange oil by complex coacervation with soybean protein isolate/gum Arabic. *Food Chemistry*, *125*(4), 1267–1272. <https://doi.org/https://doi.org/10.1016/j.foodchem.2010.10.063>
- Kawai, M., Matsumoto, T., Masuda, T., & Nakajima, A. (1992). Molecular length per mannuronic and guluronic acid residue in an alginate molecule in aqueous solutions. *Journal of Japanese Society of Biorheology*, *6*(2), 42–47. https://doi.org/10.11262/jpnbr1987.6.2_42
- Lee, K. Y., & Mooney, D. J. (2012). Alginate: Properties and biomedical applications. *Progress in Polymer Science*, *37*(1), 106–126. <https://doi.org/https://doi.org/10.1016/j.progpolymsci.2011.06.003>
- Liu, H. Y., Li, D., & Guo, S. D. (2008). Extraction and properties of gelatin from channel catfish (*Ictalurus punctatus*) skin. *LWT - Food Science and Technology*, *41*(3), 414–419. <https://doi.org/http://dx.doi.org/10.1016/j.lwt.2007.03.027>
- Liu, J., Liu, C., Liu, Y., Chen, M., Hu, Y., & Yang, Z. (2013). Study on the grafting of chitosan–gelatin microcapsules onto cotton fabrics and its antibacterial effect. *Colloids and Surfaces B: Biointerfaces*, *109*, 103–108. <https://doi.org/https://doi.org/10.1016/j.colsurfb.2013.03.040>
- Lv, Y., Yang, F., Li, X., Zhang, X., & Abbas, S. (2014). Formation of heat-resistant nanocapsules of jasmine essential oil via gelatin/gum arabic based complex coacervation. *Food Hydrocolloids*, *35*, 305–314. <https://doi.org/https://doi.org/10.1016/j.foodhyd.2013.06.003>
- Lv, Y., Zhang, X., Abbas, S., & Karangwa, E. (2012). Simplified optimization for microcapsule preparation by complex coacervation based on the correlation between coacervates and the corresponding microcapsule. *Journal of Food Engineering*, *111*(2), 225–233. <https://doi.org/https://doi.org/10.1016/j.jfoodeng.2012.02.030>
- Lv, Y., Zhang, X., Zhang, H., Abbas, S., & Karangwa, E. (2013). The study of pH-dependent complexation between gelatin and gum arabic by morphology evolution and conformational transition. *Food Hydrocolloids*, *30*(1), 323–332. <https://doi.org/https://doi.org/10.1016/j.foodhyd.2012.06.007>
- Martins, I. M., Barreiro, M. F., Coelho, M., & Rodrigues, A. E. (2014). Microencapsulation of essential oils with biodegradable polymeric carriers for cosmetic applications. *Chemical Engineering Journal*, *245*, 191–200. <https://doi.org/https://doi.org/10.1016/j.cej.2014.02.024>
- Matsuno, R., & Adachi, S. (1993). Lipid encapsulation technology - techniques and applications to food. *Trends in Food Science & Technology*, *4*(8), 256–261. [https://doi.org/https://doi.org/10.1016/0924-2244\(93\)90141-V](https://doi.org/https://doi.org/10.1016/0924-2244(93)90141-V)
- McClements, D. J. (2018). Encapsulation, protection, and delivery of bioactive proteins and peptides using nanoparticle and microparticle systems: A review. *Advances in Colloid and Interface Science*, *253*, 1–22. <https://doi.org/https://doi.org/10.1016/j.cis.2018.02.002>
- Mekhloufi, G., Sanchez, C., Renard, D., Guillemin, S., & Hardy, J. (2005). pH-Induced Structural Transitions during Complexation and Coacervation of β -Lactoglobulin and Acacia Gum. *Langmuir*, *21*(1), 386–394. <https://doi.org/10.1021/la0486786>
- Mendanha, D. V., Molina Ortiz, S. E., Favaro-Trindade, C. S., Mauri, A., Monterrey-Quintero, E. S., & Thomazini, M. (2009). Microencapsulation of casein hydrolysate by complex coacervation with SPI/pectin. *Food Research International*, *42*(8), 1099–1104. <https://doi.org/https://doi.org/10.1016/j.foodres.2009.05.007>
- Meng, Y., & Cloutier, S. (2014). Chapter 20 - Gelatin and Other Proteins for Microencapsulation. In *Microencapsulation in the Food Industry* (pp. 227–239). Academic Press.

- <https://doi.org/http://dx.doi.org/10.1016/B978-0-12-404568-2.00020-0>
- Miller, J. A., Thompson, P. A., Hakim, I. A., Chow, H.-H. S., & Thomson, C. A. (2011). d-Limonene: a bioactive food component from citrus and evidence for a potential role in breast cancer prevention and treatment. *Oncology Reviews*, 5(1), 31–42. <https://doi.org/10.1007/s12156-010-0066-8>
- Mohan, A., Rajendran, S. R. C. K., He, Q. S., Bazinet, L., & Udenigwe, C. C. (2015). Encapsulation of food protein hydrolysates and peptides: a review. *RSC Advances*, 5(97), 79270–79278. <https://doi.org/10.1039/C5RA13419F>
- Mótyán, J. A., Tóth, F., & Tőzsér, J. (2013). Research Applications of Proteolytic Enzymes in Molecular Biology. *Biomolecules*, 3(4), 923–942. <https://doi.org/10.3390/biom3040923>
- Patel, R. P., Patel, M. P., & Suthar, A. M. (2009). Spray drying technology: an overview. *Indian Journal of Science and Technology*, 2(10), 44–47.
- Prajapati, V. D., Jani, G. K., & Kapadia, J. R. (2015). Current knowledge on biodegradable microspheres in drug delivery. *Expert Opinion on Drug Delivery*, 12(8), 1283–1299.
- Rodríguez-Roque, M. J., Rojas-Graü, M. A., Elez-Martínez, P., & Martín-Belloso, O. (2013). Changes in Vitamin C, Phenolic, and Carotenoid Profiles Throughout in Vitro Gastrointestinal Digestion of a Blended Fruit Juice. *Journal of Agricultural and Food Chemistry*, 61(8), 1859–1867. <https://doi.org/10.1021/jf3044204>
- Saravanan, M., & Rao, K. P. (2010). Pectin–gelatin and alginate–gelatin complex coacervation for controlled drug delivery: Influence of anionic polysaccharides and drugs being encapsulated on physicochemical properties of microcapsules. *Carbohydrate Polymers*, 80(3), 808–816. <https://doi.org/https://doi.org/10.1016/j.carbpol.2009.12.036>
- Schmitt, C., & Turgeon, S. L. (2011). Protein/polysaccharide complexes and coacervates in food systems. *Advances in Colloid and Interface Science*, 167(1), 63–70. <https://doi.org/https://doi.org/10.1016/j.cis.2010.10.001>
- Somchue, W., Sermisri, W., Shiowatana, J., & Siripinyanond, A. (2009). Encapsulation of α -tocopherol in protein-based delivery particles. *Food Research International*, 42(8), 909–914. <https://doi.org/https://doi.org/10.1016/j.foodres.2009.04.021>
- Sootitawat, A., Bigeard, F., Yoshii, H., Furuta, T., Ohkawara, M., & Linko, P. (2005). Influence of emulsion and powder size on the stability of encapsulated d-limonene by spray drying. *Innovative Food Science & Emerging Technologies*, 6(1), 107–114. <https://doi.org/https://doi.org/10.1016/j.ifset.2004.09.003>
- Sootitawat, A., Takayama, K., Okamura, K., Muranaka, D., Yoshii, H., Furuta, T., Ohkawara, M., & Linko, P. (2005). Microencapsulation of l-menthol by spray drying and its release characteristics. *Innovative Food Science & Emerging Technologies*, 6(2), 163–170. <https://doi.org/https://doi.org/10.1016/j.ifset.2004.11.007>
- Tang, Y., Scher, H., & Jeoh, T. (2021). *Microencapsulation of chemicals and bioactives by in situ complex coacervation during spray drying*. U.S. Patent Application No. 17/178,866, Publication No. US20210316265A1.
- Tarko, T., Duda-Chodak, A., & Zajac, N. (2013). Digestion and absorption of phenolic compounds assessed by in vitro simulation methods. A review. *Rocz Panstw Zakl Hig*, 64(2), 79–84.
- Timilsena, Y. P., Wang, B., Adhikari, R., & Adhikari, B. (2016). Preparation and characterization of chia seed protein isolate–chia seed gum complex coacervates. *Food Hydrocolloids*, 52, 554–563. <https://doi.org/https://doi.org/10.1016/j.foodhyd.2015.07.033>
- Turgeon, S. L., Schmitt, C., & Sanchez, C. (2007). Protein–polysaccharide complexes and coacervates. *Current Opinion in Colloid & Interface Science*, 12(4), 166–178.

- <https://doi.org/https://doi.org/10.1016/j.cocis.2007.07.007>
- Usha, R., & Ramasami, T. (2004). The effects of urea and n-propanol on collagen denaturation: using DSC, circular dichroism and viscosity. *Thermochimica Acta*, 409(2), 201–206. [https://doi.org/https://doi.org/10.1016/S0040-6031\(03\)00335-6](https://doi.org/https://doi.org/10.1016/S0040-6031(03)00335-6)
- Virost, M., Tomao, V., Ginies, C., & Chemat, F. (2008). Total Lipid Extraction of Food Using d-Limonene as an Alternative to n-Hexane. *Chromatographia*, 68(3), 311–313. <https://doi.org/10.1365/s10337-008-0696-1>
- Wang, X., Lee, J., Wang, Y.-W., & Huang, Q. (2007). Composition and Rheological Properties of β -Lactoglobulin/Pectin Coacervates: Effects of Salt Concentration and Initial Protein/Polysaccharide Ratio. *Biomacromolecules*, 8(3), 992–997. <https://doi.org/10.1021/bm060902d>
- Wei, B., He, L., Wang, X., Yan, G. Q., Wang, J., & Tang, R. (2017). Bromelain-decorated hybrid nanoparticles based on lactobionic acid-conjugated chitosan for in vitro anti-tumor study. *Journal of Biomaterials Applications*, 32(2), 206–218.
- Weinbreck, F., de Vries, R., Schrooyen, P., & de Kruif, C. G. (2003). Complex Coacervation of Whey Proteins and Gum Arabic. *Biomacromolecules*, 4(2), 293–303. <https://doi.org/10.1021/bm025667n>
- Xiao, Z., Liu, W., Zhu, G., Zhou, R., & Niu, Y. (2014). A review of the preparation and application of flavour and essential oils microcapsules based on complex coacervation technology. *Journal of the Science of Food and Agriculture*, 94(8), 1482–1494. <https://doi.org/doi:10.1002/jsfa.6491>
- Yan, C., & Zhang, W. (2014). Chapter 12 - Coacervation Processes. In *Microencapsulation in the Food Industry* (pp. 125–137). Academic Press. <http://www.sciencedirect.com/science/article/pii/B9780124045682000121>
- Yang, Y., Anvari, M., Pan, C.-H., & Chung, D. (2012). Characterisation of interactions between fish gelatin and gum arabic in aqueous solutions. *Food Chemistry*, 135(2), 555–561. <https://doi.org/https://doi.org/10.1016/j.foodchem.2012.05.018>
- Yang, Z., Peng, Z., Li, J., Li, S., Kong, L., Li, P., & Wang, Q. (2014). Development and evaluation of novel flavour microcapsules containing vanilla oil using complex coacervation approach. *Food Chemistry*, 145, 272–277. <https://doi.org/https://doi.org/10.1016/j.foodchem.2013.08.074>
- Yeo, Y., Bellas, E., Firestone, W., Langer, R., & Kohane, D. S. (2005). Complex Coacervates for Thermally Sensitive Controlled Release of Flavor Compounds. *Journal of Agricultural and Food Chemistry*, 53(19), 7518–7525. <https://doi.org/10.1021/jf0507947>
- Zhang, W., Huang, Y., Wang, W., Huang, C., Wang, Y., Yu, Z., & Zhang, H. (2010). Influence of pH of Gelatin Solution on Cycle Performance of the Sulfur Cathode. *Journal of The Electrochemical Society*, 157(4), A443. <https://doi.org/10.1149/1.3299323>
- Zhou, P., Mulvaney, S. J., & Regenstein, J. M. (2006). Properties of Alaska pollock skin gelatin: a comparison with tilapia and pork skin gelatins. *Journal of Food Science*, 71(6), C313–C321.

Chapter 2 Industrially scalable complex coacervation process to microencapsulate food ingredients

Paper published:

Tang, Y., Scher, H., Jeoh, T. 2020. *Industrially scalable complex coacervation process to microencapsulate food ingredients. Innovative Food Science and Emerging Technologies, Innovative Food Science & Emerging Technologies, 59, 102257.*

This chapter serves as a proof of concept of the CoCo process.

2.1 Abstract

Microencapsulation by conventional complex coacervation, though highly effective and achievable at the bench-scale, is challenging to scale-up because of the complexity of the process. A novel, industrially-scalable microencapsulation process by *in situ* complex coacervation during spray drying (the ‘CoCo process’) is introduced, where the multiple steps are collapsed into one, to form dry complex coacervate microcapsules by spray drying. The CoCo process was used to encapsulate D-limonene in complex coacervated (CoCo) microcapsules using alginate and gelatin as wall materials. Insoluble CoCo particles were produced without chemical cross-linking, with extents of complex coacervation of $75 \pm 6 \%$ and $64 \pm 6 \%$ for CoCo particles with and without d-limonene, respectively, where the extent of complex coacervation was to assess the extent to which all polymers within the particles participate in complex coacervation. Up to 82.7 % of D-limonene was retained during spray drying; moreover, the CoCo matrix exhibited excellent barrier properties, retaining up to 80.0 % of total D-limonene over 72-day storage in sealed vials at room temperature.

2.2 Industrial relevance

Commercialization of microencapsulation of bioactives by complex coacervation in agricultural and food applications is hindered by the high-cost and time-intensive multistep process

consisting of emulsification, coacervation, shell hardening and drying. In this work, I overcome these limitations by developing an industrially scalable in situ complex coacervation process during spray drying ('CoCo process'). One-step complex coacervation during spray-drying opens the door to cost-effective, high-throughput, high-volume production of bioactive-containing microcapsules. The protective matrix microcapsules formed by this novel process stabilize and protect the bioactive, while allowing controlled release of the cargo for various applications in food industry and many other industries.

2.3 Introduction

Microencapsulation is attractive in many industries such as food, pharmaceutical, cosmetics, agriculture and functional materials. Complex coacervation, a particularly promising microencapsulation system, is a phase separation process where an immiscible phase is produced mainly through electrostatic interactions between two oppositely charged polymers (Warnakulasuriya & Nickerson, 2018; Yan & Zhang, 2014). Microencapsulation by complex coacervation enables high payloads achievable and controlled release possibilities, making it very attractive in many industries (Eratte et al., 2018; Gouin, 2004). However, potential commercial application of the conventional process is limited by the multiple steps and high cost (Lemetter et al., 2009; Timilsena et al., 2019) Moreover, a crosslinking step using toxic agents such as formaldehyde or glutaraldehyde, non-toxic natural cross linker such as genipin or enzymatic cross linker such as transglutaminase requires precise adjustment of pH and/or temperature and typically takes hours to complete (da Silva et al., 2019; Dong et al., 2011; Saravanan & Rao, 2010; Yang et al., 2014).

Complex coacervation is particularly suited to encapsulate volatile oils as the coacervates effectively trap the oil emulsion to minimize volatile losses (Eghbal & Choudhary, 2018). In one example, peppermint oil was encapsulated by conventional complex coacervation with gelatin and gum Arabic (Dong et al., 2011). The encapsulation process required sequential steps including emulsification of the peppermint oil in a gelatin solution, combining with the gum Arabic solution, pH adjustment using acetic acid to induce complex coacervation, enzymatic cross-linking with transglutaminase to harden the microcapsule wall, and finally, spray drying of the mixture to obtain dry complex coacervates microcapsules. In another example, whey protein and gum arabic were used to encapsulate orange essential oil. Here again, the complex coacervation suspension was formed first and then spray dried to obtain complex coacervated microcapsules (Rojas-Moreno et al., 2018).

Although effective in achieving high payload and control the release of the cargo, the conventional multistep process of microencapsulation of volatile oils in complex coacervation microcapsules remains an obstacle for commercialization. To overcome this barrier, I developed a process that enables in situ complex coacervation during spray drying (Tang et al., 2021). In this process, the feed emulsion is prepared with two negatively charged matrix polymers and a volatile base. Atomization of the feed volatilizes the base, lowering the pH to below the isoelectric point of one of the polymers to allow complex coacervation between the oppositely charged polymers. Concurrent rapid moisture removal enhances associations between the polymers to form dry complex coacervation microcapsules that are collected at the outlet of the spray dryer. This novel process microencapsulates emulsions in complex coacervation microcapsules by a low-cost, industrially-scalable spray drying process in one step without the use of a crosslinking agent (**Figure 2–1**). Spray drying is the most common and cheapest way to produce microencapsulated

food products at industrial scales (Gharsallaoui et al., 2007; Jacobs, 2014; Sosnik & Seremeta, 2015).

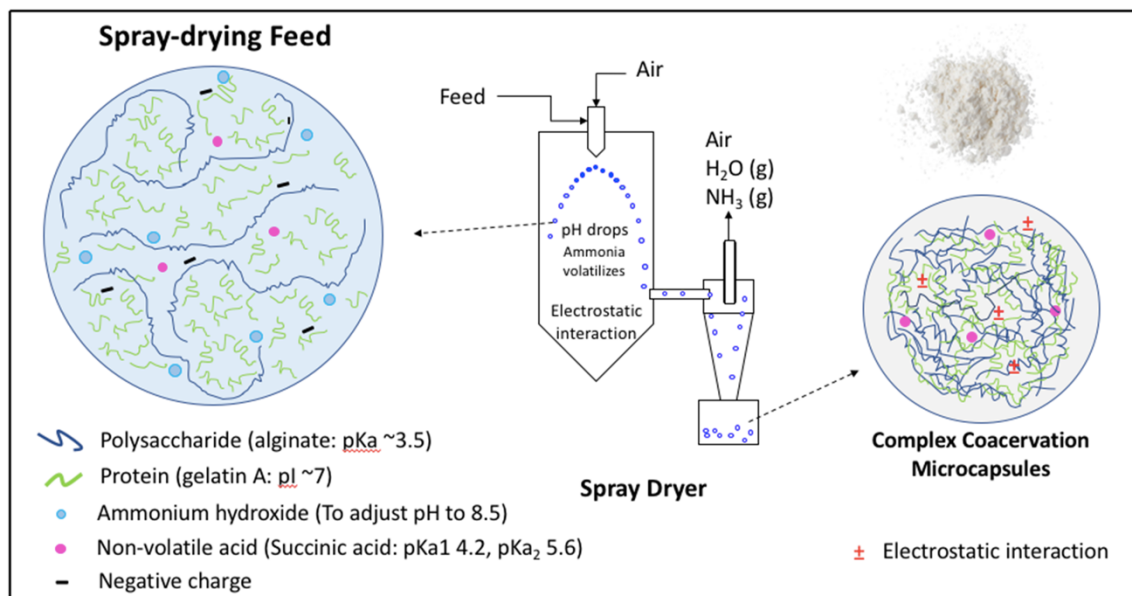


Figure 2–1. Schematic representation of the in situ complex coacervation during spray drying process (the ‘CoCo process’).

The objective of this study was to investigate the potential of this novel, industrially-scalable complex coacervation process (herein referred to as the ‘CoCo process’, **Figure 2–1**) to microencapsulate bioactive compounds. I demonstrate and characterize CoCo microparticles formed by spray drying using a widely used combination of protein and polysaccharide, gelatin and alginate, as matrix polymers. Alginate and gelatin are commonly used in various food products. A linear polysaccharide derived from algae cell wall, alginate is a good microencapsulation material in food systems due to its biocompatibility, biodegradability and nontoxicity (de Oliveira et al., 2014). Alginate is composed of alternating blocks of 1–4 linked α -L-guluronic and β -D-mannuronic acid residues (Gombotz & Wee, 2012). The charge density of this linear chain polymer makes it a very promising matrix building polymer. Gelatin is obtained from the

hydrolysis of collagen extracted from skin, white connective tissue, and bones of animals and it is a popular ingredient in food (Haug & Draget, 2011; Liu et al., 2008; Meng & Cloutier, 2014; Zhou et al., 2006). Gelatin has very good film-forming properties during spray drying which facilitates the rapid formation of a dense film to provide good protection of the core ingredient (Matsuno & Adachi, 1993). I further demonstrated the potential of the CoCo process to encapsulate D-limonene, a volatile oil. D-limonene is a monocyclic monoterpene with a pleasant citrus-like smell and many bioactivities such as antifungal, bacteriostatic and bactericidal properties, making it appealing in many industries (Ciriminna et al., 2014; Espina et al., 2013). Microencapsulation can facilitate broad application of D-limonene by preventing volatile loss and degradation during processing and storage and by enabling controlled release of the oil.

2.4 Materials and methods

2.4.1 Materials

Gelatin (type A, G6144) with isoelectric point (pI) equal to 7, D-limonene, anthrone, sulfuric acid (95-98%) and hexane were purchased from Millipore Sigma. High viscosity sodium alginate (GRINDSTED Alginate FD 155 with a pKa of 3.5) was from Dupont Nutrition and Health. Succinic acid, ammonium hydroxide, sodium hydroxide and isopropanol were purchased from Fisher Scientific. The Bio-Rad protein assay reagent containing Coomassie® Brilliant Blue G-250 dye, phosphoric acid and methanol was purchased from Bio-Rad. Carbon tape and microscopy stands were purchased from Ted Pella. Anti-foam reagent was purchased from Spectrum Chemicals Mfg Corp.

2.4.2 Methods

2.4.2.1 Formation of CoCo microcapsules during spray drying

The spray drying feed to form CoCo powders was prepared as follows: a solution with 2.5% (w/w) gelatin, 0.5% (w/w) alginate and 1% (w/w) succinic acid was adjusted to pH 8.5 using either ammonium hydroxide or sodium hydroxide (**Table 2–1**). The feed was spray dried in a Buchi B290 laboratory spray dryer (Buchi, New Castle, DE) at an inlet air temperature at 150 °C, maximum aspirator airflow rate (35 m³/h), 20% of maximum feed peristaltic pump flow rate (6 ml/min), and 40 mm nozzle pressure. The outlet temperature was 87-92 °C during spray drying.

2.4.2.2 Microencapsulation of D-limonene in the CoCo microcapsules by spray drying

D-limonene emulsions (5.71 % (w/w)) were prepared with 5:1 D-limonene to gelatin ratio. Three emulsification processes were examined: 1) coarse emulsification using an Ultra-Turrax T-18 at 12,000 rpm for 2min (IKA Works, Inc., Wilmington, DE) only; 2) coarse emulsification followed by high pressure homogenization at 20 kpsi (BEEi Nano DeBEE 30-4, BEE international, South Easton, MA) with 2 passes and cooling using iced-water; and 3) coarse emulsification followed by high pressure homogenization at 20 kpsi with four passes and cooling using room temperature water.

To form L-CoCo, the emulsion was mixed with a solution containing gelatin, alginate, succinic acid and ammonium hydroxide at pH 8.5. The final target feed composition in the spray drying feed was 2.5% (w/w) gelatin, 0.5% (w/w) alginate, 1.33% (w/w) D-limonene, and 1% (w/w) succinic acid. Ammonium hydroxide was used to adjust the spray drying feed pH to 8.5. The feed was spray dried by a Buchi B290 laboratory spray dryer at an inlet air temperature of 150 °C, maximum aspirator airflow rate (35 m³/h), 20% of maximum feed peristaltic pump flow rate (6 ml/min), and 40 mm nozzle pressure. The outlet temperature was 87-92 °C during spray drying.

Table 2–1. Formulations used in the formation of CoCo particles by spray drying. Means with same subscript letters do not differ statistically by Tukey’s test ($\alpha = 0.05$). Each sample was measured in triplicate.

CoCo Formulation ¹	Feed pH adjusted using	pH of spray-drying feed	Final pH ²	Powder yield (%)	Soluble in water? ³	Extent of Complex Coacervation (%) ⁴
1	NaOH	8.5	6.4	58.3	Yes	0±0 _a
2	NH ₄ OH	8.5	5.1	53.3	Partial	9±2 _a
3	NH ₄ OH and succinic acid	8.5	4.3	70.1	No	64±6 _b
L-CoCo ⁵	NH ₄ OH and succinic acid	8.5	4.3	61.8	No	75±6 _b

¹All the formulations contained the same concentrations of gelatin and alginate.

²Final pH of the sample after spray-drying was determined by measuring the pH of the water into which the powders were suspended. Water alone had a pH of 6.

³Solubility by visual inspection after suspending in water.

⁴Eq. 2–1.

⁵L-CoCo: D-limonene loaded complex coacervated microcapsules (CoCo microcapsules containing D-limonene as cargo).

2.4.2.3 Determination of the extent of complex coacervation

The ‘Extent of Complex Coacervation’, a metric to assess the extent to which all polymers within the particles participate in complex coacervation, was defined as the fraction of polymers that do not solubilize from the CoCo particles when the spray dried powders are suspended in water. Eq. 2–1 was used to calculate ECC:

$$\text{Extent of complex coacervation}(\%)=1-\frac{\text{Soluble gelatin+Soluble alginates (g)}}{\text{Total polymers in the spray dried powders (g)}} \times 100\%$$

To measure the extent of complex coacervation, 1% (w/v) of the spray-dried powder was dispersed in water with continuous agitation for 30 min, then incubated at 45 °C in a water bath for 10 min to facilitate the dissolution of gelatin and alginate. The pH of the suspension was measured when cooled to room temperature, followed by centrifugation at 10,000 g for 2 min. The supernatant was analyzed for dissolved gelatin and alginate. To measure the total amount of gelatin and

alginates in the CoCo particles, 1% (w/v) of the spray-dried powder was dispersed in water, and sodium hydroxide was added to bring the pH to 8.5, where the suspension pH was higher than the pI of gelatin. The suspension was incubated at 45 °C in a water bath with continuous agitation until the powders were fully dissolved. The solution was analyzed for gelatin and alginate concentrations.

2.4.2.4 Analysis of soluble gelatin and alginates

The gelatin concentration in the supernatants was measured by the Bio-Rad protein assay (Bio-Rad, Hercules, CA) based on the Bradford dye-binding method following manufacturer recommended protocols for the microplate microassay (Bradford, 1976). Gelatin was used to make the standard curve in the range of 8-30 µg/ml. The supernatant was diluted 300-fold in water prior to pipetting into the 96-well microplate. The interference of sodium hydroxide was corrected by adding known concentrations of sodium hydroxide to the gelatin standards.

The alginate concentration in the supernatants was determined using the Anthrone assay (Haldar et al., 2017). The reaction consists of heating the samples with the Anthrone reagent and concentrated sulfuric acid at 100 °C to generate a blue-green color. The supernatant was diluted 10-fold in water prior to the measurement. Alginate standard curves were prepared in the range of 0.01-0.2 mg/ml. The interference of gelatin was corrected by adding known concentrations of gelatin to the alginate standards.

2.4.2.5 Analysis of particle size distribution

The particle size distribution of the spray dried powders was measured at room temperature (25 °C) using propan-2-ol as a dispersant to prevent swelling. Measurements were conducted using a Mastersizer 3000 (Malvern Instrument, Westborough, MA) with the following parameters:

material refractive and absorption indices of 1.57 and 0.01, respectively, and propan-2-ol dispersant refractive index of 1.39 (Strobel et al., 2016). Each sample was measured in triplicate.

The D-limonene emulsion droplet size before spray drying was also measured in the Mastersizer at 25 °C using a D-limonene refractive index of 1.47 and water dispersant refractive index of 1.33. The emulsion was diluted 50-fold in water prior to the measurement. Each sample was measured in triplicate.

2.4.2.6 Morphological characterization by scanning electron microscopy (SEM)

Spray dried complex coacervate powders were mounted on double-sided carbon tape and coated with 15 nm gold using a Cressington 108 Auto Coating System (Watford, UK). The SEM images were produced by a Hitachi S-4100 FE- SEM with an electron beam acceleration voltage of 5 kV.

2.4.2.7 Measurement of volatile retention of D-limonene in complex coacervation microcapsules

The effectiveness of the microencapsulation process was evaluated by determining the volatile retention of D-limonene during spray drying. Volatile retention was calculated as follows (Jafari et al., 2007a):

$$\text{Eq. 2-2: Volatile retention (VR) (\%)} = \frac{\text{total D-limonene in the microcapsules (g)}}{\text{D-limonene in spray dryer feed (g)}} \times 100\%$$

where total D-limonene in the microcapsules is the sum of encapsulated D-limonene and surface D-limonene, and D-limonene that enters spray dryer is the D-limonene content in the spray drying feed. The weight fraction of surface D-limonene is defined as the ratio of D-limonene on the surface of powders to the spray dried powders.

To measure the surface D-limonene content, the spray-dried powder was added to hexane to a final concentration of 1% and rotated at 20 rpm for 0.5 h. Following centrifugation at 8,000 g for 5 min, the supernatant was sampled and measured by gas chromatography (GC). To measure D-limonene content in the emulsions, 10 ml isopropanol, 10 ml hexane and 5 g water were added to 5 g of the emulsion and rotated at 20 rpm for 2 h at room temperature. The mixture was allowed to sit still for 5-10 min for separation. The upper layer was separated into a clean tube and centrifuged at 15,000 g for 2 min. The supernatant was sampled and analyzed by GC. To measure the total D-limonene content of the microcapsules, spray-dried powders were dispersed in water to a final concentration of 1%, and sodium hydroxide was added to raise the pH of the suspension to above the pI of gelatin. The suspension was continuously agitated in a 45 °C in a water bath until the powders were fully dissolved. Isopropanol (10 mL) and hexane (10 mL) were added, followed by 2 h incubation at room temperature with rotation at 20 rpm. The mixture was allowed to sit still for 5-10 min to separate. The upper layer was separated into a clean tube and centrifuged at 15,000 g for 2 min. The supernatant was sampled and analyzed by GC.

The hexane phase containing D-limonene was analyzed by GC (Shimadzu 2010) with flame ionization detection equipped with a DB-FFAP column (30 m x 0.32 mm ID, film thickness 0.25 μ m). The injector and detector temperatures of the GC were set at 250 °C and 260 °C, respectively. The temperature program started at 50 °C, held for 1 min, increased to 190 °C at a rate of 20 °C /min, then held for 5 min. Helium was used as the constant carrier gas.

2.4.2.8 Statistical analysis

Data were reported as mean \pm standard deviation. ANOVA and Tukey's post hoc multiple comparison test were used to determine differences among groups. Statistical analysis was

performed using SAS[®] studio (SAS Institute Inc., Cary, NC, USA). P-values less than 0.05 were considered significant.

2.5 Results and discussion

2.5.1 In situ complex coacervation during spray drying (the ‘CoCo process’)

The conventional process of complex coacervation consists of separate steps for emulsification, coacervation, shell hardening and drying. Additionally, crosslinking using toxic agents such as formaldehyde or glutaraldehyde is often necessary to stabilize polymer associations in the shell hardening steps, which is especially incompatible with food systems. In this study, an industrially-scalable, one-step process to encapsulate cargo in dry CoCo particles by spray drying was developed. The ‘CoCo process’ (**Figure 2–1**) is designed to prevent complex coacervation prior to spray drying by maintaining a pH higher than the pKa and pI of the matrix polymers (e.g. pKa of alginate is 3.5 and pI of gelatin is 7). Volatilization of the base upon atomization of the feed in the spray dryer drops the pH, resulting in net negatively charged and net positively charged matrix polymers that associate electrostatically. Further, simultaneous water removal during the drying process enhances polymer-polymer electrostatic interactions to obviate the need for chemical crosslinking. Overall, the CoCo process yields dry, complex coacervates at the spray dryer outlet (**Figure 2–1**). Matrix microcapsules are formed in this process instead of the core-shell microcapsules formed by conventional complex coacervation process.

The CoCo process was demonstrated using alginates (pKa ~ 3.5) and gelatin A (pI ~ 7). Successful complex coacervation during spray drying relies on sufficient decrease in the droplet pH to between the pKa of the alginate and pI of gelatin to induce electrostatic interactions. The role of pH drop during spray drying on the formation of complex coacervates was tested with three

formulations (**Table 2–1**). In the first formulation, a non-volatile base, sodium hydroxide, was used as a control. The second and third formulations used a volatile base, ammonium hydroxide, to lower the pH during spray drying. Succinic acid was added in the third formulation to further lower the pH during spray drying. As a first indication of successful complex coacervation, spray dried powders from the three formulations were suspended in water to visually assess their solubility. The pH of the supernatants from the suspensions are given in **Table 2–1**. As expected, the powder prepared with sodium hydroxide (formulation 1) fully dissolved in water, indicating no complex coacervation in these particles. The powders prepared using the volatile ammonium hydroxide (formulation 2), however, remained partially undissolved in water with a supernatant pH of 5.1. When ammonium hydroxide and succinic acid were combined (formulation 3), the powder remained mostly undissolved with a supernatant pH of 4.3. These results indicate that volatilization of ammonia reduced the pH to facilitate some complex coacervation in the powder; the additional presence of succinic acid enhanced complex coacervation by driving the pH to its pKa of ~ 4, which is about 3 log units below the pI of gelatin.

Powder yield is the ratio of collected powder in collection chamber to the total dry mass of inlet feed as shown in **Table 2–1**. The powder yield was from 53% to 70% using the bench scale spray dryer, while less loss could be expected in industrial scale production.

2.5.2 *The extent of complex coacervation in CoCo particles*

To quantify an ‘extent of complex coacervation’, I measured the extent to which gelatin and alginates remained undissolved from the three formulations suspended in water (**Table 2–1**). The spray-dried powders formulated with sodium hydroxide (formulation 1) had no insoluble gelatin or alginate (**Figure 2–2**), thus confirming visual observations that the powder fully dissolved, and

no complex coacervation was achieved in these particles. The partially soluble powder of formulation 2 prepared with ammonium hydroxide had 6% and 24% undissolved gelatin and alginate, respectively (**Figure 2–2**). Finally, the largely water insoluble powder prepared with ammonium hydroxide + succinic acid (formulation 3) had 72% and 39% undissolved gelatin and alginate, respectively (**Figure 2–2**). The extent of complex coacervation was thus defined as the ratio of the undissolved gelatin and alginate to the amount of total polymer in the spray-dried CoCo samples (Eq. 2–1). By this definition, the extents of complex coacervation were $0 \pm 0 \%$, $9 \pm 2 \%$ and $65 \pm 6 \%$ for CoCo powders formulated with sodium hydroxide, ammonium hydroxide, and ammonium hydroxide + succinic acid, respectively (**Table 2–1**).

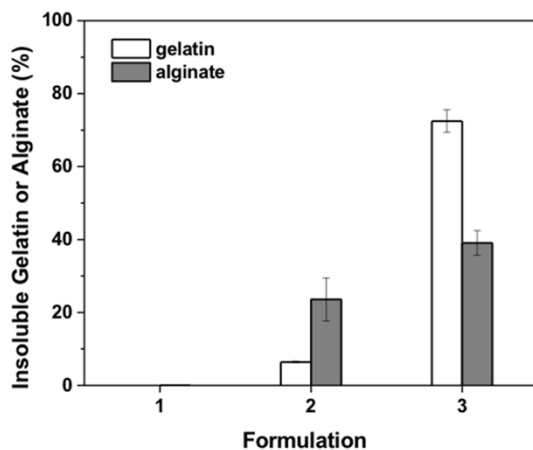


Figure 2–2. Insoluble gelatin or alginate (%) in spray dried powder formed with the formulations in Table 2–1 when suspended in water (Formulation 1: with non-volatile NaOH, Formulation 2: with volatile NH₄OH, Formulation 3: with Succinic acid and volatile NH₄OH; all formulations contained the same ratios of alginate and gelatin as detailed in the methods section).

These results thus demonstrate that the one-step CoCo process successfully forms complex coacervates during spray drying. Further, the extent of complex coacervation can be modulated by the pH during spray drying, which can be controlled by the selection of base and acid in the formulation. Electrostatic interactions, considered to be the dominant interaction for complex

coacervation, is strongly dependent on the charge density of the polymers, which is highly influenced by the pH. Further, pH not only affects charge density but can also induce structural transitions of the polymers (Mekhloufi et al., 2005). Thus, in the CoCo process, the type and concentration of acid in the feed, and the resulting pH of the feed modulated by ammonium hydroxide could affect the protein structure thus the extent of complex coacervation.

2.5.3 Volatile retention of D-limonene in L-CoCo microcapsules during spray-drying and subsequent storage

The efficacy of the CoCo process in encapsulating a volatile cargo was investigated by microencapsulating D-limonene, a volatile oil. An emulsion of D-limonene was microencapsulated in gelatin and alginate using ammonium hydroxide and succinic acid to control the pH during spray drying to form D-limonene-loaded complex coacervation microcapsules (L-CoCo). The spray dryer in-feed was formulated to target 25% dry basis D-limonene loading in L-CoCo; however, approximately 20% of D-limonene was lost during preparation of the feed (**Table 2–2**). Compared to the D-limonene content in the feed, the volatile retention of D-limonene in L-CoCo during spray drying was 82.7 ± 3.6 %, which was comparable to the microencapsulation efficiency of volatile compounds (~73.7% to 88%) by conventional complex coacervation process (de Matos et al., 2018; Ghasemi et al., 2018). As expected, the L-CoCo surfaces had minimal D-limonene (0.24 ± 0.0 %). The extent of complex coacervation in L-CoCo was 75 ± 6 % (**Table 2–1**), which was not significantly different from that of formulation 3. The D-limonene cargo had no significant effect on the extent of complex coacervation (**Table 2–1**).

Industrial spray drying is a continuous process such that the spray dried powders are removed from the collection chamber immediately, with minimal incubation time spent at outlet conditions.

In contrast, in the bench-scale batch spray dryer used in the current study, spray-dried powders remain in the collection chamber at the elevated outlet temperature (87 – 92 °C) for the duration of the batch process. The extended exposure of the L-CoCo powder to the higher outlet temperature may result in greater losses of volatile compounds in the spray dryer. The influence of the amount of time that the L-CoCo powders spent in the collection chamber on volatile retention of D-limonene was investigated by varying the feed volumes (**Table 2–2**). Almost tripling the incubation time of L-CoCo samples in the collection chamber from 12 min to 35 min (L-CoCo and LT-L-CoCo, respectively) did not significantly impact the surface D-limonene content or the volatile retention of D-limonene in the powder. These results indicate that the CoCo matrix served as an effective barrier to protect the volatile cargo during extended exposure to elevated temperatures of 87 – 92 °C.

Table 2–2. Volatile retention of L-CoCo during spray drying and storage. Means with same subscript letters in the same column do not differ statistically by Tukey’s test, where $\alpha=0.05$. Each sample was measured in triplicate.

Sample ID ¹	Emulsion size (μm) ⁷	Time in collection chamber (min)	Shelf storage (days)	D-limonene content \pm SD			
				In Feed (% d.b.)	Powder surface (% d.b.)	Spray-dried powder (% d.b.)	Volatile retention ⁸ (%)
L-CoCo ²	15	12	0	20.4 \pm 0.8	0.2 \pm 0.0 _a	16.9 \pm 0.2 _a	82.7 \pm 3.6 _a
LT-L-CoCo ³	15	35	0	20.4 \pm 0.8	0.2 \pm 0.0 _b	16.2 \pm 0.1 _a	79.4 \pm 3.3 _a
LS-L-CoCo ⁴	15	12	72	20.4 \pm 0.8	0.1 \pm 0.0 _c	16.3 \pm 0.1 _a	80.0 \pm 3.3 _a
LTLS-L-CoCo ^{3,4}	15	35	72	20.4 \pm 0.8	0.1 \pm 0.0 _d	14.3 \pm 0.2 _b	69.9 \pm 4.2 _b
LH-L-CoCo ⁵	69	12	0	20.2 \pm 1.0	0.2 \pm 0.0 _b	14.6 \pm 0.4 _b	72.6 \pm 3.8 _b
U-L-CoCo ⁶	6	12	0	19.4 \pm 1.0	0.1 \pm 0.0 _c	8.3 \pm 0.3 _c	42.5 \pm 2.0 _c

¹All samples use the same formulation as the L-CoCo (baseline) sample.

²L-CoCo sample was prepared by two-stage emulsification – coarse emulsion followed by high-pressure homogenization.

³LT: long time in collection chamber, where the outlet temperature was in the range of 87-92 °C.

⁴LS: long term storage in sealed vial at room temperature.

⁵LH: low level of homogenization. LH-L-CoCo sample was prepared by two-stage emulsification – coarse emulsion followed by low level of homogenization.

⁶U: Ultra-Turrax T-18. U-L-CoCo sample was prepared with coarse emulsion by Ultra-Turrax T-18.

⁷The volume-weighted mean diameter ($D_{4,3}$) of emulsion.

⁸Eq. 2–2. Volatile retention during spray drying does not account for ~20% of D-limonene losses during preparation of the feed.

The L-CoCo powders were stored in sealed vials in a desiccator at room temperature. After 72 days of storage, the retention of D-limonene in the LS-L-CoCo powder saw no significant loss, with the volatile retention at 80.0 ± 3.3 % (**Table 2–2**). Extended incubation at the elevated temperatures in the collection chamber, however, appeared to accelerate loss during storage; a 10% decrease in D-limonene content was observed after 72 days on the shelf of the LT-L-CoCo samples (79.4 ± 3.3 % and 69.9 ± 4.2 % volatile retention for LT-L-CoCo and LTLS-L-CoCo, respectively). Surface D-limonene content decreased by half for all samples during the 72 days of storage. Taken together, the analysis of D-limonene retention in L-CoCo samples demonstrate that the CoCo process creates a matrix of gelatin and alginate that effectively prevents the loss of volatile cargo. The CoCo matrix formed by electrostatic interactions during spray drying provides good protection during extended exposure to elevated temperatures and is effective at retaining volatile cargo during storage.

2.5.4 The influence of the emulsifying process on volatile retention of D-limonene in L-CoCo microcapsules

The D-limonene emulsions for the L-CoCo samples (**Table 2–2**) were prepared by a two-step process starting with coarse emulsification by a disperser, followed by high pressure homogenization. There were significant differences among samples prepared by different emulsification processes in terms of surface oil content and retention of D-limonene, as shown in

Table 2–2. Generally, as the emulsion is subjected to high shear and cavitation during homogenization, emulsions with submicron particle sizes are generated and particle size decreases with increasing number of passes. Lower level of homogenization, achieved by decreasing the number of passes and by cooling with iced water, resulted in an unstable emulsion with larger, agglomerated emulsion droplets (69 μm mean diameter) and decreased volatile retention (\sim - 10% compared to L-CoCo) during spray drying (LH-L-CoCo, **Table 2–2**). Eliminating high-pressure homogenization and only using a single coarse emulsification step resulted in smaller average emulsion size of 6 μm ; however, significantly greater losses were incurred during emulsification and spray drying, resulting in a volatile retention during spray drying of only 42.5 ± 2.0 % and a D-limonene content of only 8.3 ± 0.3 % (U-L-CoCo, **Table 2–2**).

Despite the high volatile retention in the L-CoCo sample, the emulsion was unstable and formed larger aggregated droplets (15 μm , **Table 2–2**). Gelatin could denature during high pressure homogenization; moreover, circulating iced water through the product-cooling heat exchanger could exacerbate the agglomeration of denatured gelatin. In the preparation of the L-CoCo feed, the emulsion is mixed with the solution of containing gelatin, alginate, succinic acid and ammonium hydroxide, which may contribute to stabilizing the emulsion. Sootitawat et al. suggested that larger emulsion size in the spray dryer feed tends to favor the evaporation of flavor (A Sootitawat et al., 2003). They found that the larger emulsion droplets shifted into smaller size after atomization, which indicates that the larger emulsion droplets are sheared into smaller droplets, resulting in loss of volatile compound during spray drying. Moreover, one study reported that small emulsion droplets decrease the number of cargo molecules per droplet and increase the number of surface active compounds, which could slow down oxidation by limiting the initiation

and propagation process (Lethuaut et al., 2002). Studies to further improve the stability of the emulsion and optimize the emulsion size to increase volatile retention is on-going.

2.5.5 Size and morphology of the CoCo microparticles

SEM images of the CoCo samples (**Figure 2–3**) show particles ranging from $\sim 1 \mu\text{m}$ to $20 \mu\text{m}$. The general morphology of the spray dried particles resembles those of cargo-loaded calcium cross-linked alginate microcapsules (CLAMs) prepared by spray drying (Santa-Maria et al., 2012; Strobel et al., 2018, 2019). No evidence of breakage or blow-holes were observed in the particles. Smaller ($\sim 1 \mu\text{m}$) CoCo particles exhibited undulations and indentations, while larger particles had smoother surfaces.

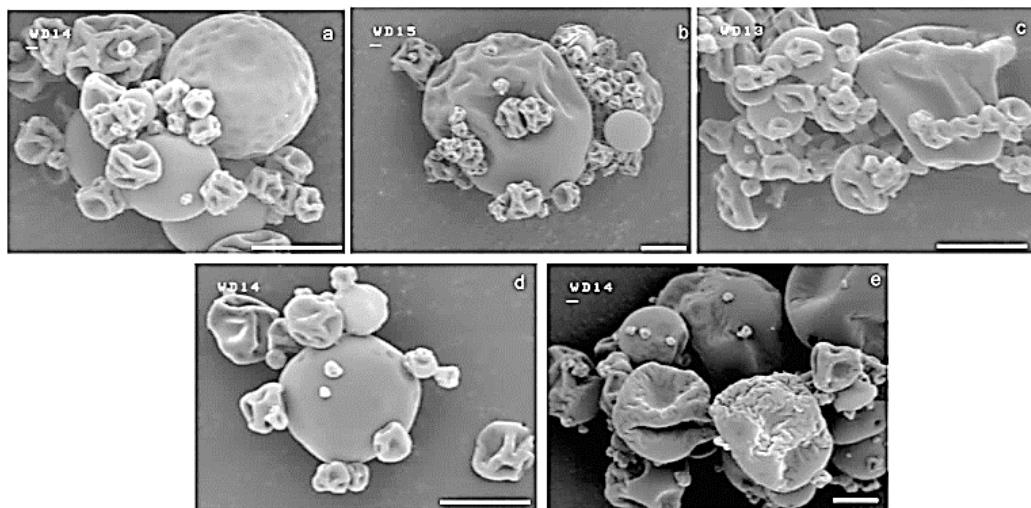


Figure 2–3. SEM images showing the external structures of CoCo particles (a–c) and L-CoCo particles (d,e). (a) Particles formulated with NaOH; (b) particles formulated with NH_4OH ; (c) particles formulated with combination of NH_4OH and succinic acid; (d) L-CoCo particles with high volatile retention; (e) U-L-CoCo particles with low volatile retention. The scale bars represent $5 \mu\text{m}$.

D-limonene loaded CoCo particles with high volatile retention of $82.7 \pm 3.6 \%$ (L-CoCo, **Figure 2–3d**) and lower volatile retention of $42.5 \pm 2.0 \%$ (C-L-CoCo, **Figure 2–3e**) appeared

very similar with few features that distinguish between the two samples. Dents, wrinkles and shrinkages were observed in all the CoCo powders. A mixture of indented and smooth surfaces observed in the spray dried complex coacervation powders is common in spray dried powders as reported in many studies (Jafari et al., 2007a). The morphology of the powder particles is purported to affect the stability of encapsulated flavors. Study showed that the volatile retention of D-limonene in small particles with more surface areas was significantly lower compared to large particles with reduced surface areas (Jafari et al., 2007b). The large CoCo particles in this work had smooth surface with less surface area could also contribute the protection of D-limonene. Soottitantawat et al. also reported that powders formed by HI CAP 100 resulted in smooth surfaces leading to lower release and oxidation rates of the encapsulated flavor compared to powders with grooved surfaces (Apinan Soottitantawat et al., 2005). L-CoCo with high volatile retention had smoother surfaces that may have contributed to preventing the loss of volatiles. Although small particles have more surface area, they experienced a quick formation of membrane to limit the loss.

In agreement with observations from the SEM images, the particle size distribution of spray dried CoCo particles generally exhibited a monomodal size distribution with a peak centered at $\sim 20 \mu\text{m}$ (**Figure 2–4**). The volume-weighted mean diameter ($D_{4,3}$) of CoCo powder formulated with volatile base was $12.9 \pm 0.0 \mu\text{m}$, which was the smallest among all the samples. The $D_{4,3}$, 10th percentile diameter ($D(0.1)$), median diameter ($D(0.5)$), and the 90th percentile diameter ($D(0.9)$) all increased with the addition of non-volatile base or acid. D-limonene loading appeared to influence the particle size distribution. The $D_{4,3}$, $D(0.1)$, $D(0.5)$, and $D(0.9)$ for the L-CoCo sample were $17.9 \pm 0.1 \mu\text{m}$, $7.3 \pm 0.0 \mu\text{m}$, $16.8 \pm 0.0 \mu\text{m}$ and $30.2 \pm 0.1 \mu\text{m}$, respectively. The CoCo process allows high throughput production of microcapsules with narrow distribution of sizes.

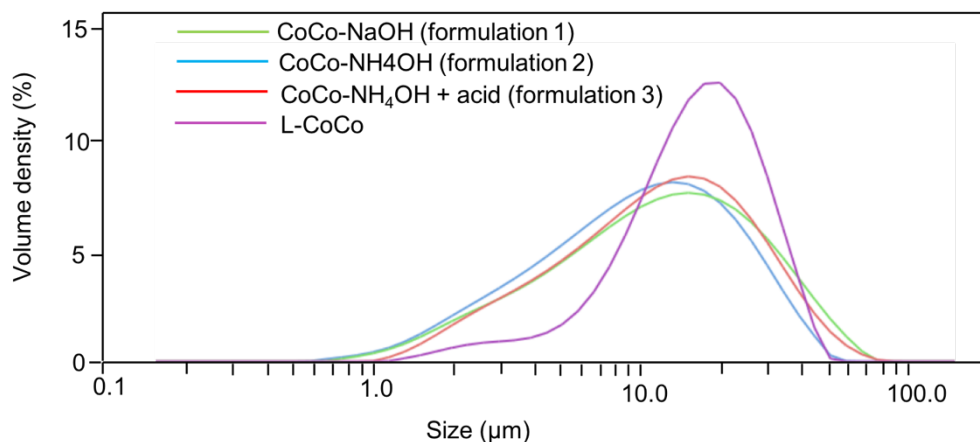


Figure 2–4. Particle size distributions of spray dried CoCo microcapsules measured in isopropanol.

The particles formed by the CoCo process ($< 50 \mu\text{m}$) are sufficiently small to be below sensory threshold, thus facilitating its application in many industries, especially the food and beverage industry. The particle size of complex coacervates formed by conventional processes is not easy to control, as particle agglomeration could happen during the coacervation step and capsules could aggregate during the cooling (shell hardening) step (Lemetter et al., 2009). Xiao et al. summarized the application of conventional complex coacervation processes for encapsulation of flavors and essential oils, showing that particle sizes range from a few microns to hundreds of microns (Xiao et al., 2014). With the formation of complex coacervates during spray drying, this novel CoCo process facilitates scalable production of complex coacervates within optimal size micrometer size ranges.

2.5.6 Opportunities to further optimize and more broadly apply the CoCo process

Besides emulsion size, there are many other factors that may affect the retention of volatile compounds and stability of encapsulated compound. The volatile retention could be further increased by the modification of wall material formulation, the concentration and type of acid in

the formulation, and the spray drying parameters. The pH during spray drying can be modulated to maximize the extent of complex coacervation between polymers that may lead to a tighter matrix to prevent the loss of volatiles. Besides that, the spray drying operation parameters including the inlet air temperature, aspirator airflow rate, feed flow rate and nozzle pressure will also affect the extent of complex coacervation by influencing the ammonia loss during spray drying and residual water level in the microcapsules. The greater the water loss during spray drying, the closer the spacing between the oppositely charged polymer molecules and hence stronger the electrostatic attractive forces. The van der Waals attractive dispersion forces will also come into play as the polymer intermolecular spacing is reduced. Hence the extent of pH lowering and the extent of water loss will determine the insolubility of the complex coacervate polymers (extent of complex coacervation). The hypothesis here is that these forces are strong enough such that a chemical cross linker will not be necessary to achieve complete insolubility.

The CoCo process is not limited to encapsulating volatile compounds but can easily be used to microencapsulate other valuable compounds. As the formation of complex coacervation microcapsules is based on electrostatic interaction between polymers, selection of polymers with an isoelectric point and anionic polymer will generate complex coacervation microcapsules that respond differently under various pH conditions, depending on the pI of protein and the pKa of polysaccharide. The pH-triggered release of the cargo by complex coacervation microencapsulation can be modulated by selection of polymers and pH of the environment, thus bringing numerous benefits to facilitate their applications in different areas. This microencapsulation process can be utilized for the protection and controlled release of bioactives, cells, pesticides, food ingredients and specialty chemicals.

2.6 Conclusions

An industrially scalable microencapsulation process by in situ complex coacervation during spray drying was developed in this work. The novel features of the CoCo process are: (1) consolidation of multiple steps into a single spray drying operation, thereby facilitating industrial scalability, (2) formation of insoluble microcapsules with good barrier properties due to electrostatic interactions coupled with intermolecular dispersion forces between polymers in the encapsulation matrix, (3) elimination of the need for chemical cross-linking, thus reducing the potential toxicity and cost of the product, (4) formation of matrix microcapsules instead of core-shell microcapsules typical of conventional complex coacervation, and (5) high throughput production of micron-sized capsules with uniform properties and narrow distribution of sizes. High retention of a volatile cargo was achieved by this novel process and the complex coacervation matrix exhibited good barrier properties to retain the volatile cargo during storage. The CoCo microcapsules formed by this process have the potential to extend the retention of volatile oils in spray dried microcapsules during spray drying and storage, and control the release of cargo for various applications.

2.7 Abbreviations used

CoCo, complex coacervated; pI, isoelectric point.

2.8 References

- Bradford, M. M. (1976). A rapid and sensitive method for the quantitation of microgram quantities of protein utilizing the principle of protein-dye binding. *Analytical Biochemistry*, 72(1), 248–254. [https://doi.org/https://doi.org/10.1016/0003-2697\(76\)90527-3](https://doi.org/https://doi.org/10.1016/0003-2697(76)90527-3)
- Ciriminna, R., Lomeli-Rodriguez, M., Demma Carà, P., Lopez-Sanchez, J. A., & Pagliaro, M. (2014). Limonene: a versatile chemical of the bioeconomy. *Chemical Communications*, 50(97), 15288–15296. <https://doi.org/10.1039/C4CC06147K>
- da Silva, T. M., de Deus, C., de Souza Fonseca, B., Lopes, E. J., Cichoski, A. J., Esmerino, E. A.,

- de Bona da Silva, C., Muller, E. I., Moraes Flores, E. M., & de Menezes, C. R. (2019). The effect of enzymatic crosslinking on the viability of probiotic bacteria (*Lactobacillus acidophilus*) encapsulated by complex coacervation. *Food Research International*, *125*, 108577. <https://doi.org/https://doi.org/10.1016/j.foodres.2019.108577>
- de Matos, E. F., Scopel, B. S., & Dettmer, A. (2018). Citronella essential oil microencapsulation by complex coacervation with leather waste gelatin and sodium alginate. *Journal of Environmental Chemical Engineering*, *6*(2), 1989–1994. <https://doi.org/https://doi.org/10.1016/j.jece.2018.03.002>
- de Oliveira, E. F., Paula, H. C. B., & de Paula, R. C. M. (2014). Alginate/cashew gum nanoparticles for essential oil encapsulation. *Colloids and Surfaces B: Biointerfaces*, *113*, 146–151.
- Dong, Z., Ma, Y., Hayat, K., Jia, C., Xia, S., & Zhang, X. (2011). Morphology and release profile of microcapsules encapsulating peppermint oil by complex coacervation. *Journal of Food Engineering*, *104*(3), 455–460. <https://doi.org/https://doi.org/10.1016/j.jfoodeng.2011.01.011>
- Eghbal, N., & Choudhary, R. (2018). Complex coacervation: Encapsulation and controlled release of active agents in food systems. *LWT*, *90*, 254–264. <https://doi.org/https://doi.org/10.1016/j.lwt.2017.12.036>
- Eratte, D., Dowling, K., Barrow, C. J., & Adhikari, B. (2018). Recent advances in the microencapsulation of omega-3 oil and probiotic bacteria through complex coacervation: A review. *Trends in Food Science & Technology*, *71*, 121–131. <https://doi.org/https://doi.org/10.1016/j.tifs.2017.10.014>
- Espina, L., Gelaw, T. K., de Lamo-Castellví, S., Pagán, R., & García-Gonzalo, D. (2013). Mechanism of Bacterial Inactivation by (+)-Limonene and Its Potential Use in Food Preservation Combined Processes. *PLOS ONE*, *8*(2), e56769. <https://doi.org/10.1371/journal.pone.0056769>
- Gharsallaoui, A., Roudaut, G., Chambin, O., Voilley, A., & Saurel, R. (2007). Applications of spray-drying in microencapsulation of food ingredients: An overview. *Food Research International*, *40*(9), 1107–1121. <https://doi.org/http://dx.doi.org/10.1016/j.foodres.2007.07.004>
- Ghasemi, S., Jafari, S. M., Assadpour, E., & Khomeiri, M. (2018). Nanoencapsulation of d-limonene within nanocarriers produced by pectin-whey protein complexes. *Food Hydrocolloids*, *77*, 152–162. <https://doi.org/https://doi.org/10.1016/j.foodhyd.2017.09.030>
- Gombotz, W. R., & Wee, S. F. (2012). Protein release from alginate matrices. *Advanced Drug Delivery Reviews*, *64*, 194–205. <https://doi.org/https://doi.org/10.1016/j.addr.2012.09.007>
- Gouin, S. (2004). Microencapsulation: industrial appraisal of existing technologies and trends. *Trends in Food Science & Technology*, *15*(7), 330–347. <https://doi.org/https://doi.org/10.1016/j.tifs.2003.10.005>
- Haldar, D., Sen, D., & Gayen, K. (2017). Development of Spectrophotometric Method for the Analysis of Multi-component Carbohydrate Mixture of Different Moieties. *Applied Biochemistry and Biotechnology*, *181*(4), 1416–1434. <https://doi.org/10.1007/s12010-016-2293-3>
- Haug, I. J., & Draget, K. I. (2011). 5 - Gelatin. In *Handbook of Food Proteins* (pp. 92–115). Woodhead Publishing. <https://doi.org/http://dx.doi.org/10.1533/9780857093639.92>
- Jacobs, I. C. (2014). Chapter 5 - Atomization and Spray-Drying Processes. In *Microencapsulation in the Food Industry* (pp. 47–56). Academic Press. <https://doi.org/http://dx.doi.org/10.1016/B978-0-12-404568-2.00005-4>

- Jafari, S. M., He, Y., & Bhandari, B. (2007a). Encapsulation of Nanoparticles of d-Limonene by Spray Drying: Role of Emulsifiers and Emulsifying Techniques. *Drying Technology*, 25(6), 1069–1079. <https://doi.org/10.1080/07373930701396758>
- Jafari, S. M., He, Y., & Bhandari, B. (2007b). Role of Powder Particle Size on the Encapsulation Efficiency of Oils during Spray Drying. *Drying Technology*, 25(6), 1081–1089. <https://doi.org/10.1080/07373930701397343>
- Lemetter, C. Y. G., Meeuse, F. M., & Zuidam, N. J. (2009). Control of the morphology and the size of complex coacervate microcapsules during scale-up. *AIChE Journal*, 55(6), 1487–1496. <https://doi.org/10.1002/aic.11816>
- Lethuaut, L., Métro, F., & Genot, C. (2002). Effect of droplet size on lipid oxidation rates of oil-in-water emulsions stabilized by protein. *Journal of the American Oil Chemists' Society*, 79(5), 425. <https://doi.org/10.1007/s11746-002-0500-z>
- Liu, H. Y., Li, D., & Guo, S. D. (2008). Extraction and properties of gelatin from channel catfish (*Ictalurus punctatus*) skin. *LWT - Food Science and Technology*, 41(3), 414–419. <https://doi.org/http://dx.doi.org/10.1016/j.lwt.2007.03.027>
- Matsuno, R., & Adachi, S. (1993). Lipid encapsulation technology - techniques and applications to food. *Trends in Food Science & Technology*, 4(8), 256–261. [https://doi.org/https://doi.org/10.1016/0924-2244\(93\)90141-V](https://doi.org/https://doi.org/10.1016/0924-2244(93)90141-V)
- Mekhloufi, G., Sanchez, C., Renard, D., Guillemin, S., & Hardy, J. (2005). pH-Induced Structural Transitions during Complexation and Coacervation of β -Lactoglobulin and Acacia Gum. *Langmuir*, 21(1), 386–394. <https://doi.org/10.1021/la0486786>
- Meng, Y., & Cloutier, S. (2014). Chapter 20 - Gelatin and Other Proteins for Microencapsulation. In *Microencapsulation in the Food Industry* (pp. 227–239). Academic Press. <https://doi.org/http://dx.doi.org/10.1016/B978-0-12-404568-2.00020-0>
- Rojas-Moreno, S., Cárdenas-Bailón, F., Osorio-Revilla, G., Gallardo-Velázquez, T., & Proal-Nájera, J. (2018). Effects of complex coacervation-spray drying and conventional spray drying on the quality of microencapsulated orange essential oil. *Journal of Food Measurement and Characterization*, 12(1), 650–660. <https://doi.org/10.1007/s11694-017-9678-z>
- Santa-Maria, M., Scher, H., & Jeoh, T. (2012). Microencapsulation of bioactives in cross-linked alginate matrices by spray drying. *Journal of Microencapsulation*, 29(3), 286–295. <https://doi.org/10.3109/02652048.2011.651494>
- Saravanan, M., & Rao, K. P. (2010). Pectin–gelatin and alginate–gelatin complex coacervation for controlled drug delivery: Influence of anionic polysaccharides and drugs being encapsulated on physicochemical properties of microcapsules. *Carbohydrate Polymers*, 80(3), 808–816. <https://doi.org/https://doi.org/10.1016/j.carbpol.2009.12.036>
- Soottitantawat, A., Yoshii, H., Furuta, T., Ohkawara, M., & Linko, P. (2003). Microencapsulation by Spray Drying: Influence of Emulsion Size on the Retention of Volatile Compounds. *Journal of Food Science*, 68(7), 2256–2262. <https://doi.org/10.1111/j.1365-2621.2003.tb05756.x>
- Soottitantawat, Apinan, Bigeard, F., Yoshii, H., Furuta, T., Ohkawara, M., & Linko, P. (2005). Influence of emulsion and powder size on the stability of encapsulated d-limonene by spray drying. *Innovative Food Science & Emerging Technologies*, 6(1), 107–114. <https://doi.org/https://doi.org/10.1016/j.ifset.2004.09.003>
- Sosnik, A., & Seremeta, K. P. (2015). Advantages and challenges of the spray-drying technology for the production of pure drug particles and drug-loaded polymeric carriers. *Advances in*

- Colloid and Interface Science*, 223, 40–54.
<https://doi.org/https://doi.org/10.1016/j.cis.2015.05.003>
- Strobel, S. A., Allen, K., Roberts, C., Jimenez, D., Scher, H. B., & Jeoh, T. (2018). Industrially-Scalable Microencapsulation of Plant Beneficial Bacteria in Dry Cross-Linked Alginate Matrix. *Industrial Biotechnology*, 14(3), 138–147. <https://doi.org/10.1089/ind.2017.0032>
- Strobel, S. A., Scher, H. B., Nitin, N., & Jeoh, T. (2016). In situ cross-linking of alginate during spray-drying to microencapsulate lipids in powder. *Food Hydrocolloids*, 58, 141–149.
- Strobel, S. A., Scher, H. B., Nitin, N., & Jeoh, T. (2019). Control of physicochemical and cargo release properties of cross-linked alginate microcapsules formed by spray-drying. *Journal of Drug Delivery Science and Technology*, 49, 440–447. <https://doi.org/https://doi.org/10.1016/j.jddst.2018.12.011>
- Tang, Y., Scher, H., & Jeoh, T. (2021). *Microencapsulation of chemicals and bioactives by in situ complex coacervation during spray drying*. U.S. Patent Application No. 17/178,866, Publication No. US20210316265A1.
- Timilsena, Y. P., Akanbi, T. O., Khalid, N., Adhikari, B., & Barrow, C. J. (2019). Complex coacervation: Principles, mechanisms and applications in microencapsulation. *International Journal of Biological Macromolecules*, 121, 1276–1286. <https://doi.org/https://doi.org/10.1016/j.ijbiomac.2018.10.144>
- Warnakulasuriya, S. N., & Nickerson, M. T. (2018). Review on plant protein–polysaccharide complex coacervation, and the functionality and applicability of formed complexes. *Journal of the Science of Food and Agriculture*, 98(15), 5559–5571. <https://doi.org/10.1002/jsfa.9228>
- Xiao, Z., Liu, W., Zhu, G., Zhou, R., & Niu, Y. (2014). A review of the preparation and application of flavour and essential oils microcapsules based on complex coacervation technology. *Journal of the Science of Food and Agriculture*, 94(8), 1482–1494. <https://doi.org/doi:10.1002/jsfa.6491>
- Yan, C., & Zhang, W. (2014). Chapter 12 - Coacervation Processes. In *Microencapsulation in the Food Industry* (pp. 125–137). Academic Press. <http://www.sciencedirect.com/science/article/pii/B9780124045682000121>
- Yang, Z., Peng, Z., Li, J., Li, S., Kong, L., Li, P., & Wang, Q. (2014). Development and evaluation of novel flavour microcapsules containing vanilla oil using complex coacervation approach. *Food Chemistry*, 145, 272–277. <https://doi.org/https://doi.org/10.1016/j.foodchem.2013.08.074>
- Zhou, P., Mulvaney, S. J., & Regenstein, J. M. (2006). Properties of Alaska pollock skin gelatin: a comparison with tilapia and pork skin gelatins. *Journal of Food Science*, 71(6), C313–C321.

Chapter 3 Volatile retention and enteric release of D-limonene by encapsulation in complex coacervated powder formed by spray drying

“Reprinted with permission from [YUTING TANG, HERBERT B. SCHER, AND TINA JEOH. ACS FOOD SCIENCE & TECHNOLOGY 2021, 1(11), 2086-2095]. Copyright [2021] American Chemical Society.”

3.1 Abstract

A novel, industrially scalable spray-drying process to form complex coacervated (CoCo) powders was applied to encapsulate D-limonene. This study investigated how to control the barrier properties of the matrix formed by the novel process to retain D-limonene in the dry powder and to control its release in aqueous media. The matrix was formed by gelatin, alginate and succinic acid to control the pH facilitating electrostatic interactions between the polymers. The CoCo powders formulated with 4% gelatin, 0.5% alginate, either 0.5% or 0.75% succinic acid demonstrated enteric release of D-limonene and minimal D-limonene release in water. The enteric release of CoCo powders correlated with the extent of complex coacervation, indicating dissolution as the primary release mechanism. The CoCo matrix also provided robust protection of the volatile compound during spray drying, where ~78% D-limonene was retained and subsequent 4 months storage at room temperature where only 2-8% D-limonene loss was incurred.

3.2 Introduction

Microencapsulation by complex coacervation offers the possibility of controlled release of high payloads and is thus extensively employed in many industrial sectors such as food, pharmaceutical and agriculture (Gouin, 2004). Commercial applications of complex coacervation, based on electrostatic interactions between two oppositely charged polymers (e.g. proteins and

anionic polysaccharides), is limited by its complicated and high-cost multistep process. The control of polymer interactions remains challenging, often requiring an additional crosslinking step to enhance polymer associations using toxic agents such as formaldehyde or glutaraldehyde, which is incompatible with many consumer-based applications (Dong et al., 2011; Saravanan & Rao, 2010; Z. Yang et al., 2014). In Chapter 2, I established a one-step, industrially scalable microencapsulation process by *in situ* complex coacervation during spray drying (herein referred to as the ‘CoCo process’) to overcome the cost and toxicity barriers for broader applicability of the process (Tang et al., 2020, 2021). This novel CoCo process uses a low-cost and industrially-scalable spray drying unit operation to form complex coacervation microcapsules. In the CoCo process, electrostatic interactions between oppositely charged polysaccharide and protein are induced during spray drying as a volatile base vaporizes and drops the pH in the atomized droplets. Rapid moisture removal during spray drying exert hydrostatic forces within the drying particles to form tight associations between the polymers, eliminating the need for chemical crosslinking. In a single operation, complex coacervated microcapsules are collected as a dry powder at the outlet of the spray dryer. The CoCo process has demonstrated potential to retain volatile cargo during spray drying and subsequent storage (Tang et al., 2020).

Controlling the barrier properties of complex coacervated (CoCo) powder is crucial to its application in various industries. For example, during spray drying and extended shelf storage, high vapor pressure cargo must be protected against volatile losses, and oxygen sensitive cargo must be protected against oxidation. In aqueous environments, the microcapsules must either prevent release and protect the cargo, or otherwise fully release under desired conditions. As a novel process, however, the potential to control the barrier properties of the matrix microcapsules in the dry state and in aqueous media remain unexplored. The barrier properties of the CoCo matrix

rely on complex coacervation driven by electrostatic interactions between oppositely charged polymers. The extent and strength of polymer-polymer interactions depends on many factors (Yan & Zhang, 2014). Polymer properties such as the molecular weight, composition, isoelectric point, acid dissociation constant, charge density and molecular structure directly impact the potential for the two ionic polymers to interact and form complex coacervates (Christophe Schmitt & Turgeon, 2011). For the select pair of polymers, typically a protein and a polysaccharide, the concentration and ratio of the polymers influence the accessibility and extent of physical interactions that facilitate complex coacervation. Solution pH can also be a significant factor influencing charge densities on the polymers and by influencing the molecular structure of the polymers (Mekhloufi et al., 2005; Y. Yang et al., 2012).

The objective of this work was to understand how to control the barrier properties of the microencapsulation matrix formed by the novel CoCo process. I hypothesized that the barrier properties of CoCo powders are related to the extent of the complex coacervation, which can be modulated by varying the formulation. In this study, alginate and gelatin were selected as the polysaccharide and protein pair, and D-limonene, a monocyclic monoterpene bioactive, was selected as the model cargo. The alginate concentration in the formulations was fixed while varying gelatin concentrations to achieve different polymer ratios. The succinic acid concentration in the formulation was also varied as a mean to influence the pH during spray drying. The D-limonene-loaded CoCo powders were assessed for volatile retention during spray drying and extended storage, and retention/release in aqueous media at varying pH.

3.3 *Materials and methods*

3.3.1 *Materials*

D-limonene, gelatin (type A with an isoelectric point of 7), n-hexane, pepsin, pancreatin 8 X USP were purchased from Sigma Aldrich (St. Louis, MO). High viscosity sodium alginate (GRINDSTED Alginate FD 155 with pKa of 3.5 was from Dupont Nutrition and Health (New Century, KS). Succinic acid, ammonium hydroxide, sodium hydroxide, sodium chloride, sulfuric acid (95~98%) and isopropanol were purchased from Fisher Scientific (Fair Lawn, NJ). The Bio-Rad protein assay reagent containing Coomassie® Brilliant Blue G-250 dye, phosphoric acid and methanol was purchased from Bio-Rad (Hercules, CA). Anti-foam reagent was purchased from Spectrum Chemicals Mfg Corp (New Brunswick, NJ). Anthrone was purchased from ACROS ORGANICS (Fair Lawn, NJ).

3.3.2 *Methods*

3.3.2.1 *Formation of CoCo powders*

All CoCo formulations in this study used a fixed concentration of 0.5% (w/w, w.b.) of alginate while varying succinic acid and gelatin concentrations in the spray drying feed (**Table 3–1**).

The spray drying feed with formulations shown in **Table 3–1** was prepared as follows (**Figure 3–1**): a coarse emulsion with a 1.2:1 gelatin to D-limonene ratio (w/w) was prepared by using an Ultra-Turrax T-18 at 12,000 rpm for 2min (IKA Works, Inc., Wilmington, DE) and an anti-foam reagent was used to reduce the foam formed during the mixing. The coarse emulsion was passed three times through a high-pressure homogenizer (BEEi Nano DeBEE 30-4 High Pressure Homogenizer) at 20 kpsi, resulting in a volume-weighted mean diameter ($D_{4,3}$) of D-limonene emulsion in the feed of around 1 μm . A solution of gelatin, alginate and succinic acid was prepared,

and ammonium hydroxide was used to adjust the solution pH to 8.5. Then, the homogenized emulsion was mixed with the solution to form spray drying feed, where ammonium hydroxide was used again to adjust the spray drying feed pH to 8.5. The feed was spray dried by a Buchi B290 laboratory spray dryer. The spray drying conditions were set as follows: inlet air temperature at 150 °C, aspirator airflow rate at maximum (35 m³/h), feed peristaltic pump at 20% of maximum (6 mL/min), and 40 mm nozzle pressure.

Table 3–1. Inlet formulations used in the formation of D-limonene-loaded CoCo microcapsules by spray drying.

Formulation ID ¹	Gelatin concentration (w/w, % w.b.) ¹	Succinic acid concentration (w/w, % w.b.) ¹	Alginate concentration (w/w, % w.b.) ^{1,2}	Target D-limonene loading (w/w, % d.b.) ³	Systematic uncertainty ⁴ $\frac{\sigma_f}{f}$
1G0.5S	1.00	0.50	0.50	25.00	0.56%
2.5G0.5S	2.50	0.50	0.50	25.00	0.32%
4G0.5S	4.00	0.50	0.50	25.00	0.22%
1G0.75S	1.00	0.75	0.50	25.00	0.50%
2.5G0.75S	2.50	0.75	0.50	25.00	0.30%
4G0.75S	4.00	0.75	0.50	25.00	0.21%
1G1S	1.00	1.00	0.50	25.00	0.45%
2.5G1S	2.50	1.00	0.50	25.00	0.28%
4G1S	4.00	1.00	0.50	25.00	0.20%

¹ The formulation ID were coded to indicate the gelatin (G) and succinic acid (S) wet basis loading in the feed. (e.g. 1G0.5S indicates a wet basis loading of 1% w/w gelatin and 0.5% w/w succinic acid).

² The alginate concentration was kept constant at 0.5% (w/w) in all formulations.

³ Target D-limonene loading in the CoCo formulation is reported on a dry basis. The actual D-limonene loading in the microcapsules after spray drying is reported in Figure 3-3b in results.

⁴ For formulation preparation, the source of systematic error for D-limonene loading (f) is the analytical balance. The analytical balances are used and the accuracy specification for analytical balances are ± 0.01 g (for D-limonene weighing) and ± 0.0001 g (for other components weighing). The uncertainty in a scale measuring device (σ) is equal to the smallest increment divided by 2. For propagating uncorrelated uncertainties,

$$\sigma_f^2 = \sum \left(\frac{\partial f}{\partial x_i} \sigma_i \right)^2$$

Systematic error can also come from the operational instrument (spray dryer) used in the sample generation. The temperature control accuracy for spray dryer Buchi B290 is $\pm 3^{\circ}\text{C}$ and the impact is assumed to be negligible. During the experiment, the systematic error has been reduced as much as possible: the spray dryer parameters have been carefully adjusted to the same parameter setting each time; the balance has been calibrated and tared every time.

Although the target D-limonene loading in CoCo microcapsules was 25% (d.b.) (Table 3–1), approximately 6-28% of D-limonene was consistently lost during the emulsification process to prepare the feed (Figure 3–1).

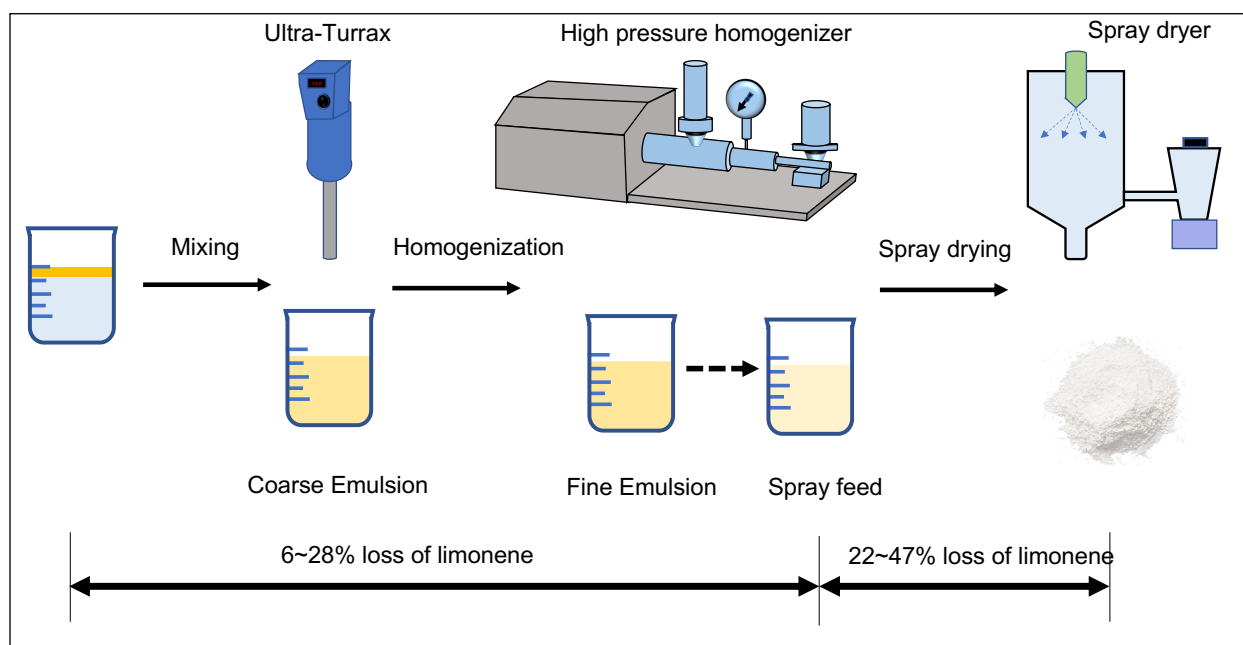


Figure 3–1. A schematic representation of the process to encapsulate D-limonene in complex coacervated (CoCo) powder by spray-drying.

3.3.2.2 Emulsion size and particle size measurement

D-limonene droplet size in the feed and spray dried particle size were measured by Mastersizer 3000 (Malvern Instrument, Westborough, MA) (Strobel et al., 2016). The settings for the analyzer were as follows: material type of D-limonene with refractive index 1.47, dispersant

type of water with dispersant refractive index of 1.33, temperature: 25 °C. Each sample was measured in triplicate.

Spray dried powders were dispersed with sonication in propan-2-ol to prevent swelling. To ensure proper sample dispersion, sonication was used and stopped until volume-weighted mean diameter ($D_{4,3}$) stabilized. The settings for the analyzer were as follows: material type of particle with refractive index 1.57 and absorption index 0.01, dispersant type of propan-2-ol with dispersant refractive index of 1.37, temperature: 25 °C. Each sample was measured in triplicate.

3.3.2.3 Water activity measurement

Water activity of the sample was measured in duplicate by AquaLab® model Series 3 TE (Decagon, Devices, Inc., Pullman, Washington).

3.3.2.4 Measurement of volatile retention of D-limonene in CoCo microcapsules and microencapsulation efficiency

The microencapsulation yield here was expressed as volatile retention -Equation 3-1:

$$\text{Volatile retention (VR) (\%)} = \frac{\text{total D-limonene in the microcapsules (g)}}{\text{D-limonene in spray dryer feed (g)}} \times 100\%$$

Surface D-limonene, D-limonene in emulsion and encapsulated D-limonene in microcapsules were measured to calculate VR.

To measure surface D-limonene, 0.05 g spray-dried powders was added to 10 mL hexane and rotated at 20 rpm for 10min. After that, the extract mixtures were centrifuged at 8000 g for 2 min. The supernatant was sampled and analyzed by gas chromatography (GC).

To measure D-limonene in emulsion, 10 mL isopropanol, 10 mL hexane and 9.5 g water were added to 0.5 g of emulsion. The mixture was rotated at 20 rpm for 2 h at room temperature and

allowed to sit still for 5–10 min to separate. The volume of the top hexane layer containing D-limonene was measured, then sampled and analyzed by GC.

To measure total D-limonene in microcapsules, spray-dried powders were dispersed in water to a final concentration of 1% (w/v) and sodium hydroxide was added to raise the pH of the suspension to above the pI of gelatin. The sample was incubated in 45 °C water bath for 10 min with continuous agitation to facilitate the dissolution of gelatin, after which the sample was rotated end-over-end at 20 rpm until the powders were fully dissolved. Once dissolved, 6 mL isopropanol and 10 mL hexane were added and followed by 1 h rotation at 20 rpm. The extract mixtures were centrifuged at 1000 g for 10 min. The volume of the top hexane layer containing D-limonene was measured, then sampled and analyzed by GC. Each powder sample was extracted in triplicate.

Microencapsulation efficiency was calculated as the ratio of encapsulated D-limonene to the total D-limonene. Encapsulated D-limonene was calculated as the total D-limonene minus the surface D-limonene.

3.3.2.5 Shelf-life study

For measurement of volatile retention of D-limonene during long-term storage, spray dried microcapsules were stored in sealed vials in a desiccator at room temperature. The samples were taken out after 4 months and the retained D-limonene in the microcapsules during storage was measured as described above. Each powder sample was extracted in triplicate.

3.3.2.6 Release of D-limonene in water, simulated gastric and intestinal fluids

The extent to which CoCo powders release D-limonene in distilled water (pH 5.8), simulated gastric fluid (SGF, 8.78 mg/mL sodium chloride at pH 1.8 with pepsin activity of 2000 U/mL

(Swackhamer et al., 2019)) and simulated intestinal fluid (SIF, 50 mM phosphate buffer at pH 7.4 with 9.6 mg/mL pancreatin 8 X USP based on trypsin activity of 100 TAME U/mL) (Strobel et al., 2016) were measured. The powders were dispersed in the respective fluids at 0.5% (w/v) and incubated at 37°C (for samples in SGF and SIF) and room temperature (for samples in water). and rotated end-over-end at 20 rpm. After 2 h incubation, 10 mL of hexane was added and mixed very gently for 30 s before centrifuging at 10,000 g for 5 min. The supernatant was separated and mixed with 6 mL isopropanol. Following a 15 min extraction time, the mixtures were centrifuged at 1,000 g for 10 min. The volume of the top layer containing D-limonene was measured, then sampled and analyzed by GC. Each powder sample was released in triplicate.

3.3.2.7 Gas chromatography (GC) to determine D-limonene contents in extracts

The hexane phase containing D-limonene was analyzed by gas chromatography (Shimadzu 2010) with flame ionization detection equipped with a capillary column (DB-FFAP, 30 m x 0.32 mm ID, film thickness 0.25 µm). The injector temperature of GC was set at 250 °C and the detector was set at 260 °C. The temperature program started at 50 °C, held for 3 min and then increased to 190 °C at a rate of 20 °C /min before holding for 1 min and then increased to 200 °C at a rate of 10 °C /min before holding for 6 min. Helium was used as the carrier gas. Standard curve of D-limonene ranged from 0.0078 mg/mL to 2 mg/mL.

3.3.2.8 Measure the percent of coacervated gelatin and alginate in aqueous media

To assess the extent to which all polymers within the particles participate in complex coacervation, I defined the ‘Extent of Complex Coacervation (ECC)’ metric, i.e. the ratio of the mass of matrix polymers involved in complex coacervation to the total mass of matrix polymers

in spray dried powders (Tang et al., 2020). Coacervated alginate and gelatin in the powders remain insoluble when dispersed in distilled water (pH 5.8) where the pH is lower than the pI of gelatin. The ECC is determined by measuring the fraction of undissolved polymers when spray dried powders are suspended in aqueous media.

Equation 3–2:

$$\text{ECC (\%)} = 1 - \frac{\text{Total Soluble polymers (g)}}{\text{Total polymers in the spray dried powders (g)}} \times 100\%$$

To measure the amount of soluble gelatin and alginate, spray-dried powders were dispersed in water (1% (w/v)) and continuously agitated for 2 h at room temperature and then in a 45 °C water bath for 10 min. The suspension pH was measured when cooled to room temperature. After that, the suspension was centrifuged at 10,000 g for 2 min to obtain the supernatant for further measurement. To measure the amount of total gelatin and alginate, 1% spray-dried powders were dispersed in water with NaOH to bring up the pH to 9. The sample was continuously agitated for 2 h at room temperature and then in a 45 °C water bath. The sample was fully dissolved.

The soluble gelatin concentration in the supernatant and total gelatin concentration were assayed by the Bradford method following manufacturer specified protocols (Bradford, 1976). Soluble alginate concentration in the supernatant and total alginate concentration were assayed by the Anthrone method (DuBois et al., 1956). Each sample was measured in triplicate. The interference of gelatin was corrected after the gelation concentration was determined (C Schmitt et al., 1999).

3.3.2.9 Statistical analysis

Data were reported as mean ± standard deviation. ANOVA and Tukey's post hoc multiple comparison test were used to determine differences among factor levels. Statistical analysis was

performed using JMP (SAS Institute Inc., Cary, NC, USA). P-values less than 0.05 were considered significant.

3.4 Results

3.4.1 D-limonene loaded CoCo powders prepared by spray drying

3.4.1.1 Particle size distribution of D-limonene-loaded CoCo powders

D-limonene loaded complex coacervated (CoCo) powders were prepared by spray drying with varying concentrations of gelatin and succinic acid (**Table 3–1**). The alginate concentration was held constant for all formulations, while gelatin concentration was varied to achieve different polymer ratios, and succinic acid concentration was varied to adjust the pH during spray drying. The hypothesis was that varying polymer ratios and pH would influence the interactions between alginate and gelatin, impacting properties of the CoCo particles.

The D-limonene loaded CoCo powders generally exhibited monomodal size distributions centered between 12 and 16 μm (**Figure 3–2**), in the range of previously reported sizes for microcapsules formed by complex coacervation of a few to hundreds of micrometers (Jun-xia et al., 2011; Leclercq et al., 2009). Powders formed using the lowest gelatin concentration (1% w/w w.b. in the feed) could not be dispersed in isopropanol and thus could not be sized. Higher gelatin concentrations were needed to generate dispersible powder, suggesting one role of gelatin in the formulation is to prevent particle aggregation.

The CoCo powder from formulation 4G0.5S yielded the smallest volume-weighted mean diameter ($D_{4,3}$) of $14.1\pm 0.0\ \mu\text{m}$, with 10th percentile ($D(0.1)$), median ($D(0.5)$), and 90th percentile ($D(0.9)$) diameters of $4.3\pm 0.0\ \mu\text{m}$, $12.0\pm 0.0\ \mu\text{m}$, $26.9\pm 0.0\ \mu\text{m}$, respectively. The CoCo powder with the largest mean diameter $D_{4,3}$ of $18.5\pm 0.3\ \mu\text{m}$ was formed using the 2.5G1S formulation.

Powder formed with 1S tended to have larger D(90). There was no clear trend relating formulation to the particle sizes.

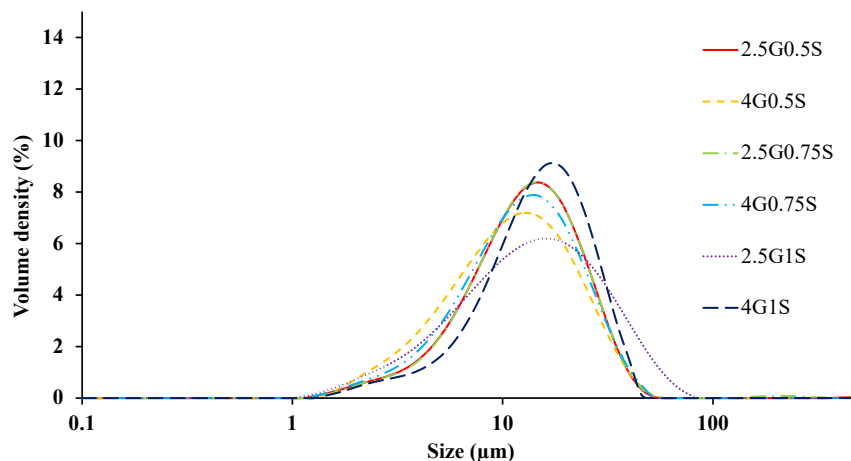


Figure 3–2. Volume weighted particle size distributions of spray dried CoCo powders dispersed in isopropanol. The formulations for the samples are given in Table 3–1.

3.4.1.2 Encapsulation efficiency and water activity of D-limonene-loaded CoCo powders

The CoCo microcapsules had minimal D-limonene on the surfaces (**Table 3–2**). For most of the formulations, the surface D-limonene content of the CoCo powders was 0.1~0.3% (w/w, d.b.) and the microencapsulation efficiencies were up to 97~99%. The surface D-limonene contents in two formulations with 1% gelatin and either 0.75% or 1% succinic acid were significantly higher than the others, indicating that with higher succinic acid concentration, less gelatin could result in more D-limonene on the surface of the microcapsules (1G0.75S and 1G1S) and low microencapsulation efficiency.

At each level of succinic acid in the formulation, increasing gelatin concentrations resulted in higher water activity of the microcapsules (**Table 3–2**). Higher concentration of succinic acid in the formulation was expected to lower the final pH during spray drying resulting in different extent of interaction between gelatin and alginate, but since succinic acid is a weak acid, increasing its

concentration in the feed did not result in big changes in pH. High concentrations of gelatin may act as buffer to prevent the pH drop even with increased amount of succinic acid.

Table 3–2. Surface D-limonene content, water activity and pH of CoCo powders. Means with same letters do not differ statistically by Tukey's test ($\alpha = 0.05$).

Formulation	Surface D-limonene (%)	Microencapsulation efficiency (%)	Surface D-limonene after storage (%) ¹	Water activity	Final pH ²
1G0.5S	0.3±0.1 _b	97.1±0.9 _a	0.3±0.0 _a	0.466±0.002 _{c,d}	4.70
2.5G0.5S	0.3±0.1 _b	98.0±0.6 _a	0.9±0.0 _a	0.509±0.026 _{b,c,d}	4.81
4G0.5S	0.3±0.0 _b	97.9±0.2 _a	0.8±0.3 _a	0.534±0.001 _{b,c,d}	5.03
1G0.75S	1.8±0.7 _a	89.9±3.8 _b	1.6±1.1 _a	0.996±0.002 _a	4.77
2.5G0.75S	0.1±0.1 _b	99.4±0.2 _a	0.2±0.0 _a	0.423±0.015 _d	4.91
4G0.75S	0.2±0.0 _b	99.0±0.2 _a	0.6±0.1 _a	0.675±0.264 _{a,b,c,d}	5.07
1G1S	2.3±0.3 _a	80.4±2.2 _c	0.6±0.0 _a	0.860±0.166 _{a,b,c}	4.41
2.5G1S	0.3±0.0 _b	97.5±0.1 _a	0.5±0.0 _a	0.897±0.070 _{a,b}	4.61
4G1S	0.3±0.0 _b	97.5±0.0 _a	0.5±0.2 _a	0.414±0.040 _d	5.00

¹ The storage condition: the powder was stored in sealed vial and put in desiccator at room temperature for 4 months.

² Final pH of the sample after spray-drying was determined by measuring the pH of the water into which 1% of powders were suspended. Water alone had a pH of 6.

3.4.2 Volatile retention of D-limonene in CoCo microcapsules during spray drying

The volatile retention of D-limonene in the various CoCo formulations during spray drying was assessed on the dry basis D-limonene content in the feed (**Figure 3–1**). Up to ~78% of D-limonene was retained during spray drying in most of the formulations (**Figure 3–3a**). This result was comparable to the microencapsulation efficiency of volatile components (~74% to 88%) by conventional complex coacervation and our previous work (de Matos et al., 2018; Ghasemi et al., 2018; Tang et al., 2020). Succinic acid concentration in the feed played an important role in retaining the volatile compound during spray drying, while the influence of gelatin concentration

on volatile retention of D-limonene during spray drying depended on the succinic acid content in the feed. With 0.75% (w/w) succinic acid in the feed, the gelatin concentration did not significantly impact volatile retention of D-limonene in the CoCo powders (**Figure 3–3a**). At 0.5% (w/w) succinic acid in the feed, higher concentrations of gelatin helped in retaining more D-limonene; however, the opposite trend was observed with 1% (w/w) succinic acid in the feed. Although 25% (d.b.) D-limonene loading in CoCo microcapsules was targeted (**Table 3–1**), losses during emulsification (6~28%, **Figure 3–1**) and spray drying yielded maximum D-limonene loadings of $17.5 \pm 1.5\%$ (d.b.) with 7% loss during the feed preparation (**Figure 3–3b**). On industrial scale production, the loss of D-limonene in preparation could be similar to that on the bench scale and more iteration work on reducing the loss of D-limonene in preparation should be done to make the production more economically viable.

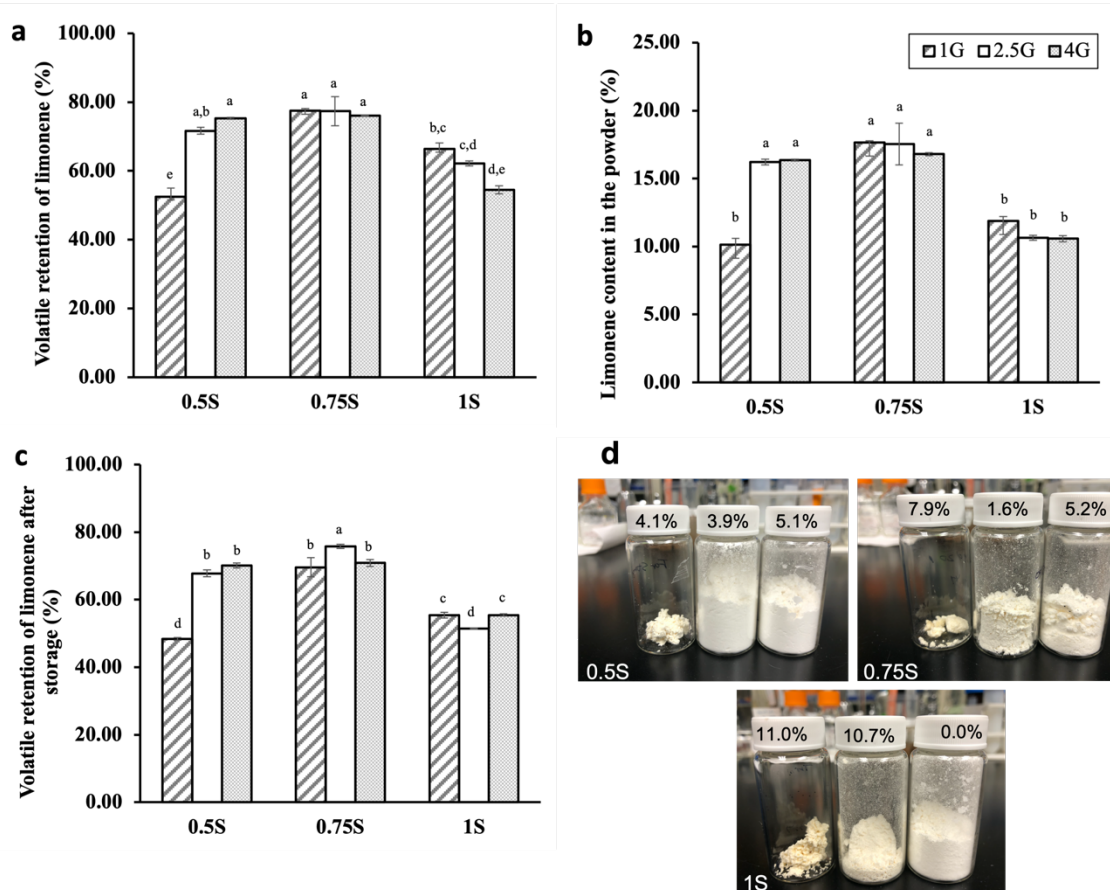


Figure 3–3. a: Volatile retention of D-limonene in CoCo microcapsules after spray drying; b: D-limonene content in CoCo microcapsules formed by spray drying using formulations; c: Volatile retention of D-limonene in CoCo microcapsule after 4 months storage; d: The D-limonene loaded CoCo powders stored in sealed vials after 4 months. At each level of succinic acid, the powder in vial from left to right was generated from formulation with gelatin concentration of 1%, 2.5% and 4% respectively. Each vial is labeled with percent of D-limonene loss after 4 months storage. Means with same letters do not differ statistically by Tukey's test ($\alpha = 0.05$).

3.4.3 Volatile retention of D-limonene in CoCo microcapsules during storage

The CoCo powders containing D-limonene were stored in sealed vials in a desiccator at room temperature for 4 months (**Figure 3–3c,d**). The D-limonene loss ranged from 0 to 11%, indicating that the matrix formed by spray drying was able to protect the volatile cargo during storage. Formulation 1G01S and 2.5G1S were the two formulations with the highest losses of 11.0% and 10.7%, respectively. A visual assessment revealed that powders with the lowest concentrations of

gelatin (1G0.5S, 1G0.75S, and 1G1S) caked and yellowed during storage (**Figure 3–3d**), suggesting that for formulations with high succinic acid concentration, a concurrent increase in gelatin improves powder quality.

3.4.4 The potential for enteric release of D-limonene from CoCo powders

The complex coacervated matrix can serve as a diffusion barrier in water to prevent leakage and provide protection of the cargo in aqueous environments. The extent to which the CoCo matrices could retain D-limonene in water, SGF and SIF was investigated.

The CoCo powders were generally effective at retaining D-limonene in water, with some composition-dependent variations (**Figure 3–4a**). Less D-limonene was released with higher concentrations of gelatin regardless of succinic acid content. Specifically, 7.2~11.7% of the loaded D-limonene was released from CoCo powders formed with 4% (w/w) gelatin, while 14.3~21.1% of the loaded D-limonene was released from powders formulated with 2.5% (w/w) gelatin. The D-limonene released from powders formulated with 1% (w/w) gelatin varied between 14.4~42.1%. Gelatin concentration in the formulation was the key factor affecting the release of D-limonene in water, with higher gelatin content resulting in less D-limonene release.

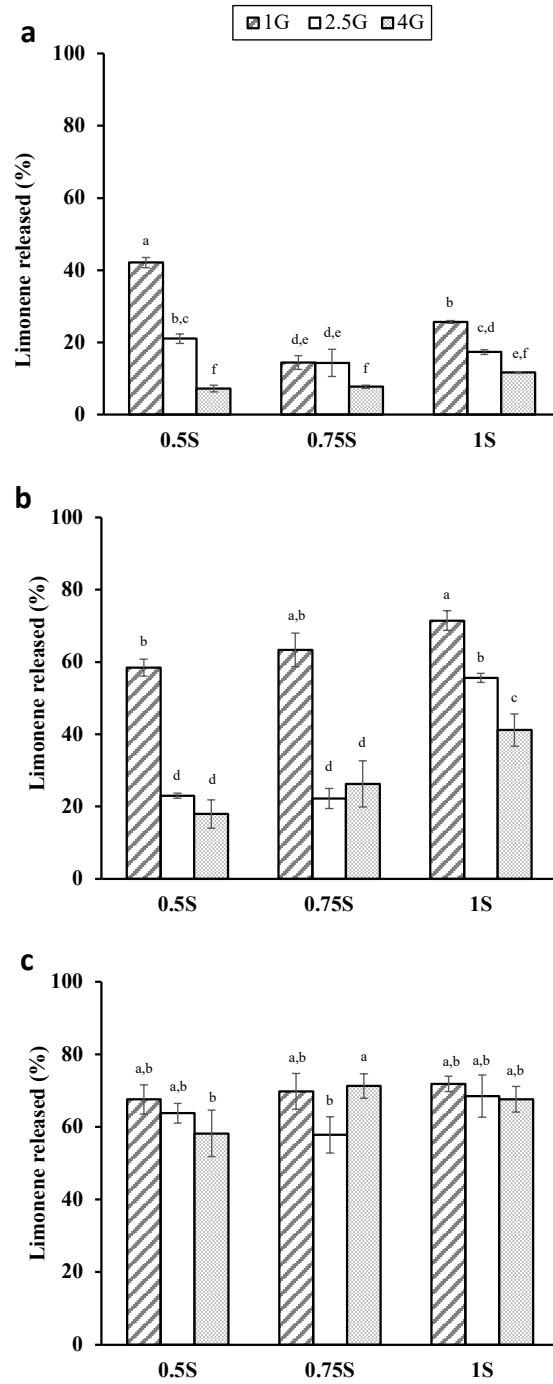


Figure 3–4. Release of D-limonene from CoCo microcapsules after 2 h. D-limonene release in water (pH 5.8, room temperature) (a), SGF (pH 1.8, 37 °C) (b) and SIF (pH 7.4, 37 °C) (c) was assessed by dispersing powders in each fluid and incubating with end-over-end rotation for 2 h. Means with same letters do not differ statistically by Tukey's test ($\alpha = 0.05$).

The CoCo powders released D-limonene in SGF more readily than in water, releasing between 18.0-71.4% in 2 hours (**Figure 3–4b**). Similar to the release of D-limonene in water, at each level of succinic acid, less D-limonene was released as the concentration of gelatin increased. Powders with the highest concentration of succinic acid (1%) was least effective at retaining D-limonene in SGF, releasing 41.7-71.4% regardless of gelatin content. The lowest D-limonene release in SGF of 18.0~26.3% were achieved by powders formed with low and medium succinic acid concentration (0.5 and 0.75%) and medium and high gelatin concentration (2.5% and 4%) (2.5G0.5S, 4G0.5S, 2.5G0.75S and 4G0.75S).

In SIF, up to 57.8~71.8% of D-limonene was released from the CoCo powders for all the formulations (**Figure 3–4c**). The higher pH is expected to disrupt the interactions between alginate and gelatin to dissolve the powders and facilitate release of the encapsulated D-limonene. However, some D-limonene remained unreleased after 2h incubation, possibly due to incomplete dissociation of the matrix.

3.4.5 The ECC as a measure of barrier properties

The ECC, i.e. the fraction of coacervated gelatin and alginate forming the particle matrix (Equation 3–2) that remain insoluble in water, is expected to impact the retention of D-limonene in the CoCo powders. In the formulations examined in this study, the ECC is driven by the retention of gelatin in the powders (**Figure 3–5**). Formulations with 0.5% succinic acid resulted in very high portions (up to 73%~84%) of undissolved (coacervated) gelatin (**Figure 3–5a**) but very low portions (7%~14%) of undissolved (coacervated) alginate (**Figure 3–5b**). Up to 21%~37% of coacervated alginate was formed in the formulations with 0.75% succinic acid, but the portion of coacervated gelatin decreased to 37~68%. The formulations with 1% succinic acid also resulted in

high portions of coacervated gelatin (60%~96%) and moderate levels of coacervated alginate (13%~28%). Overall, increasing the gelatin to alginate ratio increased both the ratio of coacervated gelatin and coacervated alginate, and higher gelatin concentration in the formulation resulted in higher ECC (Figure 3–5c).

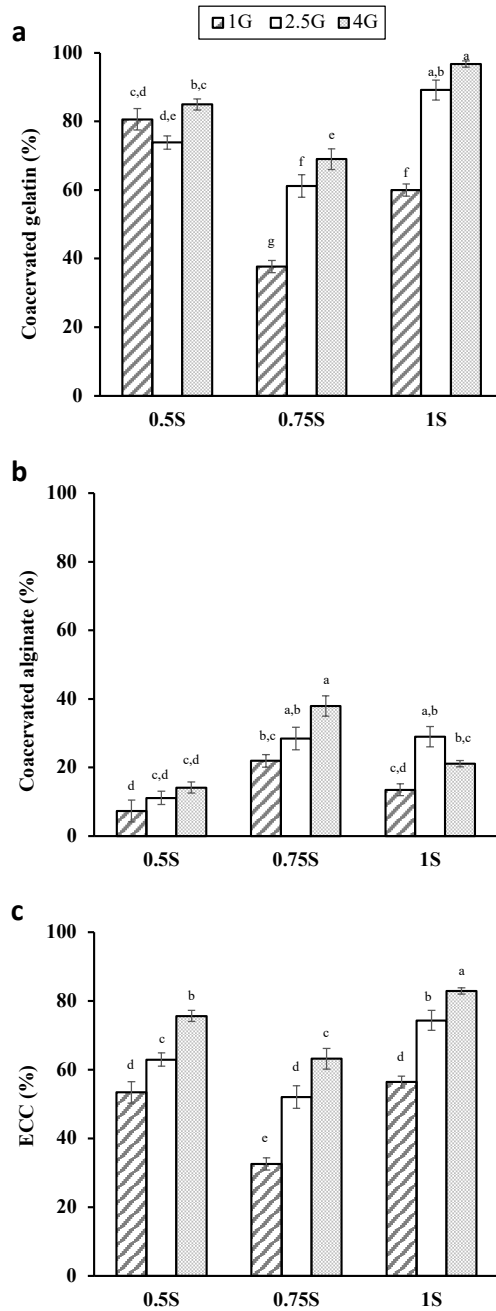


Figure 3–5. a: Coacervated gelatin; b: coacervated alginate; and c: the ECC in CoCo powders. Means with same letters do not differ statistically by Tukey's test ($\alpha = 0.05$).

There was a correlation between the release of D-limonene in water and SGF, and the ECC (Figure 3–6). In general, higher extents of complex coacervation resulted in less release of D-limonene in water and SGF from the CoCo microcapsules (Figure 3–6). However, at different succinic acid levels, the ECC needed to achieve certain level of release differed. Increasing succinic acid levels in the feed formulation from 0.5 to 0.75% improved D-limonene retention, but at lower ECC. Further increasing succinic acid levels to 1% increased ECC but resulted in poorer retention of D-limonene in both water and SGF. The intended role of succinic acid in the formulations was to control droplet pH at the pKa of 4.2 to facilitate effective coacervation of net negatively charged alginates and net positively charged gelatin during spray drying. ECC can be a relative quantitative indicator of effectiveness of the coacervated matrix as a barrier in water and SGF. However, Figure 3–6 shows there are qualitative differences in the resulting CoCo matrices that cannot be captured by the ECC metric.

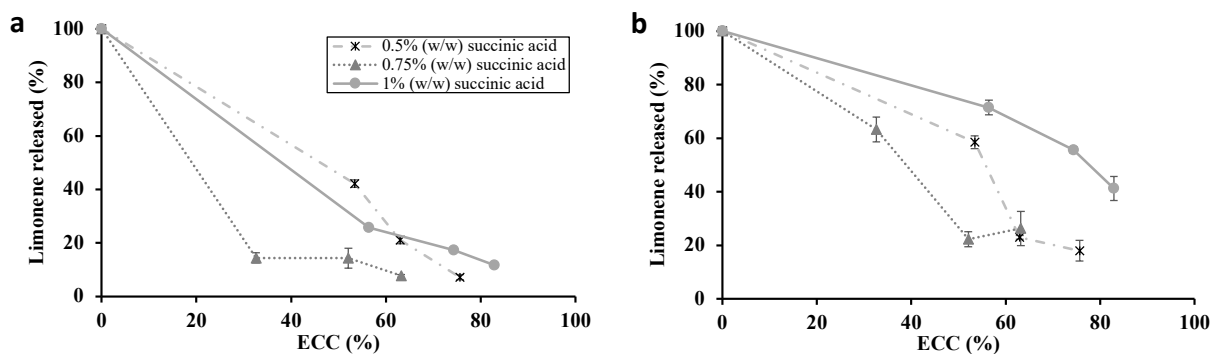


Figure 3–6. The relationship between the ECC and the release of D-limonene in: a: water, and b: SGF. Lines are drawn to guide the eye.

Of the formulations tested, 4G0.75S (Table 3–1) was one of the most successful at retaining D-limonene during spray drying (Figure 3–3a) and storage (Figure 3–3c), and in conferring

enteric release (**Figure 3–4**). Focusing on the 4G0.75S, the undissolved (coacervated) fraction of gelatin was highest in water ($80\pm 2\%$), less in the SGF ($66\pm 0\%$) and lowest in SIF (0%) (**Figure 3–7a**). The extent of undissolved alginate+gelatin in the powder sample in each medium trended with undissolved gelatin (**Figure 3–7a**), and less D-limonene released in aqueous media when more of the matrix polymers remained undissolved (**Figure 3–7b**). These results suggest that dissolution of the CoCo matrix is the main mechanism of D-limonene release from the CoCo powders into the various aqueous media within the 2 hour incubation.

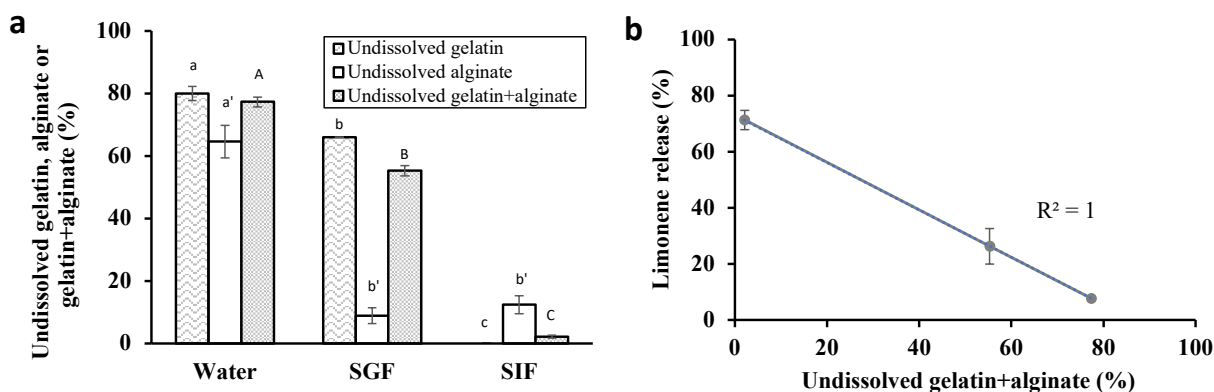


Figure 3–7. a: Undissolved alginate, undissolved gelatin and undissolved matrix polymers (alginate+gelatin) from the 4G0.75S CoCo sample in various aqueous media. b: The relationship between ECC and the release of D-limonene in aqueous media from the 4G0.75S CoCo sample (Table 3–1).

3.5 Discussion

3.5.1 The effect of the ECC on volatile retention and controlled release of D-limonene

In this study, I investigated how the gelatin-alginate polymer matrix formed by the CoCo process protects D-limonene in the dry powder and controls the release of D-limonene in aqueous media. During the CoCo process, drying, pH change and polymer-polymer interactions occur simultaneously and rapidly. The CoCo powder particles contain both coacervated and

uncoacervated polymers within which the encapsulated cargo (payload) is incorporated. The ECC, the portion of polymer involved in complex coacervation in the CoCo powder samples, was thus defined as a metric to help understand how the barrier properties of CoCo powder could be controlled. The ECC of the CoCo powders was assessed by dispersing the powder in liquid media to dissolve out the non-coacervated polymers.

Unsurprisingly, the ECC had no impact on the volatile retention of D-limonene in the dry CoCo powder either during formation or during storage. In the dry state, regardless of whether gelatin and alginate were coacervated, the polymers were fully present and part of the matrix acting as a physical barrier to limit D-limonene volatilization. The succinic acid concentration in the formulation, varied to control pH and thus ECC during the CoCo process, however, did play a role in the resulting powder quality and D-limonene retention. Too much succinic acid content in the CoCo matrix encouraged yellowing and clumping of the powder, which were not beneficial for retaining D-limonene. A possible explanation for this is that higher succinic acid content in the CoCo matrix could result in more surface D-limonene during storage, facilitating the formation of D-limonene oxide to form the yellowish color.

Complex coacervated matrices are reportedly resistant to dissolution in acidic media and offers rapid release under alkaline conditions. For example, Lin & Metters (Lin & Metters, 2006) reported slow release of only up to 10% of astaxanthin oleoresin in gastric juice over 2h from gelatin-alginate microcapsules formed by conventional complex coacervation, and significant higher release in intestinal fluid. This enteric release characteristic was consistent from the CoCo powders produced in this study. Moreover, release of D-limonene from the CoCo powders in water and SGF were related to the ECC (**Figure 3–6**); i.e. the more uncoacervated matrix polymers dissolved, the less D-limonene was retained in the media. The primary release mechanism of cargo

from biodegradable microcapsules includes diffusion, dissolution, swelling, erosion or a combination of these mechanisms (Lin & Metters, 2006; Prajapati et al., 2015). When the matrix is soluble, the release rate of the cargo from microcapsules is expected to be dominated by the dissolution rate of the polymer (Prajapati et al., 2015). In this study, higher ECC, i.e. higher retention of coacervated (and thus insoluble) polymer in the CoCo powders released less D-limonene, regardless of the media properties. I thus conclude that the dissolution of the CoCo matrix is the dominant mechanism of cargo release in aqueous media. Furthermore, in alkaline conditions at pH above the pKa and pI of the matrix polymers, cargo release is triggered by the dissociation of the complex coacervates, again consistent with conventionally formed complex coacervated gelatin-alginate and pectin-alginate microcapsules (Saravanan & Rao, 2010).

In this study, ECC was used as a metric to relate the coacervated polymer ratio to barrier properties controlling cargo release in aqueous media. While correlations between ECC and D-limonene release in the various aqueous media were observed, the ECC did not capture qualitative differences in the CoCo matrices resulting from varying succinic acid levels. For example, **Figure 3–6** showed that the trend of higher ECC resulting in less D-limonene release in aqueous media was consistent for CoCo particles formed with different succinic acid levels in the feed; however, the actual relationship between ECC and D-limonene release differed with succinic acid levels used. Increasing the succinic acid concentration from 0.5 to 0.75% in the spray drying feed resulted in CoCo powders retaining higher levels of D-limonene at lower ECC; but further increasing to 1.0% succinic acid resulted in CoCo powders retaining less D-limonene at the same ECCs. I hypothesize that modulating succinic acid levels adjusts the pH in the atomized droplets during spray drying to facilitate stronger electrostatic interactions between gelatin and alginate, which may not manifest as higher ECC, but could improve the matrix barrier properties. However, when

succinic acid is present in excess in the CoCo particles, dissolution of the acid in aqueous media could create pores in the matrix and facilitate faster D-limonene release even at higher ECC. These are speculations at this time, and further studies are needed to better understand the impact of formulation on the matrix barrier properties of the CoCo powders.

3.5.2 Modulating the ECC by formulation

The ECC of CoCo powders could be modulated by formulation, where higher ratios of gelatin to alginate led to higher ECC. Increasing the gelatin concentration introduces more positively charged polymers during the CoCo process, and increases the possibility of complex coacervation with negatively charged alginates. I observed that the ratio of coacervated gelatin was consistently much higher than the ratio of coacervated alginate in this study, suggesting that gelatin may be flexible and can adapt its molecular conformation to improve associations with alginates. Gelatin is obtained from tropocollagen (300,000 Da) composed of three alpha-peptide, about 300 nm long and 1.5 nm thick (Bhattacharjee & Bansal, 2005; Gorgieva & Kokol, 2011; Usha & Ramasami, 2004). The high shear preparation of the CoCo feed is likely to denature gelatin (~25kD and ~ 30 nm). The root mean square end-to-end distance of alginate with average molecular weight of 28,200 and high G/M ratio (G/M=1.8) was calculated as 48 nm (Kawai et al., 1992). The alginate used in this study of molecular weight of 172,800±458 (Jeoh et al., 2021), was approximately 6-fold larger. Taken together, I surmise that the gelatin-alginate matrix formed in this study could be envisioned as multiple flexible, smaller gelatin polymers cross-linking extended alginate polymers. Further studies varying alginate and gelatin sources, and matrix characterization would be needed to better understand the nature of the alginate-gelatin complex coacervated matrices formed by the CoCo process.

Succinic acid, a dicarboxylic acid with pKa 1 of 4.61 and pKa 2 of 5.61, has been widely used in the agricultural, food and pharmaceutical industries (Song & Lee, 2006). Succinic acid was selected in this work because it is safe and can achieve the desired solution pH in the particles during spray drying. A previous study in our group to form ion-mediated crosslinked alginate by controlling the pH during spray drying demonstrated that succinic acid poised the pH in the droplets during spray drying to near its pKa 1, solubilizing the calcium salt and inducing the crosslinking between calcium ion and alginates (Strobel et al., 2016b). I speculated that pH ~ 4~5 may be the ideal range to facilitate the interactions between alginate with pKa of 3.5 and gelatin with pI of 7. In addition to succinic acid, other organic acids such as maleic acid and citric acid could also be candidates for the CoCo process. Our preliminary study showed that 1% maleic acid and citric acid in the formulation with 2.5% gelatin and 0.5% alginate was able to drop the pH to 4.5 and 5.5 respectively (Supplementary **Figure 3-1**). A wide range of pH could be achieved by modulating the type and concentration of the acid to investigate the effect of pH on the barrier properties of the CoCo matrix. Moreover, the selection of acid not only affects the complex coacervation process by modulating the pH, but also could affect the matrix structure.

In this study, the best performing formulation used 4% gelatin and 0.75% succinic acid in the feed (4G0.75S) to generate CoCo powders with the high D-limonene loading of 16.8%, high retention during spray drying of 76.0%, high retention after 4 months of storage of 70.9%. The 4G0.75S CoCo sample was also successfully retained the majority of the encapsulated D-limonene in water and in gastric fluids, while releasing in the intestinal fluid. In other words, this formulation successfully conferred enteric release to this CoCo powder. Finally, this formulation exhibited superior powder quality.

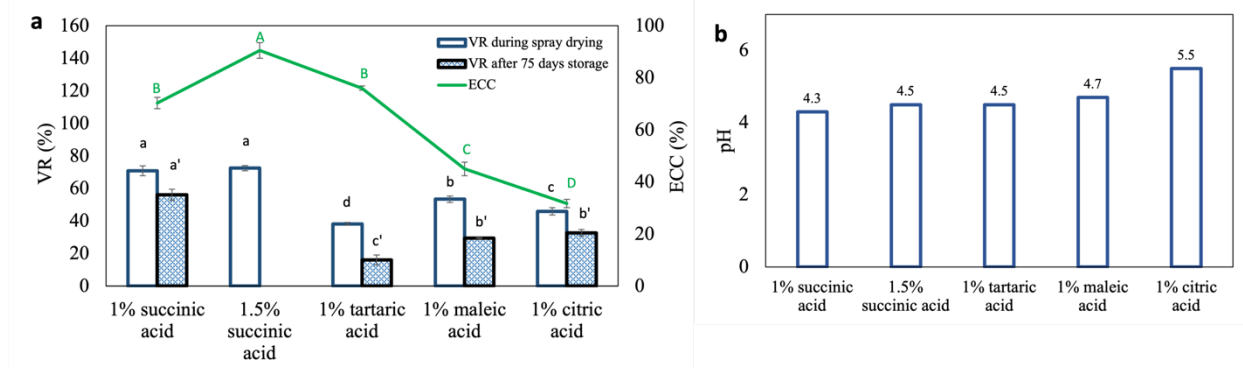
3.6 Conclusions

This study investigated how to control the barrier properties of gelatin-alginate CoCo powders using the novel CoCo process. For controlling the release of cargo in aqueous media, the extent of complex coacervation (ECC) is important, which can be modulated by varying the polymer ratio and acid concentration in the formulation. Higher extents of complex coacervation were achieved by increasing the gelatin concentration (increasing gelatin to alginate ratio) in the formulation. For retaining the cargo during spray drying and subsequent dry storage, controlling the ECC was not important. Overall, the study showed that the gelatin-alginate matrix formed by the CoCo process was capable of retaining 78% of D-limonene during spray drying in powders and providing enteric release. The novelty of this work included: (1) an understanding of controlling properties of the microcapsules formed by the novel industrial scalable *in situ* complex coacervation process, and (2) understanding the role of the ECC on the microcapsule barrier and controlled release properties. Ultimately, the utility of CoCo powders in food can be broadened by varying the encapsulated cargo; e.g., for controlled delivery of flavoring agents, antimicrobials, pre- or probiotics, or nutraceuticals.

3.7 Abbreviations

CoCo, complex coacervated/complex coacervation; pI, isoelectric point; ECC, extent of complex coacervation. SGF, simulated gastric fluid; SIF, simulated intestinal fluid.

3.8 Supplemental information



Supplementary Figure 3–1. The volatile retention of D-limonene in CoCo powder during spray drying and after 75 days storage and the ECC of D-limonene microcapsules formed with different concentration of acid, 2.5% gelatin and 0.5% alginate. The volatile retention of D-limonene after storage from powder formulated with 1.5% succinic acid was not measured (a); The pH of 1% (w/v) D-limonene microcapsules formed with different concentration of acid (b).

Supplementary Table 3–1. Particle size of CoCo powders (μm).

Formulation ¹	D _{4,3}	D(0.1)	D(0.5)	D(0.9)
2.5G0.5S	17.6±3.6 _{a,b}	5.6±0.0 _c	13.9±0.1 _c	28.1±0.4 _c
4G0.5S	14.1±0.0 _b	4.3±0.0 _f	12.0±0.0 _e	26.9±0.0 _d
2.5G0.75S	17.2±0.7 _{a,b}	5.7±0.0 _b	14.0±0.0 _c	28.4±0.1 _c
4G0.75S	15.1±0.1 _{a,b}	5.1±0.0 _d	13.2±0.1 _d	27.9±0.3 _c
2.5G1S	18.5±0.3 _a	4.6±0.0 _e	14.7±0.0 _b	37.5±0.1 _a
4G1S	17.4±0.0 _{a,b}	6.5±0.0 _a	16.1±0.0 _a	30.3±0.1 _b

3.9 References

- Bhattacharjee, A., & Bansal, M. (2005). Collagen Structure: The Madras Triple Helix and the Current Scenario. *IUBMB Life*, 57(3), 161–172. <https://doi.org/10.1080/15216540500090710>
- Bradford, M. M. (1976). A rapid and sensitive method for the quantitation of microgram quantities of protein utilizing the principle of protein-dye binding. *Analytical Biochemistry*, 72(1), 248–254. [https://doi.org/10.1016/0003-2697\(76\)90527-3](https://doi.org/10.1016/0003-2697(76)90527-3)
- de Matos, E. F., Scopel, B. S., & Dettmer, A. (2018). Citronella essential oil microencapsulation by complex coacervation with leather waste gelatin and sodium alginate. *Journal of Environmental Chemical Engineering*, 6(2), 1989–1994. <https://doi.org/10.1016/j.jece.2018.03.002>
- Dong, Z., Ma, Y., Hayat, K., Jia, C., Xia, S., & Zhang, X. (2011). Morphology and release profile of microcapsules encapsulating peppermint oil by complex coacervation. *Journal of Food Engineering*, 104(3), 455–460. <https://doi.org/10.1016/j.jfoodeng.2011.01.011>

- DuBois, M., Gilles, K. A., Hamilton, J. K., Rebers, P. A., & Smith, F. (1956). Colorimetric Method for Determination of Sugars and Related Substances. *Analytical Chemistry*, 28(3), 350–356. <https://doi.org/10.1021/ac60111a017>
- Ghasemi, S., Jafari, S. M., Assadpour, E., & Khomeiri, M. (2018). Nanoencapsulation of d-limonene within nanocarriers produced by pectin-whey protein complexes. *Food Hydrocolloids*, 77, 152–162. <https://doi.org/https://doi.org/10.1016/j.foodhyd.2017.09.030>
- Gorgieva, S., & Kokol, V. (2011). Collagen- vs. Gelatine-Based Biomaterials and Their Biocompatibility: Review and Perspectives. In *Biomaterials: Applications for Nanomedicine* (pp. 18–52). IntechOpen. <https://doi.org/10.5772/24118>
- Gouin, S. (2004). Microencapsulation: industrial appraisal of existing technologies and trends. *Trends in Food Science & Technology*, 15(7), 330–347. <https://doi.org/https://doi.org/10.1016/j.tifs.2003.10.005>
- Jeoh, T., Wong, D. E., Strobel, S. A., Hudnall, K., Pereira, N. R., Williams, K. A., Arbaugh, B. M., Cunniffe, J. C., & Scher, H. B. (2021). How alginate properties influence in situ internal gelation in crosslinked alginate microcapsules (CLAMs) formed by spray drying. *PLOS ONE*, 16(2), e0247171. <https://doi.org/10.1371/journal.pone.0247171>
- Jun-xia, X., Hai-yan, Y., & Jian, Y. (2011). Microencapsulation of sweet orange oil by complex coacervation with soybean protein isolate/gum Arabic. *Food Chemistry*, 125(4), 1267–1272. <https://doi.org/https://doi.org/10.1016/j.foodchem.2010.10.063>
- Kawai, M., Matsumoto, T., Masuda, T., & Nakajima, A. (1992). Molecular length per mannuronic and guluronic acid residue in an alginate molecule in aqueous solutions. *Journal of Japanese Society of Biorheology*, 6(2), 42–47. https://doi.org/10.11262/jpnbr1987.6.2_42
- Leclercq, S., Harlander, K. R., & Reineccius, G. A. (2009). Formation and characterization of microcapsules by complex coacervation with liquid or solid aroma cores. *Flavour and Fragrance Journal*, 24(1), 17–24. <https://doi.org/https://doi.org/10.1002/ffj.1911>
- Lin, C.-C., & Metters, A. T. (2006). Hydrogels in controlled release formulations: Network design and mathematical modeling. *Advanced Drug Delivery Reviews*, 58(12), 1379–1408. <https://doi.org/https://doi.org/10.1016/j.addr.2006.09.004>
- Mekhloufi, G., Sanchez, C., Renard, D., Guillemin, S., & Hardy, J. (2005). pH-Induced Structural Transitions during Complexation and Coacervation of β -Lactoglobulin and Acacia Gum. *Langmuir*, 21(1), 386–394. <https://doi.org/10.1021/la0486786>
- Prajapati, V. D., Jani, G. K., & Kapadia, J. R. (2015). Current knowledge on biodegradable microspheres in drug delivery. *Expert Opinion on Drug Delivery*, 12(8), 1283–1299.
- Saravanan, M., & Rao, K. P. (2010). Pectin–gelatin and alginate–gelatin complex coacervation for controlled drug delivery: Influence of anionic polysaccharides and drugs being encapsulated on physicochemical properties of microcapsules. *Carbohydrate Polymers*, 80(3), 808–816. <https://doi.org/https://doi.org/10.1016/j.carbpol.2009.12.036>
- Schmitt, C., Sanchez, C., Thomas, F., & Hardy, J. (1999). Complex coacervation between β -lactoglobulin and acacia gum in aqueous medium. *Food Hydrocolloids*, 13(6), 483–496. [https://doi.org/https://doi.org/10.1016/S0268-005X\(99\)00032-6](https://doi.org/https://doi.org/10.1016/S0268-005X(99)00032-6)
- Schmitt, Christophe, & Turgeon, S. L. (2011). Protein/polysaccharide complexes and coacervates in food systems. *Advances in Colloid and Interface Science*, 167(1), 63–70. <https://doi.org/https://doi.org/10.1016/j.cis.2010.10.001>
- Song, H., & Lee, S. Y. (2006). Production of succinic acid by bacterial fermentation. *Enzyme and Microbial Technology*, 39(3), 352–361. <https://doi.org/https://doi.org/10.1016/j.enzmictec.2005.11.043>

- Strobel, S. A., Scher, H. B., Nitin, N., & Jeoh, T. (2016). In situ cross-linking of alginate during spray-drying to microencapsulate lipids in powder. *Food Hydrocolloids*, *58*, 141–149. <https://doi.org/https://doi.org/10.1016/j.foodhyd.2016.02.031>
- Swackhamer, C., Zhang, Z., Taha, A. Y., & Bornhorst, G. M. (2019). Fatty acid bioaccessibility and structural breakdown from in vitro digestion of almond particles. *Food & Function*, *10*(8), 5174–5187. <https://doi.org/10.1039/C9FO00789J>
- Tang, Y., Scher, H. B., & Jeoh, T. (2020). Industrially scalable complex coacervation process to microencapsulate food ingredients. *Innovative Food Science & Emerging Technologies*, *59*, 102257. <https://doi.org/https://doi.org/10.1016/j.ifset.2019.102257>
- Tang, Y., Scher, H., & Jeoh, T. (2021). *Microencapsulation of chemicals and bioactives by in situ complex coacervation during spray drying*. U.S. Patent Application No. 17/178,866, Publication No. US20210316265A1.
- Usha, R., & Ramasami, T. (2004). The effects of urea and n-propanol on collagen denaturation: using DSC, circular dichroism and viscosity. *Thermochimica Acta*, *409*(2), 201–206. [https://doi.org/https://doi.org/10.1016/S0040-6031\(03\)00335-6](https://doi.org/https://doi.org/10.1016/S0040-6031(03)00335-6)
- Yan, C., & Zhang, W. (2014). Chapter 12 - Coacervation Processes. In *Microencapsulation in the Food Industry* (pp. 125–137). Academic Press. <http://www.sciencedirect.com/science/article/pii/B9780124045682000121>
- Yang, Y., Anvari, M., Pan, C.-H., & Chung, D. (2012). Characterisation of interactions between fish gelatin and gum arabic in aqueous solutions. *Food Chemistry*, *135*(2), 555–561. <https://doi.org/https://doi.org/10.1016/j.foodchem.2012.05.018>
- Yang, Z., Peng, Z., Li, J., Li, S., Kong, L., Li, P., & Wang, Q. (2014). Development and evaluation of novel flavour microcapsules containing vanilla oil using complex coacervation approach. *Food Chemistry*, *145*, 272–277. <https://doi.org/https://doi.org/10.1016/j.foodchem.2013.08.074>

Chapter 4 The effect of ethylcellulose on retention and release of D-limonene encapsulated by complex coacervated microcapsules formed by spray drying

4.1 Abstract

The application of D-limonene in food products faces substantial barriers related to the volatility and instability of D-limonene. The study of controlled release of D-limonene in aqueous media explores opportunities to develop effective delivery strategies for hydrophobic compounds. In this study, the CoCo process was applied to encapsulate D-limonene based on the coacervation between alginate and gelatin and the effect of ethylcellulose in the CoCo microcapsules on D-limonene retention and release was investigated. D-limonene retention in coacervated gelatin and alginate microcapsules was up to $75.7\% \pm 1.3\%$ after spray drying, followed with $\sim 10\%$ D-limonene loss and low oxidation after 3-weeks of storage. The inclusion of ethylcellulose in the CoCo formulation aimed to reinforce the matrix. However, ethylcellulose in the CoCo microcapsules resulted in escalated volatilization and oxidation in spray dried powders and modulated release of D-limonene in different pH environments. This chapter addresses how the latex polymer like ethylcellulose could modulate the release of D-limonene either in dry powder state or in aqueous environment for its targeted application.

4.2 Introduction

D-limonene a monocyclic monoterpene with a citrus-like smell, offers many bioactivities including antifungal, bacteriostatic and bactericidal properties (Ciriminna et al., 2014). In the food industry, D-limonene can be found in many food products such as chewing gum, citrus juices, vegetables, herbs, candy and drinks (Calo et al., 2015). Specifically, D-limonene can be used as

food preservative as it exhibits antifungal, bacteriostatic and bactericidal properties (Espina et al., 2013). More commonly, it has been used as a flavoring agent in some food products such as fruit beverages and ice creams (Espina et al., 2013). In addition, D-limonene is a potential diet supplement for its anti-inflammatory and anti-stress properties (d'Alessio et al., 2013). However, the application of D-limonene in food products or as nutraceuticals is highly challenging as it is volatile and sensitive to process or environmental stresses. Microencapsulation of D-limonene can facilitate the application of D-limonene by providing a barrier for prolonged shelf life and controlled release.

There have been extensive studies for the formulation and process development of latex dispersion for film coating, applying to solid substrates for odor and taste masking, improvement of appearance, and protection of environmental conditions (Ahmed et al., 2020; Lecomte et al., 2004; Petereit & Weisbrod, 1999). A latex dispersion, a colloidal dispersion, can be prepared from any existing thermoplastic water insoluble polymer, forming a thin film as water evaporates if the operational conditions are above the glass transition temperature of the latex polymer (Keddie & Routh, 2010). Ethylcellulose (EC), one kind of latex polymer, is an ethyl ether of cellulose that has been widely used in the pharmaceutical industry as it is insoluble and impermeable to water (Wasilewska & Winnicka, 2019). It has been used for moisture protection and taste masking. No study has investigated how the combination of latex polymers and a complex coacervation system protect the cargo under environmental stresses such as heat, moisture and pH.

Microencapsulation of D-limonene by the CoCo process can protect D-limonene from volatilization during spray drying and storage and provide enteric release as demonstrated in chapter 2 and 3 (Tang et al., 2020, 2021). It is not clear whether the incorporation of latex polymers can reinforce the protective matrix for D-limonene retention and release. The effect of

ethylcellulose in the CoCo microcapsules on D-limonene retention and release was studied in this study. **Figure 4–1** is the schematic of the formation of bioactive loaded CoCo powder with/without latex polymer using the CoCo process.

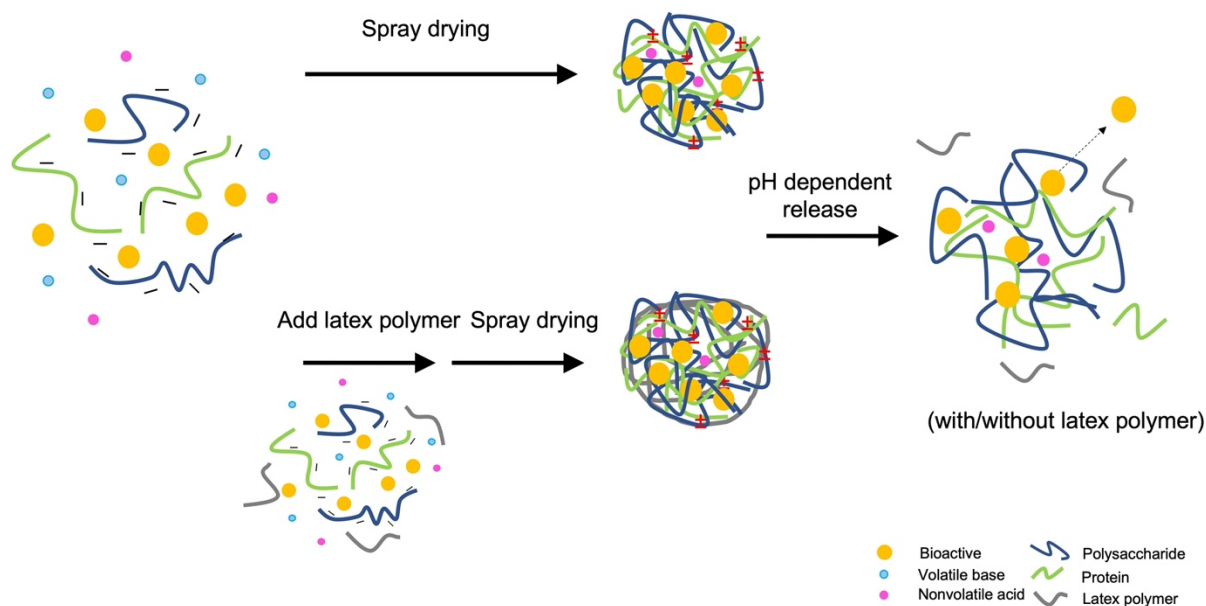


Figure 4–1. Schematic representation of the formation of CoCo powder with/without latex and its following release.

4.3 Materials and methods

4.3.1 Materials

D-limonene, gelatin (type A with an isoelectric point of 7), n-hexane, pepsin, pancreatin 8x USP were purchased from Sigma Aldrich (St. Louis, MO). High viscosity sodium alginate (GRINDSTED Alginate FD 155 with pKa of 3.5 was from Dupont Nutrition and Health (New Century, KS). Succinic acid, ammonium hydroxide, sodium hydroxide, sodium chloride and isopropanol were purchased from Fisher Scientific (Fair Lawn, NJ). Anti-foam reagent was purchased from Spectrum Chemicals Mfg Corp (New Brunswick, NJ). Aquacoat® ECD 30 (aqueous colloidal dispersion of ethylcellulose polymer) was provided by Colorcon (Harleysville,

PA) and tributyl citrate was purchased from TCI America (Portland, OR). D-limonene, carvone and limonene oxide standard were purchased from Sigma Aldrich (St. Louis, MO).

4.3.2 Methods

4.3.2.1 Formation of the CoCo microcapsules with/without ethylcellulose

D-limonene loaded microcapsules were prepared as described in Chapter 3. A coarse emulsion with a 1.2:1 gelatin to D-limonene ratio (w/w) was prepared by using an Ultra-Turrax T-18 at 12,000 rpm for 2min (IKA Works, Inc., Wilmington, DE), where an anti-foam reagent was used to reduce the foam formed during the mixing. The coarse emulsion was passed three times through a high-pressure homogenizer (BEEi Nano DeBEE 30-4 High Pressure Homogenizer) at 20 kpsi. A CoCo solution containing gelatin, alginate and succinic acid was prepared, where ammonium hydroxide was used to adjust the solution pH to 8.5. 25% of tributyl citrate based on the mass of ethylcellulose was added to the Aquacoat® ECD 30 dispersion (referred to as ethylcellulose dispersion) and rotated at 20rpm overnight before adding to the CoCo formulation. The emulsion and the CoCo solution with or without ethylcellulose dispersion was mixed to form the spray drying feed. **Table 4–1** shows the compositions in each formulation. The feed was spray dried by a Buchi B290 laboratory spray dryer. The spray drying conditions were set as follows: inlet air temperature at 150 °C, aspirator airflow rate at maximum (35 m³/h), feed peristaltic pump at 20% of maximum (6 ml/min), and 40 mm nozzle pressure.

Table 4–1. Formulations to form D-limonene-loaded CoCo powders with or without ethylcellulose.

Sample ID	Concentration in spray dryer inlet suspension (w/w, %)					
	Total solid	EC dispersion	Alginate	Gelatin	Succinic acid	D-limonene
CoCo	7.00	0.00	0.50	4.00	0.75	1.75
Low-EC CoCo	7.67	0.50	0.50	4.00	0.75	1.92
High-EC CoCo	9.33	1.75	0.50	4.00	0.75	2.33

4.3.2.2 Emulsion size and particle size measurement

D-limonene droplet size in the feed and spray dried particle size were measured by Mastersizer 3000 (Malvern Instrument, Westborough, MA) (Strobel et al., 2016). For the size measurement of D-limonene emulsion, material type of D-limonene was with refractive index 1.47, and dispersant type of water was with dispersant refractive index of 1.33. For the size measurement of spray dried powders, powders were dispersed in propan-2-ol to prevent swelling. Sonication to ensure good dispersion was applied until volume-weighted mean diameter ($D_{4,3}$) stabilized. Material type of particle was with refractive index 1.57 and absorption index 0.01, and dispersant type of propan-2-ol was with dispersant refractive index of 1.37. Temperature was ~ 25 °C. Each sample was measured in triplicate.

4.3.2.3 Measurement of volatile retention of D-limonene in CoCo microcapsules with/without ethylcellulose

Volatile retention of D-limonene was expressed as the ration of total D-limonene in the microcapsules to total D-limonene in the spray drying feed.

To measure total D-limonene in the spray drying feed, 10ml isopropanol, 10ml hexane and 9.5g water were added to 0.5 g of emulsion. The mixture was rotated at 20 rpm for 2 h at room

temperature and allowed to sit still for 5–10 min to separate. The volume of the top hexane layer containing D-limonene was measured, then sampled and analyzed by GC.

Spray-dried powders were dispersed in water to a final concentration of 1% (w/v), where sodium hydroxide was added to raise the pH of the suspension to above the pI of gelatin. The sample was rotated end-over-end at 20 rpm for 2h, including incubated in 45 °C water bath for 10 min to facilitate the dissolution of gelatin. Once the powders were fully dissolved, 6 ml isopropanol and 10 ml hexane were added and followed by 1 h rotation at 20 rpm. The extract mixtures were centrifuged at 1000 g for 10 min. The volume of the top hexane layer containing D-limonene was measured, then sampled and analyzed by GC. Each powder sample was extracted in triplicate.

0.05g spray-dried powders was added to 10ml hexane and rotated at 20 rpm for 10min. After that, the extract mixtures were centrifuged at 8000 g for 2 min. The supernatant was sampled and analyzed by gas chromatography (GC) to measure surface D-limonene.

4.3.2.4 Shelf-life study of D-limonene CoCo microcapsules with/without ethylcellulose

The microcapsules were subjected to three different conditions after spray drying to evaluate the release and oxidation of D-limonene over time. Samples were weighted to 0.1g (for total D-limonene) or 0.05g (for surface D-limonene) and spread in a thin layer in a 15-ml glass bottle (20 ×48 mm) in triplicate per time point for each storage condition. All the glass bottle was put in an airtight container (BD GasPak™). Storage condition 1 had controlled relative humidity, with 75% RH using saturated NaCl solution (RH 75%); storage condition 2 also had controlled relative humidity, with less than 10% RH using saturated KOH solution (RH 10%); storage condition 3 had no environmental controls, with ~30% RH (RH ~30%) as shown in **Figure 4–2**.

The samples were taken out at each time point (1, 2, and 3 weeks) and the retained D-limonene in the microcapsules during storage was measured as described above. Each powder sample was extracted in triplicate.

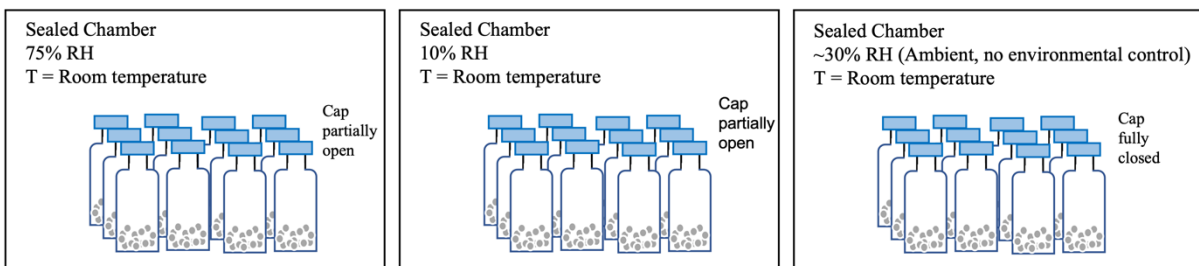


Figure 4–2. The storage conditions for shelf-life study of D-limonene CoCo microcapsules with/without ethylcellulose.

4.3.2.5 Release of D-limonene from the microcapsules in water, simulated gastric and intestinal fluids

The powder was dispersed in distilled water (pH 5.8), simulated gastric fluid (SGF, 8.78 mg/ml sodium chloride at pH 1.8 with pepsin activity of 2000 U/ml (Swackhamer et al., 2019)) and simulated intestinal fluid (SIF, 50 mM phosphate buffer at pH 7.4 with 9.6 mg/ml pancreatin 8x USP based on trypsin activity of 100 TAME U/mL) (Strobel et al., 2016). Specifically, the powders were dispersed in the respective fluids at 0.5% (w/v) in triplicate per time points and incubated at 37 °C (SGF and SIF) or room temperature (water) and rotated end-over-end at 20 rpm. At each time points, 10 mL of hexane was added and mixed very gently for 30 s before centrifuging at 10,000g for 5min. The supernatant was separated and mixed with 6 ml isopropanol. The mixtures were centrifuged at 1,000 g for 10 min after 15 min extraction time. The volume of the top layer containing D-limonene was measured, then sampled and analyzed by GC. Each powder sample was released in triplicate.

4.3.2.6 Gas chromatography (GC) to determine D-limonene contents in extracts

The hexane phase containing D-limonene was analyzed by gas chromatography (Shimadzu 2010) with flame ionization detection equipped with a capillary column (DB-FFAP, 30 m x 0.32 mm ID, film thickness 0.25 μm). The injector temperature of GC was set at 250 $^{\circ}\text{C}$ and the detector was set at 260 $^{\circ}\text{C}$. The temperature program started at 50 $^{\circ}\text{C}$, held for 3 min and then increased to 190 $^{\circ}\text{C}$ at a rate of 20 $^{\circ}\text{C}/\text{min}$ before holding for 1 min and then increased to 200 $^{\circ}\text{C}$ at a rate of 10 $^{\circ}\text{C}/\text{min}$ before holding for 6 min. Helium was used as the carrier gas. Standard curve of D-limonene, carvone and limonene oxide ranged from 7.8-2000 $\mu\text{g}/\text{mL}$, 0.16-20 $\mu\text{g}/\text{mL}$ and 0.78-50 $\mu\text{g}/\text{mL}$ respectively.

4.3.2.7 Statistical analysis

Data were reported as mean \pm standard deviation. ANOVA and Tukey's post hoc multiple comparison test were used to determine differences among factor levels. Statistical analysis was performed using JMP (SAS Institute Inc., Cary, NC, USA). P-values less than 0.05 were considered significant.

4.4 Results and discussion

4.4.1 Volatile retention of D-limonene in CoCo microcapsules after spray drying

The effect of ethylcellulose in the CoCo microcapsules on the volatile retention of D-limonene after spray drying was investigated. The hypothesis was that the inclusion of ethylcellulose would form an extra layer of protection for D-limonene along with the CoCo matrix. Interestingly, the inclusion of ethylcellulose in the CoCo powder was markedly less effective at preventing D-

limonene from volatilizing during spray drying; the volatile retention in the CoCo, the low-EC CoCo and the high-EC CoCo were $77.7 \pm 1.3\%$, $42.1 \pm 0.5\%$ and $19.7 \pm 0.2\%$, respectively (**Figure 4-3a**). The surface D-limonene in spray dried microcapsules increased dramatically with the increase of ethylcellulose content (**Figure 4-3a**). The significant effects of ethylcellulose in the CoCo microcapsules suggest that the ethylcellulose drives the hydrophobic compound like D-limonene to the surface of the matrix. Higher surface D-limonene content enables easier volatilization of D-limonene, resulting in lower volatile retention. Besides that, as shown in **Figure 4-3b**, the size of D-limonene emulsion in the feed decreased as the ethylcellulose content increased in the formulation. The ethylcellulose dispersion is stabilized by sodium lauryl sulfate (SLS) and cetyl alcohol, which could be highly effective to decrease the size of D-limonene emulsion. The smaller emulsion size with increased surface area could also facilitate the volatilization of D-limonene. In summary, higher surface D-limonene combined with smaller D-limonene emulsion size in the feed led to significantly lower volatile retention of D-limonene during spray drying.

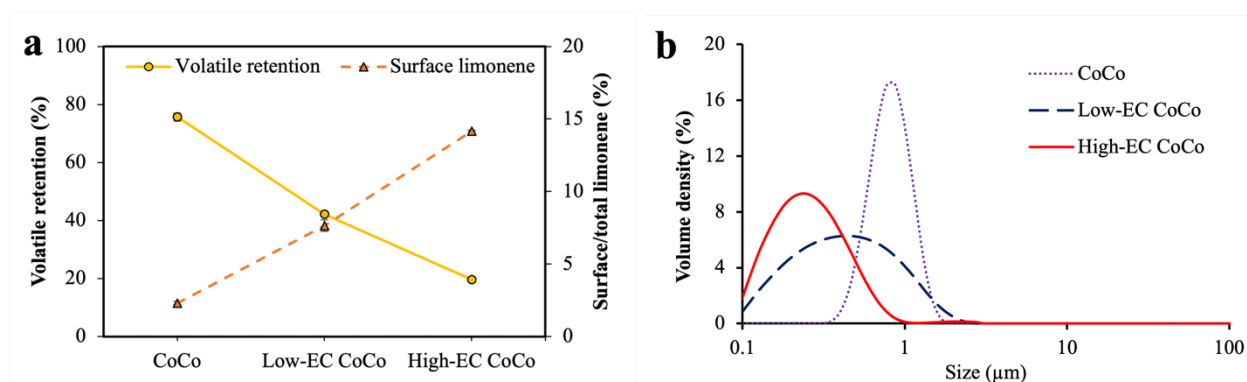


Figure 4-3. a: Volatile retention of D-limonene in the CoCo microcapsules during spray drying; b: Emulsion size of D-limonene in the CoCo feed with different concentration of ethylcellulose.

There have been extensive studies investigating the relation of volatile retention and emulsion size which remains controversial. As mention by Chang et al., large atomized droplets requires

more time to form film, resulting in lower retention (Chang et al., 1988). Soottitantawat et al. reported that the increasing emulsion size from 0.65 μm to 2 μm resulted in remarkably decreased retention of flavors in different carrier combinations (maltodextrin with Gun Arabic/soybean soluble polysaccharide/HI-CAP 100) (A Soottitantawat et al., 2003). This implies that large emulsion droplets sheared to small droplets during atomization and facilitated the volatilization. They also reported that some flavors retention increased with the increasing emulsion size. With the emulsion size in a range from 1 μm to 4 μm , the volatile retention reached maximum for ethyl butyrate and ethyl propionate with emulsion size of ~ 1.8 and ~ 3 μm respectively. Too fine or too large emulsion resulted in a decreasing retention. This study demonstrated that the volatile retention increased as the emulsion size increased from 0.3 μm to 0.9 μm (**Figure 4–3**). The likely explanation is that the smaller size of D-limonene in the feed leads to larger surface area of D-limonene droplet, increasing the chances of D-limonene to volatile during spray drying. The controversial findings indicated that there could be optimal emulsion size to high retention depending on the wall materials and the processing conditions.

In another set of studies, I compared the volatile retention from the two formulations with different emulsion size (**Figure 4–4**). In L gelatin formulation, the emulsion prepared with a 0.2 D-limonene to gelatin ratio (w/w) was unstable, leading to varied emulsion size in the feed and poor reproducibility of volatile retention. The H gelatin formulation prepared with a 1.2 D-limonene to gelatin ratio (w/w) resulted in stable and small emulsion size in the feed, followed by significantly higher volatile retention with good reproducibility. This study indicated the stable emulsion with optimal emulsion size could be vital to achieve high volatile retention. However, more systematic study by comparing the same formulation with different emulsion size in the feed can be explored to elucidate the effect of emulsion size on the volatile retention of D-limonene.

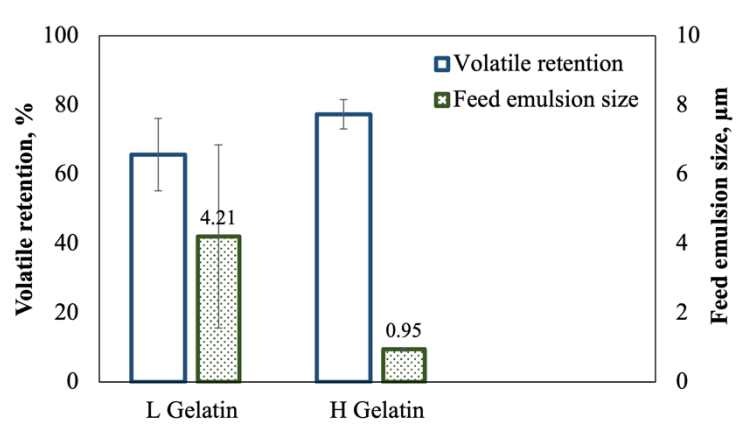


Figure 4–4. The volatile retention of D-limonene in microcapsules generated from different formulation during spray drying and the emulsion size in the feed: L gelatin: 2.5% gelatin, 0.5% alginate and 1% succinic acid, 25% D-limonene based on dry inlet feed (w/w) where D-limonene emulsion was prepared with a 0.2 D-limonene to gelatin ratio (w/w); H gelatin: 2.5% gelatin, 0.5% alginate and 0.75% succinic acid, 25% D-limonene based on dry inlet feed (w/w) where D-limonene emulsion was prepared with a 1.2 D-limonene to gelatin ratio (w/w).

Emulsifier that affects the emulsion size and the complex coacervation at the interface of D-limonene emulsion can be another factor that can impact the volatile retention. In another set of experiment, different emulsifier was used in the formulation to form D-limonene loaded CoCo microcapsules. In **Figure 4–5**, formulation using whey protein isolate (WPI) and soy protein isolate (SPI) as the emulsifier resulted in significantly higher volatile retention of 83.8% and 79.9% respectively, along with the emulsion size of 1.00 and 1.09 µm. Formulation with casein as emulsifier yielded emulsion size of 0.90 µm and volatile retention of 64.8%. Formulation with Tween 85 as emulsifier yielded smallest emulsion size of 0.35 µm and the lowest volatile retention of 60.3%. Small holes have been observed in the surface of casein CoCo and Tween 85 CoCo microcapsules and could be relevant to the lower volatile retention of D-limonene (shown in supplementary information-**Figure 4-1**). Study has also shown that emulsifier like Tween 20 that has slow absorption rate, failing to stabilize newly formed small droplets and lack of good film formation ability, resulted in poor retention of volatiles (Jafari et al., 2007a). Emulsifier can

influence the volatile retention of D-limonene in three ways: (1) emulsifier influences the emulsion size and there may be optimal emulsion size to maximum the volatile retention of D-limonene in specific matrix; (2) the protein emulsifier can form globular/flexible layers at the interface that influences the formation of complex coacervates at the interface and the stronger interaction at the interface may lead to better protection of D-limonene during spray drying. Non-protein emulsifier may not be able to form a barrier as good as protein emulsifier to protect D-limonene during spray drying. (3) the diffusivity of D-limonene through the emulsifier layer can impact the loss of D-limonene. Further work on investigation the distribution of complex coacervates at the interface can be explored to understand the influence of protein emulsifier on volatile retention of D-limonene.

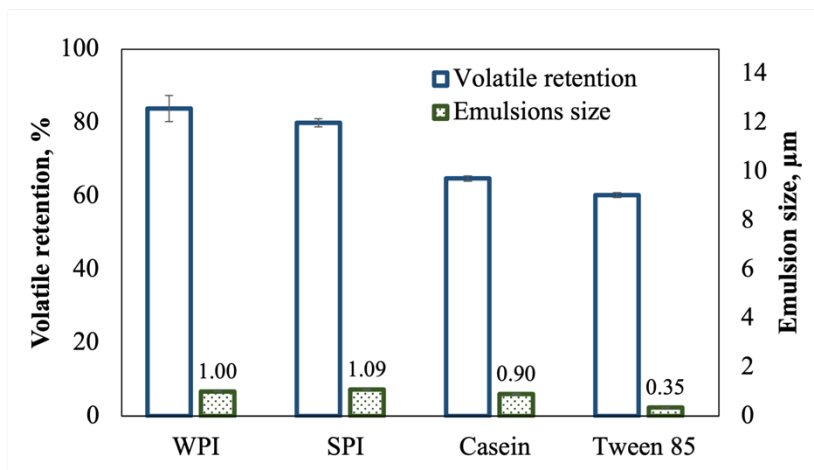


Figure 4-5. The volatile retention of D-limonene in the CoCo microcapsules formulated with different emulsifier during spray drying and the emulsion size for each formulation. The detailed formulation was shown in supplementary information Table 4-1.

To sum up, volatile retention of flavors during spray drying could depend on the distribution of the flavors, the emulsion size and the emulsion stability and emulsifier type in the matrix.

4.4.2 Retention and oxidation of D-limonene in CoCo microcapsules during storage

D-limonene CoCo microcapsules with different content of ethylcellulose was stored at conditions with different relative humidity. This part of the study was to investigate whether the inclusion of ethylcellulose working as moisture barrier would be effective at retaining D-limonene at different relative humidity levels.

Figure 4–6a shows that relative humidity has a significant effect on volatile retention during storage. Up to $89.9 \pm 0.4\%$ and $88.6 \pm 0.8\%$ of D-limonene in the CoCo microcapsules were retained at 10% and ~30% relative humidity after 3 weeks, whereas D-limonene retention dropped to $5.0 \pm 2.1\%$ at 75% relative humidity. The surface D-limonene content was $9.0 \pm 1.4\%$ after one week at 75% relative humidity, compared to less than $1.2 \pm 0.0\%$ at lower relative humidity conditions as shown in **Figure 4–6a'**. This suggests that high relative humidity condition facilitates the migration of D-limonene to the surface of the matrix, resulting in dramatic decrease of D-limonene in the microcapsules. One possible explanation is that the surface is hydrophilic, and water displays D-limonene from the surface at high humidity, leading to more D-limonene loss. The influence of high relative humidity on volatile retention was consistent with the findings reported by Soottitantawat et al. (Apinan Soottitantawat et al., 2004). The high relative humidity also led to the destruction of the matrix, resulting in the D-limonene droplets released in the powders. **Figure 4–7** shows the appearance of D-limonene CoCo powder stored at different relative humidity conditions after 1 week. It was clear that the CoCo powder stored at high relative humidity clumped together and experienced structure changes.

The higher ethylcellulose content in the CoCo microcapsules further promoted the accumulation of surface D-limonene, especially at high relative humidity as shown in **Figure 4–6a'-c'**. In addition, the difference in ethylcellulose content in the CoCo microcapsules had

substantial effect on the volatile retention in 10% relative humidity condition. As shown in **Figure 4–6a-c**, the volatile retention of D-limonene in high- ethylcellulose CoCo microcapsules dropped to $76.6\pm 1.3\%$ in 10% relative humidity condition and it was significantly lower compared to that in the CoCo and the low-EC CoCo microcapsules, suggesting that the inclusion of ethylcellulose in the CoCo microcapsules is not beneficial for retaining D-limonene under low relative humidity condition. No significant differences were noted when comparing the volatile retention of D-limonene in the CoCo and the EC CoCo microcapsules in 75% relative humidity condition, which reveals the lack of efficiency of ethylcellulose in the CoCo microcapsules as moisture barrier to slow down to the release of D-limonene. These findings indicated ethylcellulose the CoCo microcapsules could not only drive D-limonene to the surface during spray drying, but also facilitated D-limonene diffusing through the matrix to the surface during storage even under low RH conditions.

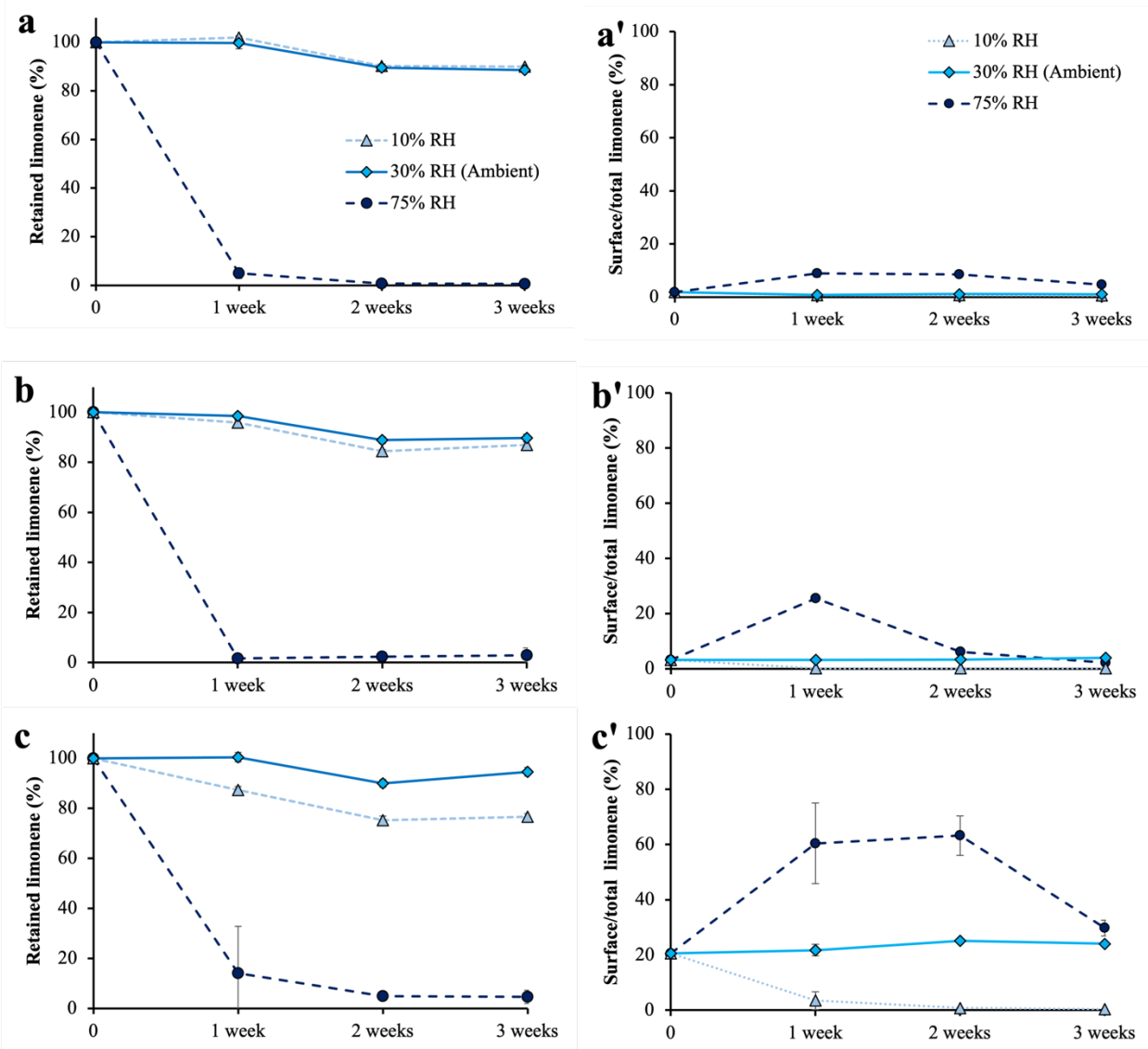


Figure 4-6. The volatile retention of D-limonene (a-c) and the surface D-limonene content (a'-c') in microcapsules stored at different storage conditions: CoCo (a and a'), low-EC CoCo (b and b'), and high-EC Coco (c and c') microcapsules.

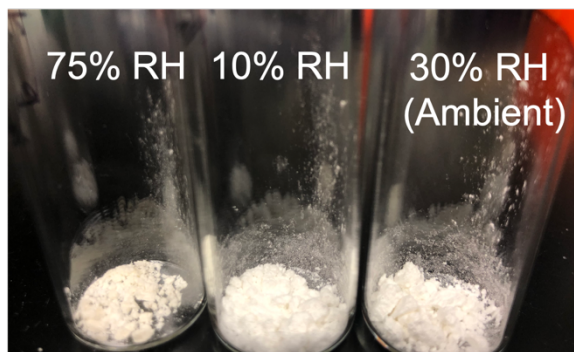


Figure 4–7. The appearance of D-limonene loaded CoCo powders stored at different conditions after 1 week.

The formation of oxidation products of D-limonene in microcapsules during storage is shown in **Figure 4–8**. Carvone and limonene oxide were measured as the indicators of D-limonene oxidation. The relative humidity can influence the formation of carvone (**Figure 4–8a-b**). Less formation of carvone was detected at higher RH (30%) compared to 10% RH condition, whereas the influence of relative humidity on the formation of limonene oxide was not significant (**Figure 4–8c and d**).

The presence of ethylcellulose in the CoCo microcapsules could accelerate the carvone formation as shown in **Figure 4–8a-b**. Similar effect was observed with limonene oxide formation (**Figure 4–8c-d**). Interestingly, limonene oxide content in the high-EC CoCo microcapsules was much higher than that in the CoCo microcapsules and the low-EC CoCo microcapsules after spray drying. However, it dropped significantly in the high EC CoCo microcapsules after 1 week storage. Slightly higher limonene oxide content was detected in the low-EC CoCo microcapsules compared to the CoCo microcapsules. Ethylcellulose in the CoCo microcapsules influenced the carvone and limonene oxide formation during storage likely through impacting the D-limonene distribution in the matrix. Ethylcellulose in the CoCo microcapsules promoted the migration of D-limonene to

surface and facilitates the oxidation, which was consistent with the implication from the volatile retention of D-limonene during spray drying and storage.

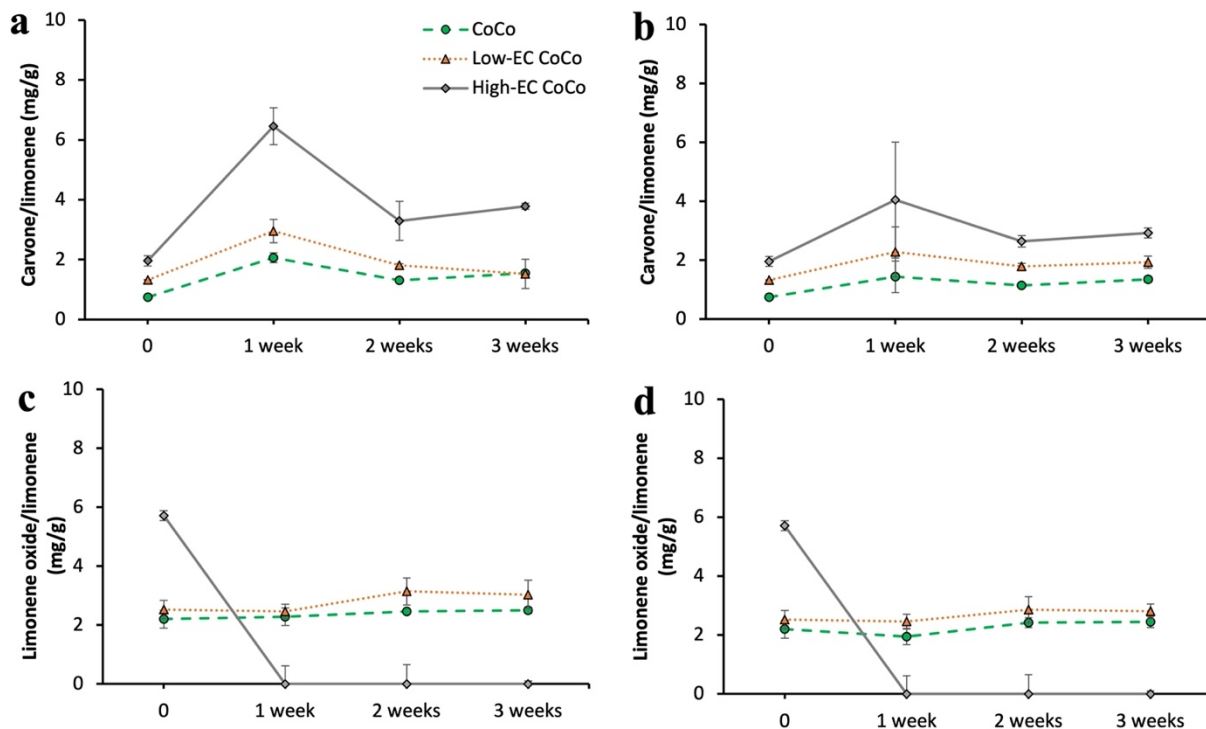


Figure 4–8. The formation of carvone (a and b) and limonene oxide (c and d) in D-limonene loaded microcapsules with/without ethylcellulose stored at 10% RH condition (a and c) and 30% RH (ambient condition) (b and d). The formation of carvone and limonene oxide in microcapsules stored at 75% RH condition was not shown because it was below the detection limits.

4.4.3 Controlled release of D-limonene from CoCo microcapsules in aqueous media

The release of D-limonene from microcapsules was investigated in water, SGF and SIF. **Figure 4–9a** shows the release of D-limonene from microcapsules in water for up to 6 hours. The difference in ethylcellulose loading in the CoCo powders impacted the release profile of D-limonene. In water, the high-EC CoCo microcapsules released $25.2 \pm 1.6\%$ of D-limonene in 2 hour, compared to $14.8 \pm 0.7\%$ from the low-EC CoCo microcapsules and $9.4 \pm 1.0\%$ from the

CoCo microcapsules. There was no significant increase of D-limonene release in water from the CoCo microcapsules regardless of the ethylcellulose content after 6 hours, demonstrating the CoCo microcapsules with or without ethylcellulose provided robust protection for retaining D-limonene in the matrix.

Faster release of D-limonene from the high-EC CoCo microcapsules in SGF was also observed at 30 min, where $25.2 \pm 1.2\%$ of D-limonene was released from the high-EC CoCo microcapsules, compared to $20.0 \pm 0.6\%$ from the low-EC CoCo microcapsules and $14.1 \pm 1.6\%$ from the CoCo microcapsules. There are two possible reasons for ethylcellulose in the CoCo microcapsules accelerating the release of D-limonene in water and SGF. First, D-limonene in the CoCo microcapsules formulated with smaller D-limonene emulsion size in the feed might diffuse out through the pores of the matrix more easily. Second, the release study in Chapter 3 demonstrated that the extent of complex coacervation, defined as the ratio of polymers coacervated to the total polymers in the matrix, influenced the release of D-limonene in water and SGF. The inclusion of ethylcellulose in the CoCo microcapsules may interfere with the complex coacervation of gelatin and alginate in the low pH conditions, leading to faster release of the cargo.

In contrast to the role of ethylcellulose in the CoCo particles on D-limonene release in water and SGF, the high-EC CoCo microcapsules appeared to be more effective at slowing down the release of D-limonene in SIF than the CoCo microcapsules without ethylcellulose. Specifically, up to $58.4 \pm 7.9\%$ of D-limonene was released from CoCo microcapsules in 5 min and increased to $83.0 \pm 2.4\%$ in 30 min, whereas the high-EC CoCo microcapsules could significantly decrease the initial burst release of D-limonene in SIF with 35.7 ± 0.1 and 41.4 ± 5.5 of D-limonene release in 5 and 10 min, respectively. The inclusion of ethylcellulose in the CoCo microcapsules attenuates the burst release of D-limonene in SIF, likely due to its effect at slowing down the solution

penetration into the matrix and the following dissolution of the matrix. The ethylcellulose in the CoCo microcapsules only showed this effect in SIF, indicating this effect could be negligible for D-limonene release when the interaction of polymers in the microcapsules in the media (e.g. in water and SGF) was strong enough.

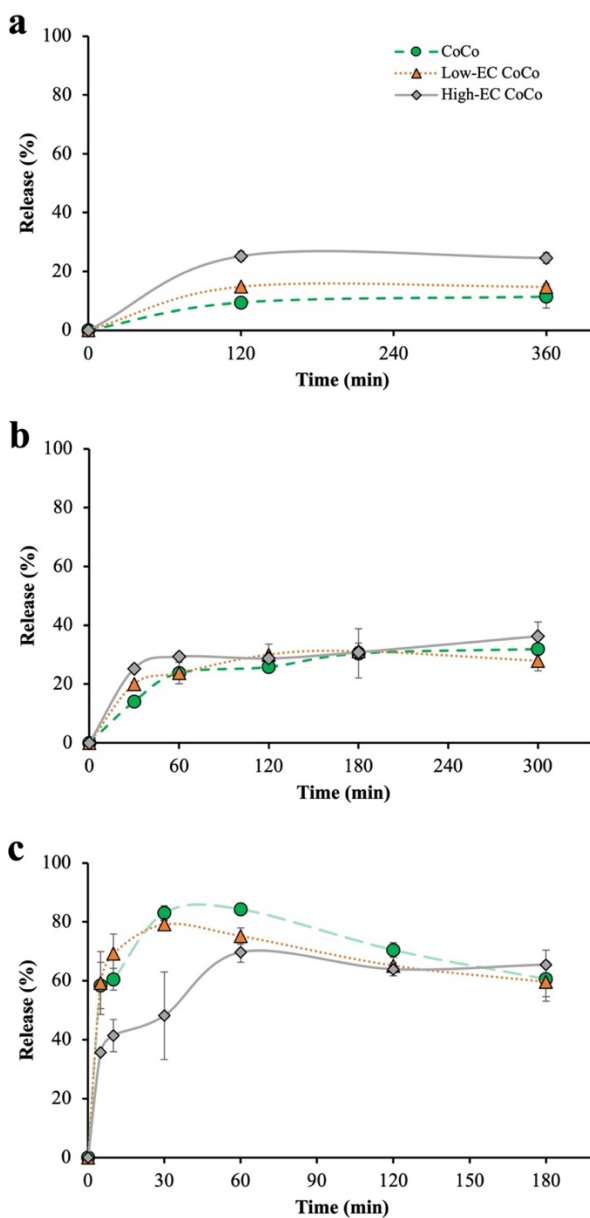


Figure 4-9. The kinetics release of D-limonene from the CoCo microcapsules with/without ethylcellulose in water (a), SGF (b) and SIF (c).

4.4.4 SEM and particle size of CoCo microcapsules

Particle size distribution of the CoCo microcapsules formulated with or without ethylcellulose were reported on a volume basis (**Figure 4–10**). The microcapsules all exhibited monomodal size distribution (**Figure 4–10**). The volume-weighted mean diameter ($D_{4,3}$), 10th percentile ($D(0.1)$), median ($D(0.5)$), and 90th percentile ($D(0.9)$) of CoCo particles were independent of the ethylcellulose content in the microcapsules. The $D_{4,3}$ of CoCo microcapsules, low-EC CoCo microcapsules and high-EC CoCo microcapsules were $15.1\pm 0.1\ \mu\text{m}$, $10.2\pm 0.4\ \mu\text{m}$, and $13.2\pm 0.8\ \mu\text{m}$ respectively and they were significantly different from each other.

There have been study reporting the microcapsules with large particle showed higher stability, (Apinan Soottitantawat et al., 2005). Large particles had less effective surface areas, resulting lower release rate and the oxidation rate of D-limonene. However, in this study, the higher surface D-limonene content and smaller emulsion size could be the primary reasons leading to the lower volatile retention of D-limonene in the CoCo microcapsules with high ethylcellulose content. Some studies also pointed out that the release rate and the oxidation rate of D-limonene were relevant to the emulsion size during storage (Jafari et al., 2007b; Apinan Soottitantawat et al., 2005). The smaller emulsion droplets had more effective surface areas that can lead to lower stability of D-limonene. In future work, tracking the emulsion size in the microcapsules during storage may lead to a better understanding of how to improve the retention and stability of D-limonene during storage.

The morphology of the microcapsules is shown in **Figure 4–11**. The microcapsules presented with irregular shape, where dents and shrinkage were prevalent. Large particles had less shrinkage compared to the small particles. Especially, the dimples feature along the surface of the particles

was observed for the EC CoCo microcapsules and was prevalent for the high-EC CoCo microcapsules. This feature could come from the evaporation of surface D-limonene during SEM, indicating surface D-limonene concentration increased with the ethylcellulose content and resulting in low retention of D-limonene.

The morphology of the microcapsules can influence the volatile retention of D-limonene during spray drying and storage. There have been reports that particles with smooth surfaces possessed less surface areas for D-limonene to release and contact with oxygen compared to groove surfaces (Apinan Soottitantawat et al., 2005). Many studies demonstrated that particles with more inner and outer surface oils usually had lower retention and poorer stability as they were easier to release and contact with oxygen (A Soottitantawat et al., 2003; Apinan Soottitantawat et al., 2005).

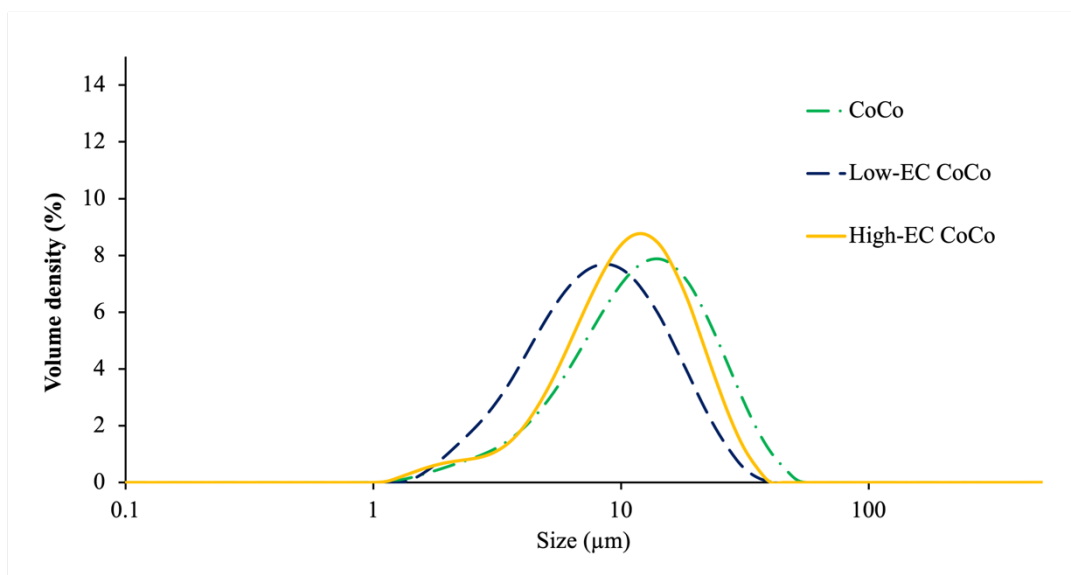


Figure 4–10. The size distribution of D-limonene loaded CoCo microcapsules with/without ethylcellulose.

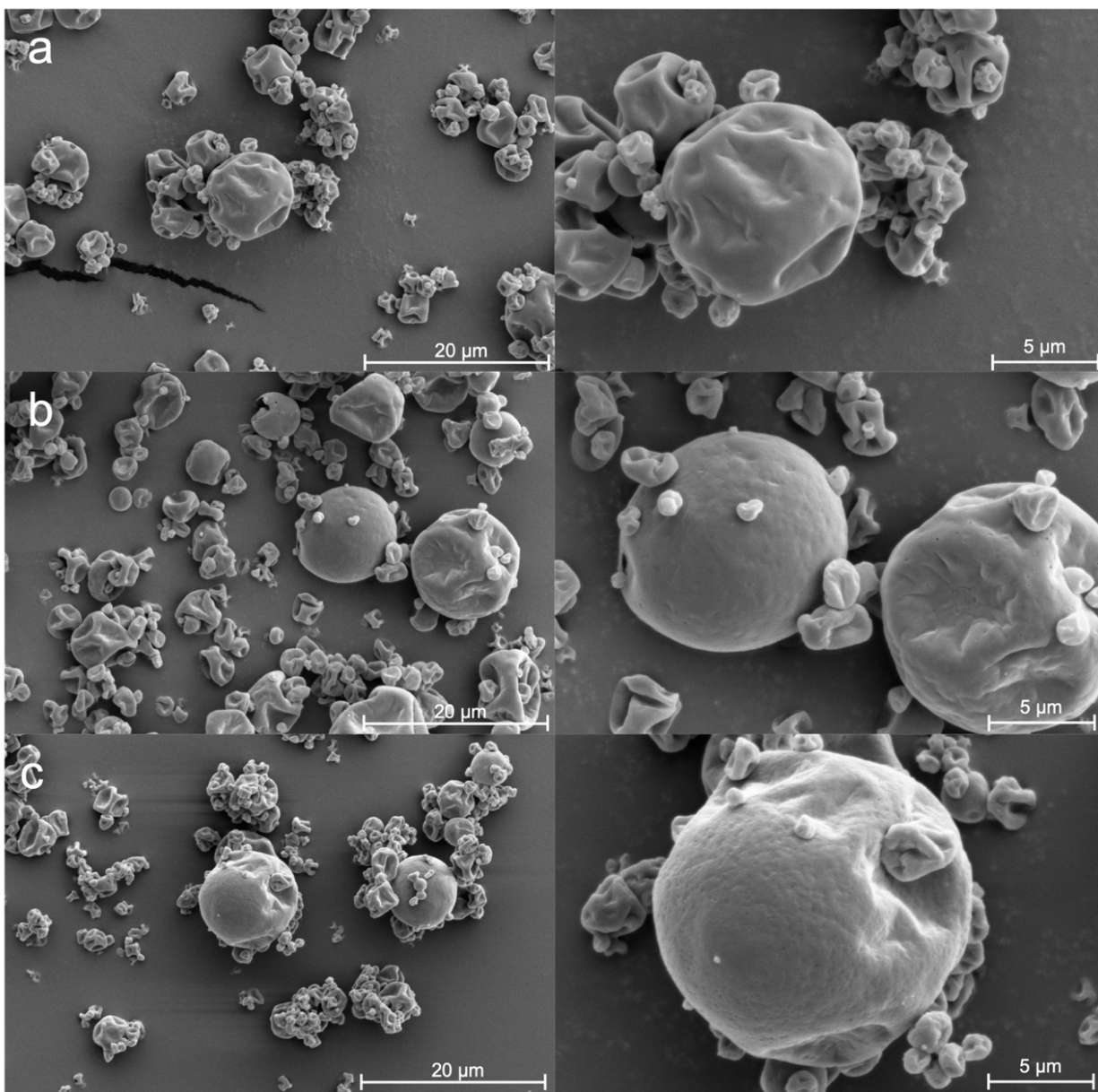


Figure 4–11. The SEM of microcapsules: CoCo (a), low-EC CoCo (b) and high-EC CoCo (c).

4.5 Conclusions

This work studied how the incorporation of a latex polymer -ethylcellulose influenced the volatile retention of D-limonene in dry powders and the release of D-limonene in aqueous environment. The CoCo microcapsules with ethylcellulose were markedly less efficient at retaining D-limonene during spray drying and storage. First, ethylcellulose could drive D-

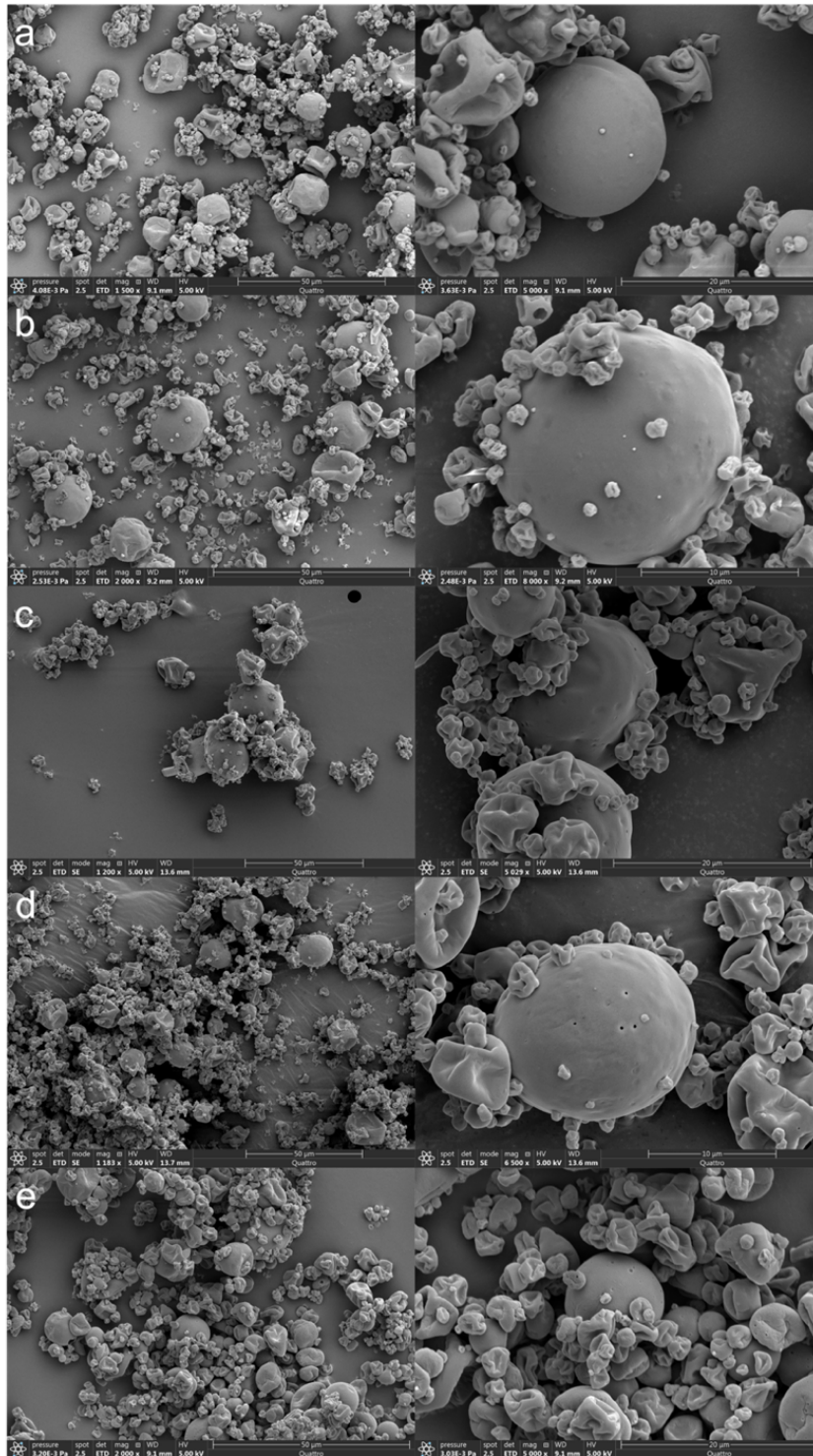
limonene to the surface of the matrix and the surfactant in ethylcellulose dispersion was effective to decrease the D-limonene emulsion size, leading to significant loss of D-limonene after spray drying. Second, instead of working as a moisture barrier, the inclusion of ethylcellulose in the CoCo microcapsules promoted the migration of D-limonene to the surface during storage, especially at high relative humidity conditions, resulting in escalated release and oxidation of D-limonene in dry powders during storage. The ethylcellulose in CoCo microcapsules also accelerated the release of D-limonene in water and SGF and slowed the initial release of D-limonene in SIF. Specially, ethylcellulose in the CoCo microcapsules sped up the release of D-limonene in water and SGF likely by affecting the complex coacervation between alginate and gelatin. Moreover, D-limonene with smaller emulsion size in the CoCo microcapsules with ethylcellulose might diffuse out through the pores of the matrix more easily. However, ethylcellulose in the CoCo microcapsules could slow down the burst release of D-limonene in SIF possibly by slowing down the penetration of water to the matrix.

Overall, ethylcellulose in the CoCo microcapsules resulted in escalated volatilization and oxidation in spray dried powders and modulated the release of D-limonene in different pH environments.

4.6 Abbreviations

CoCo, complex coacervated/complex coacervation; EC: ethylcellulose; pI, isoelectric point; ECC, extent of complex coacervation. SGF, simulated gastric fluid; SIF, simulated intestinal fluid; RH, relative humidity.

4.7 Supplementary information



Supplementary Figure 4–1. SEM of the CoCo microcapsules formed with different emulsifier: WPI (a), SPI (b), gelatin (c), casein (d) and Tween 85 (e).

Supplementary Table 4–1. Formulations used in the formation of D-limonene-loaded CoCo microcapsules using different emulsifier by spray drying.

Formulation ID ¹	Emulsifier used	Emulsifier (w/w, % w.b.)	Gelatin concentration (w/w, % w.b.) ¹	Succinic acid concentration (w/w, % w.b.) ¹	Alginate concentration (w/w, % w.b.) ^{1,2}
WPI-CoCo	Whey protein isolate	0.29	2.50	1.00	0.50
SPI-CoCo	Soy protein isolate	0.29	2.50	1.00	0.50
G-CoCo	Gelatin	0.29	2.50	1.00	0.50
Casein-CoCo	Casein	0.29	2.50	1.00	0.50
T85-CoCo	Tween 85	0.29	2.50	1.00	0.50

¹ The formulation ID were coded to indicate the emulsifier.

² Target D-limonene loading in the CoCo formulation is reported on a dry basis. The actual D-limonene loading depends on the specific coacervation process.

4.8 References

- Ahmed, A. R., Mota, J. P., Shahba, A. A.-W., & Irfan, M. (2020). *Chapter 3 - Aqueous polymeric coatings: New opportunities in drug delivery systems* (R. B. T.-D. D. A. Shegokar (ed.); pp. 33–56). Elsevier. <https://doi.org/https://doi.org/10.1016/B978-0-12-821222-6.00003-8>
- Calo, J. R., Crandall, P. G., O’Bryan, C. A., & Ricke, S. C. (2015). Essential oils as antimicrobials in food systems – A review. *Food Control*, *54*, 111–119. <https://doi.org/https://doi.org/10.1016/j.foodcont.2014.12.040>
- Chang, Y. I., Scire, J., & Jacobs, B. (1988). Effect of Particle Size and Microstructure Properties on Encapsulated Orange Oil. In *Flavor Encapsulation* (Vol. 370, pp. 10–87). American Chemical Society. <https://doi.org/doi:10.1021/bk-1988-0370.ch010>
- Ciriminna, R., Lomeli-Rodriguez, M., Demma Carà, P., Lopez-Sanchez, J. A., & Pagliaro, M. (2014). Limonene: a versatile chemical of the bioeconomy. *Chemical Communications*, *50*(97), 15288–15296. <https://doi.org/10.1039/C4CC06147K>
- d’Alessio, P. A., Ostan, R., Bisson, J.-F., Schulzke, J. D., Ursini, M. V., & Béné, M. C. (2013). Oral administration of d-Limonene controls inflammation in rat colitis and displays anti-inflammatory properties as diet supplementation in humans. *Life Sciences*, *92*(24), 1151–1156. <https://doi.org/https://doi.org/10.1016/j.lfs.2013.04.013>
- Espina, L., Gelaw, T. K., de Lamo-Castellví, S., Pagán, R., & García-Gonzalo, D. (2013). Mechanism of Bacterial Inactivation by (+)-Limonene and Its Potential Use in Food Preservation Combined Processes. *PLOS ONE*, *8*(2), e56769. <https://doi.org/10.1371/journal.pone.0056769>
- Jafari, S. M., He, Y., & Bhandari, B. (2007a). Encapsulation of Nanoparticles of d-Limonene by Spray Drying: Role of Emulsifiers and Emulsifying Techniques. *Drying Technology*, *25*(6), 1069–1079. <https://doi.org/10.1080/07373930701396758>
- Jafari, S. M., He, Y., & Bhandari, B. (2007b). Role of Powder Particle Size on the Encapsulation Efficiency of Oils during Spray Drying. *Drying Technology*, *25*(6), 1081–1089.

- <https://doi.org/10.1080/07373930701397343>
- Keddie, J. L., & Routh, A. F. (2010). *An Introduction to Latex and the Principles of Colloidal Stability BT - Fundamentals of Latex Film Formation: Processes and Properties* (J. L. Keddie & A. F. Routh (eds.); pp. 1–26). Springer Netherlands. https://doi.org/10.1007/978-90-481-2845-7_1
- Lecomte, F., Siepmann, J., Walther, M., MacRae, R. J., & Bodmeier, R. (2004). Polymer blends used for the aqueous coating of solid dosage forms: importance of the type of plasticizer. *Journal of Controlled Release*, 99(1), 1–13. <https://doi.org/https://doi.org/10.1016/j.jconrel.2004.05.011>
- Petereit, H.-U., & Weisbrod, W. (1999). Formulation and process considerations affecting the stability of solid dosage forms formulated with methacrylate copolymers. *European Journal of Pharmaceutics and Biopharmaceutics*, 47(1), 15–25. [https://doi.org/https://doi.org/10.1016/S0939-6411\(98\)00083-6](https://doi.org/https://doi.org/10.1016/S0939-6411(98)00083-6)
- Soottitantawat, A., Yoshii, H., Furuta, T., Ohkawara, M., & Linko, P. (2003). Microencapsulation by Spray Drying: Influence of Emulsion Size on the Retention of Volatile Compounds. *Journal of Food Science*, 68(7), 2256–2262. <https://doi.org/10.1111/j.1365-2621.2003.tb05756.x>
- Soottitantawat, Apinan, Bigeard, F., Yoshii, H., Furuta, T., Ohkawara, M., & Linko, P. (2005). Influence of emulsion and powder size on the stability of encapsulated d-limonene by spray drying. *Innovative Food Science & Emerging Technologies*, 6(1), 107–114. <https://doi.org/https://doi.org/10.1016/j.ifset.2004.09.003>
- Soottitantawat, Apinan, Yoshii, H., Furuta, T., Ohgawara, M., Forssell, P., Partanen, R., Poutanen, K., & Linko, P. (2004). Effect of Water Activity on the Release Characteristics and Oxidative Stability of d-Limonene Encapsulated by Spray Drying. *Journal of Agricultural and Food Chemistry*, 52(5), 1269–1276. <https://doi.org/10.1021/jf035226a>
- Strobel, S. A., Scher, H. B., Nitin, N., & Jeoh, T. (2016). In situ cross-linking of alginate during spray-drying to microencapsulate lipids in powder. *Food Hydrocolloids*, 58, 141–149. <https://doi.org/https://doi.org/10.1016/j.foodhyd.2016.02.031>
- Swackhamer, C., Zhang, Z., Taha, A. Y., & Bornhorst, G. M. (2019). Fatty acid bioaccessibility and structural breakdown from in vitro digestion of almond particles. *Food & Function*, 10(8), 5174–5187. <https://doi.org/10.1039/C9FO00789J>
- Tang, Y., Scher, H. B., & Jeoh, T. (2020). Industrially scalable complex coacervation process to microencapsulate food ingredients. *Innovative Food Science & Emerging Technologies*, 59, 102257. <https://doi.org/https://doi.org/10.1016/j.ifset.2019.102257>
- Tang, Y., Scher, H., & Jeoh, T. (2021). *Microencapsulation of chemicals and bioactives by in situ complex coacervation during spray drying*. U.S. Patent Application No. 17/178,866, Publication No. US20210316265A1.
- Wasilewska, K., & Winnicka, K. (2019). Ethylcellulose—A Pharmaceutical Excipient with Multidirectional Application in Drug Dosage Forms Development. In *Materials* (Vol. 12, Issue 20). <https://doi.org/10.3390/ma12203386>

Chapter 5 Enteric release of therapeutic peptides encapsulated by complex coacervated microcapsules formed by spray drying

5.1 Abstract

Oral delivery of therapeutic peptides faces substantial barriers as the peptides are highly susceptible to denaturation, aggregation or hydrolysis during digestion. This study explored the potential of the CoCo process to encapsulate peptides for enteric release using five peptides - semaglutide, liraglutide, GLP-1, gonadorelin acetate and oxytocin acetate as model peptides. The formulation development demonstrated that promising enteric release of semaglutide and liraglutide could be achieved with 0.25 parts latex polymers -1.0 part CoCo polymers made by gelatin, alginate and succinic acid. Specifically, only $12.3 \pm 0.7\%$ of semaglutide and $24.0 \pm 0.5\%$ of liraglutide were released in simulated gastric fluid in 2h from complex coacervation microcapsules with the inclusion of ethylcellulose, while more than 88% of peptides was released in simulated intestinal fluid. This work demonstrated the physicochemical properties of the peptides were relevant to the oral bioavailability of peptide and the CoCo process could energize the development of the oral delivery of peptide for medical use.

5.2 Introduction

Peptides, which are short chains of amino acids, provide numerous health benefits and play important roles in treating various diseases (Lau & Dunn, 2018). For peptide formulation development in pharmaceutical industry, there are many challenges including the hydrophilicity/hydrophobicity of peptide influencing its incorporation, the stability affected by environmental factors such as temperature, light and pH, the bioavailability in digestive conditions, bitterness leading to limitations in oral formulation, hygroscopicity leading to physicochemical

instability etc. (Elias et al., 2008; McClements, 2018; Udenigwe, 2014). Subcutaneous injection has established for peptide delivery. For example, peptide such as semaglutide used for the treatment of type 2 diabetes was approved for medical use as an injection version (tradename: Ozempic®). Semaglutide binds to albumin, making it more resistant to the degradation by dipeptidyl peptidase-4 (Bækdal et al., 2021). Trulicity® and Victoza®, known as GLP-1 agonists used for the treatment of type 2 diabetes, are another two injectable non-insulin medications. Oral delivery of peptide is especially desirable due to dosing convenience, patient acceptance, potential shorter treatment period and low cost. However, the oral delivery of peptide is highly challenging (McClements, 2018), and the challenges are related to the normal physiological roles of the gastrointestinal tract (Drucker, 2020). First, peptides are susceptible to denaturation, aggregation, or hydrolysis in the stomach due to the low pH and the presence of proteolytic enzymes. Second, the gastrointestinal tract has a set of cellular and mucus barriers, restricting the passage of peptide (Drucker, 2020). Different strategies including permeation enhancer, modulation of pH, direct enzyme inhibition, peptide cyclization, mucus-penetrating agents, as well as cell penetrating peptides etc. have been designed to overcome these barriers (Drucker, 2020). So far, Rebelsus® approved in 2019 is the first and only oral tablet version of glucagon-like peptide 1 receptor agonist semaglutide (Brayden et al., 2020; Drucker, 2020). The tablet containing 10 mg of semaglutide and 300 mg of sodium N-[8-(2-hydroxybenzoyl)amino] caprylate (SNAC; also known as salcaprozate sodium) protects the peptide in the stomach through a localized increase in pH, prohibiting pepsin activation and also facilitating the absorption of semaglutide across the gastric epithelium as a permeation enhancer (Buckley et al., 2018). SNAC and sodium caprate (C10; also known as decanoic acid) are the few enhancers have demonstrated safety and efficacy to process towards clinical trials (Twarog et al., 2019). Silica nanoparticles have emerged as a

biodegradable inorganic nanocarrier for oral drug delivery (Abeer et al., 2020). For example, silica-coated nanoparticles formulated with two established excipients and stabilizers, zinc chloride and L-arginine, has been studied for insulin oral delivery (Hristov et al., 2020). However, hydrogel for oral peptide delivery has made very limited progress toward clinical use.

Microencapsulation is one solution to facilitate the application of peptides by protecting peptides against stressful conditions, masking bitterness, providing targeted release and improving bioavailability and stability of peptides (Sarabandi et al., 2020). Among the different techniques of microencapsulation, complex coacervation is a promising technique to offer intrinsic advantages and unique properties in terms of high payloads, controlled release under circumstances such as thermal and mechanical stress and digestion (Gouin, 2004). However, the high-cost and multi-step process of conventional complex coacervation process makes it highly challenging to scale up (Dong et al., 2011; Saravanan & Rao, 2010; Yang et al., 2014). In this study, the CoCo process was used (Tang et al., 2020, 2021). This novel process forms complex coacervation microcapsules using a low-cost and industrially scalable spray drying process.

A latex dispersion is a colloidal dispersion that can be prepared from any existing thermoplastic water insoluble polymer. It forms a thin film as water evaporates if the operational conditions are above the glass transition temperature (T_g) of the latex polymer (Keddie & Routh, 2010). Latex polymers dispersions have been extensively studied for film coating, thereby applying to solid substrates for the protection of substances from environmental conditions. The aqueous-based film coating technologies have made significance improvements in drug release (Ahmed et al., 2020; Lecomte et al., 2004; Petereit & Weisbrod, 1999). For example, there are many kinds of aqueous based polymers used for controlled release coating. Ethylcellulose (EC) is an ethyl ether of cellulose and is widely used in pharmaceutical industry. Ethylcellulose is

insoluble and impermeable to water and has been used for moisture protection and taste masking (Wasilewska & Winnicka, 2019). Enteric-coating polymer latexes, such as polymethacrylates like copolymer of methacrylic acid and methyl methacrylate or ethyl acrylate, cellulose derivatives like cellulose acetate phthalate (CAP), hydroxypropyl methylcellulose phthalate, hydroxypropyl methylcellulose acetate succinate, and vinyl derivatives (polyvinyl acetate phthalate (PVAP)), can be used for enteric coating (Zu et al., 2007). Enteric polymers demonstrate resistances to gastric fluids due to the un-ionized acidic functional groups and dissolve readily in intestinal fluids by forming salts with alkalis or amines to release drugs (Zu et al., 2007). There have been extensive efforts to improve the efficacy of coating, including optimization of curing conditions, modulating the T_g by the optimization of polymer blend coating and plasticizer type and content, and the addition of hydrophilic excipients (Ahmed et al., 2020). However, no study has investigated how the combination of latex polymers and a complex coacervation system protects the cargo under gastric conditions.

In this study, five peptides were used as model peptides: semaglutide, liraglutide, GLP-1, gonadorelin acetate and oxytocin acetate. Semaglutide, liraglutide and GLP-1 are peptides for diabetes treatment (Knudsen & Lau, 2019; Wang et al., 2015). Gonadorelin acetate is used for treating diseases related to gonadotropin-releasing hormone (Rastogi et al., 2019). Oxytocin acetate is therapeutically used for induce or stimulate labor and to prevent post-partum hemorrhage (Hawe et al., 2009). The study aimed to investigate the potential of the CoCo process to encapsulate peptides for enteric release, as well as how the incorporation of latex polymer to the CoCo system protects peptides under gastric conditions. **Figure 4–1** in Chapter 4 is the schematic of the formation of bioactive loaded CoCo powder with/without latex polymer using the CoCo process. Alginate and gelatin were used as matrix building polymer (Tang et al., 2020). I

hypothesized that: (1) the formation of the CoCo matrix protects peptide from releasing in simulated gastric environment and enables the release of majority peptide in simulated intestinal environment; (2) the incorporation of the latex polymer serves as an extra layer of protection for the peptide in gastric environment; (3) alginate classified as an anionic mucoadhesive polymer could facilitate the passage of peptide through mucus layer (Gombotz & Wee, 2012). This work explored the opportunities for the development of the oral peptide delivery using a cost-effective process.

5.3 *Materials and methods*

5.3.1 *Materials*

Peptides (semaglutide with batch No. of P210303-F003, liraglutide with batch No. of P200117-B012, GLP-1 with batch No. of P210118-A032, gonadorelin acetate with batch No. of P201014-A020 and oxytocin acetate with batch No. of P200516-A013) were provided by Wuxi STA (SynTheAll Pharmaceutical Co., Ltd).

Gelatin (type A with an isoelectric point of 7) was purchased from Sigma Aldrich (St. Louis, MO). High viscosity sodium alginate (GRINDSTED Alginate FD 155 with pKa of 3.5) was from Dupont Nutrition and Health. Succinic acid, ammonium hydroxide, sodium chloride, hydrochloric acid, sodium hydroxide, monopotassium phosphate and dipotassium phosphate were purchased from Fisher Scientific (Fair Lawn, NJ). MilliQ water with a minimum resistivity of 18 MU-cm (Millipore, Billerica, MA) was used for all experiments (referred in text as water).

Aquacoat® ECD 30 (aqueous colloidal dispersion of ethylcellulose polymer) and Sureteric® aqueous enteric coating system were provided by Colorcon (Harleysville, PA) and tributyl citrate was purchased from TCI America (Portland, OR). EUDRAGIT® L 30 D-55 and PLASACRYL

HTP 20 were provided by Evonik (Piscataway, NJ). Aquacoat® CPD 30 was provided by IFF Nutrition and Bioscience (Newark, DE).

ETOCAS 35 (HLB of 13) and Tween 80 (HLB of 15) were from Croda.

5.3.2 Methods

5.3.2.1 Formation of peptide loaded CoCo microcapsules with the latex polymer by the CoCo process

The CoCo process feed consisted of 0.582% (w/w) gelatin, 0.109% (w/w) alginate and 0.109% (w/w) succinic acid and 0.2 % (w/w) peptide. The pH of the feed was adjusted to 8~8.8 using ammonium hydroxide before adding peptide.

The Aquacoat® ECD 30 is 30% ethylcellulose stabilized by sodium lauryl sulfate (SLS) and cetyl alcohol (referred to as EC). The EUDRAGIT® L 30 D-55 is methacrylic acid copolymer, which is type C methacrylic acid and ethyl acrylate copolymer with ratio of 1:1 (referred to as MAC). Sureteric® aqueous enteric coating system is specially blended combination of polyvinyl acetate phthalate, plasticizers and other processing ingredients (referred to as PVAP). The Aquacoat® CPD 30 is 30% solid with 80% cellulose acetate phthalate (CAP) included (referred to as CAP).

All the latex (EC, MAC, PVAP and CAP) CoCo feed contained 0.582% (w/w) gelatin, 0.109% (w/w) alginate and 0.109% (w/w) succinic acid, 0.2% peptide and 25% of latex polymer based on the CoCo solid content of the CoCo feed. In addition, the EC CoCo feed contained 25% of tributyl citrate based on the mass of ethylcellulose in the feed. The MAC CoCo feed contained 17% of PLASACRYL HTP 20 based on the mass of methacrylic acid copolymer in the feed. The CAP CoCo feed contained 35% of tributyl citrate based on the mass of cellulose acetate phthalate in the

feed. These levels of plasticizer were added to the latex polymer, so that the outlet temperature of the spray dryer was above the glass transition temperature of the latex polymer-plasticizer combination. For the controlled experiment, the controlled feed was prepared as the same but without peptide in each formulation. The formulations and the corresponding sample IDs are shown in **Table 5–1**.

The feed was spray dried by a Buchi B290 laboratory spray dryer. The spray drying conditions were set as follows: inlet air temperature at 150 °C, aspirator airflow rate at maximum (35 m³/h), feed peristaltic pump at 20% of maximum (6 ml/min), and 40 mm nozzle pressure (0.41 bar).

5.3.2.2 Release of peptides from microcapsules in water, simulated gastric fluid and intestinal fluids

To determine the extent of peptide release in aqueous media, the peptides loaded powder and the control powder (containing no peptide) were dispersed in MilliQ water, simulated gastric fluid (SGF, 8.78 mg/ml sodium chloride at pH 1.8) and simulated intestinal fluid (SIF, 50 mM phosphate buffer at pH 7.4) and 50 mM phosphate buffer at pH 8.5 (PB 8.5). The CoCo powder and CoCo powder with latex polymer were dispersed in the respective fluids at 0.1% (w/v) and 0.2% (w/v). The dispersion in water was rotated at 20 rpm at room temperature for 2 h or 20 h. The dispersion in PB 8.5 was rotated at 20 rpm at room temperature for 2 h or 20 h including incubated at 37 °C water bath for 10 min. The dispersion in SGF and SIF was incubated at 37 °C and rotated at 20 rpm for 2 h or 20 h. The release was done by duplicate for each sample.

Table 5–1. Formulations used in the formation of peptide loaded CoCo powders by spray drying.

Latex polymer	Sample IDs	Peptide	Formulation
Ethylcellulose (EC)	Semaglutide EC CoCo	Semaglutide	0.582% (w/w) gelatin, 0.109% (w/w) alginate and 0.109% (w/w) succinic acid, 0.2% peptide, 25% of EC based on the solid content of the CoCo feed and 25% of tributyl citrate based on the mass of EC in the feed
	Liraglutide EC CoCo	Liraglutide	
	GLP-1 EC CoCo	GLP-1	
	Gonadorelin EC CoCo	Gonadorelin acetate	
	Oxytocin EC CoCo	Oxytocin acetate	
Methacrylic acid copolymer (MAC)	Semaglutide MAC CoCo	Semaglutide	0.582% (w/w) gelatin, 0.109% (w/w) alginate and 0.109% (w/w) succinic acid, 0.2% peptide, 25% of MAC based on the solid content of the CoCo feed and 17% of PLASACRYL HTP 20 based on the mass of EC in the feed
	Liraglutide MAC CoCo	Liraglutide	
	GLP-1 MAC CoCo	GLP-1	
	Gonadorelin MAC CoCo	Gonadorelin acetate	
	Oxytocin MAC CoCo	Oxytocin acetate	
Polyvinyl acetate phthalate (PVAP)	Semaglutide PVAP CoCo	Semaglutide	0.582% (w/w) gelatin, 0.109% (w/w) alginate and 0.109% (w/w) succinic acid, 0.2% peptide, 25% of PVAP based on the solid content of the CoCo feed
Cellulose acetate phthalate (CAP)	Semaglutide CAP CoCo	Semaglutide	0.582% (w/w) gelatin, 0.109% (w/w) alginate and 0.109% (w/w) succinic acid, 0.2% peptide, 25% of CAP based on the solid content of the CoCo feed and 35% of tributyl citrate based on the mass of CAP in the feed
N/A	Semaglutide CoCo	Semaglutide	0.582% (w/w) gelatin, 0.109% (w/w) alginate and 0.109% (w/w) succinic acid, 0.2% peptide
	Liraglutide CoCo	Liraglutide	
	GLP-1 CoCo	GLP-1	
	Gonadorelin CoCo	Gonadorelin acetate	
	Oxytocin CoCo	Oxytocin acetate	

5.3.2.3 Quantification of the released peptides

5.3.2.3.1 Quantification of peptide release in aqueous media

At the 2 h time point, 1 ml aliquot was withdrawn from the sample and centrifuged at 10,000 g for 2 min (for the CoCo and the MAC CoCo sample) and 20,000 g for 2 or 5 min for (EC, PVAP and CAP sample). At 20 h time point, another 1 ml aliquot was withdrawn from sample and treated by the same procedure as described above. 200 µl of the supernatant was added to the 96 well UV plate and each sample was measured triplicated at A280 for semaglutide, liraglutide and GLP-1 sample, A278 for gonadorelin acetate sample and A274 for oxytocin acetate sample by Synergy 4 microplate reader from Bio Tek. The baseline was corrected at A340. The interference of gelatin was corrected by the controlled sample without peptide.

5.3.2.3.2 Quantification of semaglutide release from microcapsules in SGF

Semaglutide has a low solubility in low pH media and ETOCAS 35 with a 5:1 ETOCAS 35 to peptide ratio was added to facilitate the solubilization of released semaglutide in SGF. For 2 h/20 h release, the ETOCAS 35 was added after the sample was incubated and rotated at 37 °C for 1h 30 min/19 h 30 min and sample was put back to 37 °C incubator and rotated at 20 rpm for 30 min to solubilize the released semaglutide and the total release time was 2 h/20 h. At end of release, 1ml aliquot was withdrawn and centrifuged at 20,000 g for 2 min. 200 µl of the supernatant were added to the 96 well UV plate and each sample was measured triplicated. The release was done duplicated.

5.3.2.3.3 *Quantification of liraglutide release from microcapsules in water and SGF*

1.5 mg/ml of Tween 80 was added to facilitate the solubilization of liraglutide from the CoCo powder with and without latex polymer in water and SGF. For 2 h/20 h release, the Tween 80 was added after the sample was incubated and rotated at 37 °C for 1h 40 min/19 h 40 min and sample was put back to 37 °C incubator and rotated at 20 rpm for 20 min to solubilize the released liraglutide and the total release time was 2 h/20 h. At end of release, 1ml aliquot was withdrawn and centrifuged at 20,000 g for 2 min. 200 µl of the supernatant were added to the 96 well UV plate and each sample was measured triplicated. The release was done duplicated.

5.3.2.4 *Standard curves for each peptide*

5.3.2.4.1 *Standard curve for peptide dissolve well in water, PB 8.5, SGF and SIF*

10 mg peptide was dissolved in 20 ml MilliQ, PB 8.5, SGF and SIF. The peptide in water was rotated at 20 rpm at room temperature for 2 h. The peptide in PB 8.5 was rotated at 20 rpm at room temperature for 2 h including incubated at 37 °C water bath for 10 min. The peptide in SGF and SIF was incubated at 37 °C and rotated at 20 rpm for 2 h. The peptide standard was prepared in a range of 0 to 0.5 mg/ml and 200 µl of the standard was added to the 96 well UV plate and each sample was measured triplicated at A280 for semaglutide, liraglutide and GLP-1, A278 for gonadorelin acetate and A274 for oxytocin acetate.

5.3.2.4.2 *Standard curve for semaglutide in SGF*

5 mg semaglutide was dispersed in 10 ml SGF for 30 min. Then, 26.5 mg of ETOCAS 35 was added and the standard was incubated at 37 °C and rotated at 40 rpm for 1h until it's clear. The standard was centrifuged at 20,000g for 2 min. To eliminate the interference of ETOCAS 35, same

amount of ETOCAS 35 was added to 10 ml SGF and went through the same procedure (as control). The peptide standard was prepared in a range of 0 to 0.5 mg/ml and 200 µl of the standard was added to the 96 well UV plate and each sample was measured triplicated at A280.

5.3.2.4.3 *Standard curve for liraglutide in water and SGF*

10 mg liraglutide was dispersed in 20 ml water and SGF for 30 min. Then, 30 mg of Tween 80 was added. The standard in water was rotated at 20 rpm at RT for 20 min until it's clear. The standard in SGF was incubated at 37 °C and rotated at 20 rpm for 20 min until it's clear. The standard was centrifuged at 20,000 g for 2 min. To eliminate the interference of Tween 80, the same amount of Tween 80 was added to 20 ml water and SGF and went through the same procedure (as control). The peptide standard was prepared in a range of 0 to 0.5 mg/ml and 200 µl of the standard was added to the 96 well UV plate and each sample was measured triplicated at A280.

5.3.2.5 *Particle size measurement of peptide loaded microcapsules*

Spray dried powders were dispersed in propan-2-ol and sonicated for 1 or 2 min until good dispersion was observed, the sample was then added to the dispersion unit and circulated until the initial sample obscuration was stable before initiating measurement. The settings for the analyzer were as follows: material type of particle with refractive index 1.57 and absorption index 0.01, dispersant type of propan-2-ol with dispersant refractive index of 1.37, temperature: 25 °C. Each sample was measured in triplicate.

5.3.2.6 SEM of peptide loaded microcapsules

Spray dried CoCo powders were mounted on double- sided carbon tape and coated with 10 nm gold. The SEM images were produced by the Thermo Fisher Quattro S environmental SEM with an electron beam acceleration voltage of 5 kV and spot size of 3.0.

5.3.2.7 Statistical analysis

Data were reported as mean \pm standard deviation. ANOVA and Tukey's post hoc multiple comparison test were used to determine differences among factor levels. Statistical analysis was performed using JMP (SAS Institute Inc., Cary, NC, USA). P-values less than 0.05 were considered significant.

5.4 Results

5.4.1 2h release profile of peptides from CoCo microcapsules in aqueous media

The release of semaglutide in aqueous solutions from microcapsules generated from four formulations after a 2 h incubation is shown **Figure 5–1a**. In water, 18.3% of the loaded semaglutide was released from the CoCo powder, significantly more than that released from the latex CoCo powders. All the latex polymers showed impressive performance in preventing semaglutide release in water. In SGF, only 12.3% and 17.8% of the loaded semaglutide was released from the EC CoCo and PVAP CoCo powders, significantly less than that of 23.1%, 40.3% and 38.3% from the CAP CoCo, the MAC CoCo and the CoCo powder, respectively. In SIF, up to 88.4 to 93.8% of the loaded semaglutide was released from powders generated from five formulations. The dissolution of the matrix has led to the overwhelming release of the peptide. The latex CoCo system demonstrated promising enteric release behavior.

The 2 h release profile of liraglutide from microcapsules is shown in **Figure 5–1b**. Up to 84.0% of liraglutide was released from the CoCo powder in water after 2 h incubation, while only small fraction of liraglutide (0.0% and 3.4%) was released from the EC and MAC CoCo powder. 73.2% of liraglutide was released from the CoCo powder in SGF, which significantly dropped to 24.0% and 31.6% release from the EC and MAC CoCo powder, respectively. Complete release of liraglutide was observed in SIF for all the three formulations. Similar to the semaglutide release profile, the CoCo powder with the latex polymer, especially the EC CoCo powder exhibited promising enteric release and helped to retain liraglutide in water.

The 2 h release profile of GLP-1 from microcapsules is shown in **Figure 5–1c**. Very small fraction of GLP-1 was released from all the three microcapsules in water. Robust protection of GLP-1 in water was achieved in either the latex CoCo or the CoCo microcapsules alone. In SGF, 41.2% of GLP-1 was released from the EC CoCo powder, 71.6% of GLP-1 was released from the MAC powder and up to 82.7% of GLP-1 was released from the CoCo powder. Although the EC CoCo microcapsules was able to maintain up to 60% of GLP-1 in SGF, it was not as effective as that for semaglutide and liraglutide. The majority of GLP-1 was released in SIF for all the three formulations.

The 2 h release profile of gonadorelin acetate is shown in **Figure 5–1d**. The lowest release fraction of gonadorelin acetate was 45.8% in the MAC CoCo powder in water. 54.3% of gonadorelin acetate was released from the EC CoCo powder in water. The CoCo formulation alone also provided some protection for gonadorelin acetate in water but released 67.0% of gonadorelin acetate. Nearly complete release of gonadorelin acetate in SGF and SIF were observed.

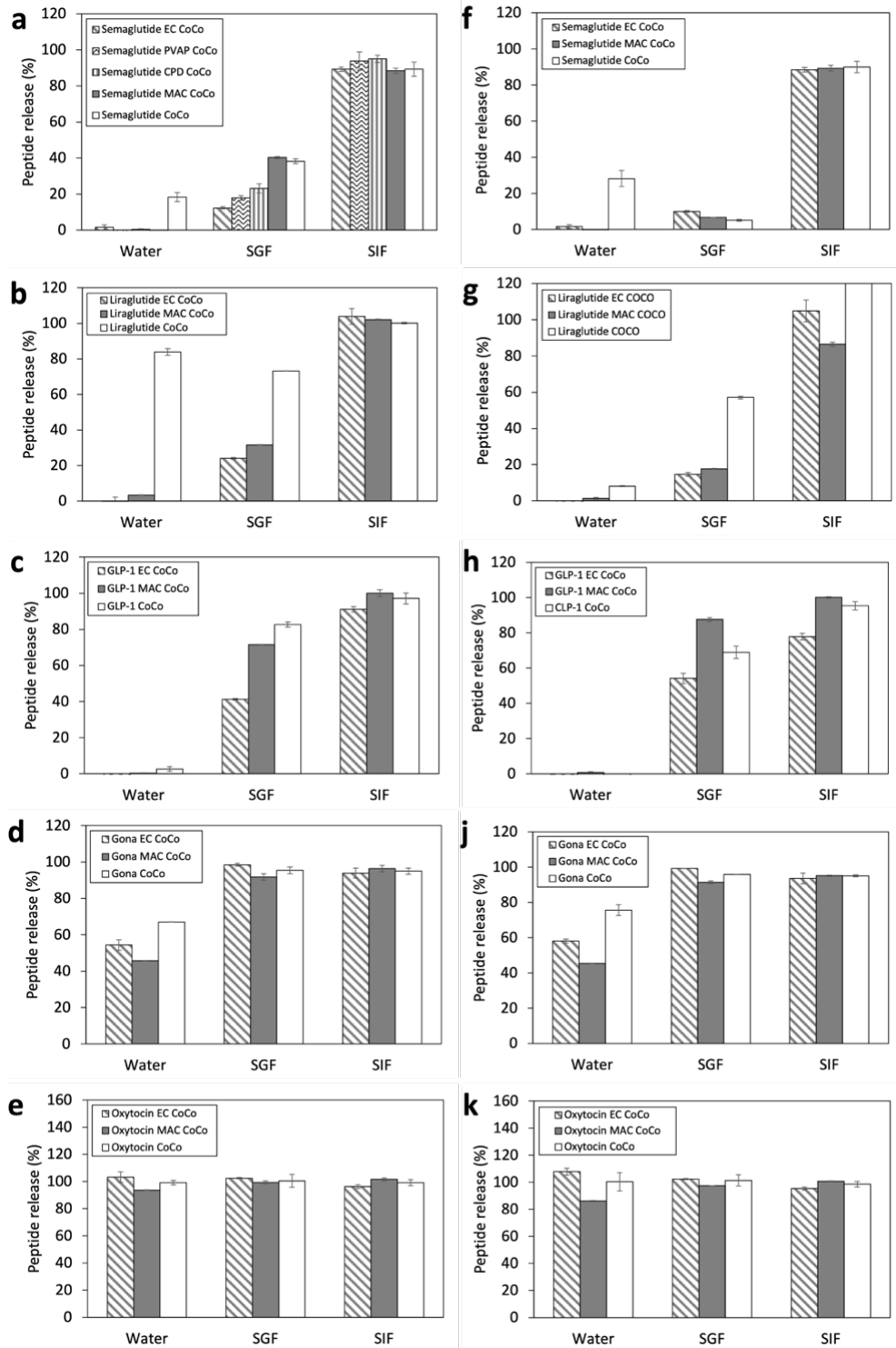


Figure 5–1. 2 h (a, b, c, d, e) and 20h (f, g, h, j, k) release profile of peptides from CoCo microcapsules with latex polymer and the CoCo microcapsules: semaglutide (a, f); liraglutide (b, g); GLP-1 (c, h); gonadorelin acetate (Gona) (d, j); oxytocin acetate (e, k). Ethylcellulose (EC), polyvinyl acetate phthalate (PVAP), cellulose acetate phthalate (CAP), methacrylic acid copolymer (MAC).

The 2 h release profile of oxytocin acetate is shown in **Figure 5–1e**. More than 90% of oxytocin acetate was released from the latex CoCo and the CoCo microcapsules in water, SGF and SIF for microcapsules. No protection of oxytocin acetate was accomplished by either the latex CoCo powder or the CoCo powder alone. Oxytocin acetate is very challenging to retain in the CoCo matrix in aqueous environments.

5.4.2 20h release profile of peptides from CoCo microcapsules in aqueous media

The release profile of semaglutide after 20 h incubation is shown in **Figure 5–1f**. The release of semaglutide from the CoCo powder was increased from 18.3% to 28.1% after 18 hours longer incubation in water. The very small fraction of semaglutide from the EC and MAC CoCo powder in water was released after longer incubation. It indicated that the addition of latex polymers in the CoCo microcapsules provided long term protection for semaglutide in water. The released fraction of semaglutide from microcapsules in SGF after 20 h incubation was decreased from all the three powders and it could be linked to the degradation of semaglutide in SGF. No change has been observed for semaglutide release from the microcapsules in SIF after 20 h incubation compared to 2 h incubation.

The release profile of liraglutide after a 20 h incubation is shown in **Figure 5–1g**. The release of liraglutide from the EC and MAC CoCo powder in water after 20 h was consistent with the results of 2 h release profile. However, only 8.1% of liraglutide was released after 20 h from the CoCo powder in water, compared to 84.0% of liraglutide released after 2 h incubation. There could be some interaction between liraglutide and the matrix and hinder its release during long term

incubation. The released liraglutide in SGF after 20 h incubation was lower than the released fraction of 2 h, indicating the degradation of liraglutide in SGF. In another study, I tested the stability of liraglutide in different media after a 20 h incubation (**Figure 5–2**). Only 46% of liraglutide was recovered after 20 h incubation in SGF, suggesting that the decrease in liraglutide seen 20 h incubation in SGF is due to degradation. The increased signal of liraglutide in SIF after 20 h explained that the percent of liraglutide release from the CoCo powder was beyond 100% in **Figure 5–1g**.

The release profile of GLP-1 after 20 h incubation is shown in **Figure 5–1h**. Almost no GLP-1 was released from the microcapsules in water after long time incubation. The released fraction of GLP-1 was increased from 41.2% to 54.1% in the EC CoCo powder after 20 h SGF incubation and increased from 71.6% to 87.6% in the MAC CoCo powder, while the released GLP-1 was decreased to 68.9% to 82.7% from the CoCo powder. The decrease has also observed for released GLP-1 in the EC CoCo powder in SIF. The interaction of GLP-1 with the matrix or the degradation of GLP-1 could contribute to this phenomenon.

The release profile of gonadorelin acetate after 20 h incubation is shown in **Figure 5–1j**. For gonadorelin acetate release in water, 4% more gonadorelin acetate was released from the EC CoCo powder, 8% more gonadorelin acetate was released from the CoCo powder and almost no more gonadorelin acetate was released from the MAC CoCo powder. The release of gonadorelin acetate in SGF and SIF after 20 h was consistent with the result of 2 h incubation.

The release profile of oxytocin acetate after 20 h incubation is shown in **Figure 5–1k**. The results were consistent with the result of 2 h incubation.

In summary, the 20h release profile indicated that the degradation of semaglutide, liraglutide and GLP-1 in SGF. A matrix that helps retain these peptides in matrix in SGF is crucial to maintain the bioactivity of these peptides.

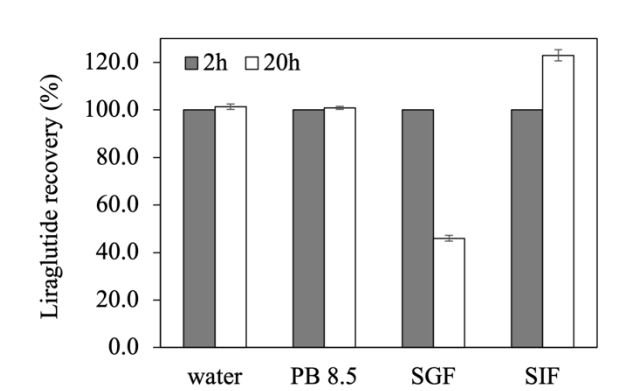


Figure 5–2. Recovery of liraglutide in different media after 20h incubation (Water and PB 8.5 at room temperature; SGF and SIF at 37°C).

5.4.3 SEM of the peptides loaded CoCo microcapsules

SEMs images show the surface structure of the peptide loaded CoCo microcapsules with/without the latex polymer (**Figure 5–3**). All the microcapsules presented round surfaces, or irregular surfaces with dents, wrinkles or shrinkages. Smooth surface was more prevalent for larger particles. No significant structural difference was noted when comparing one peptide to another.

The inclusion of EC in the formulation may lead to a different surface structure. The surface of the EC CoCo microcapsules featured the prevalence of submicron-sized dimples for most of the peptide samples (e.g. semaglutide, liraglutide, gonadorelin acetate and oxytocin acetate). Surfaces with small bumps have been observed for GLP-1 and gonadorelin EC loaded CoCo powders. The surface of the oxytocin EC CoCo powders exhibited a tendency to connect to its neighboring particles. The influence of other latex polymer on powder surface structure was not significant as shown in **Figure 5–3a**.

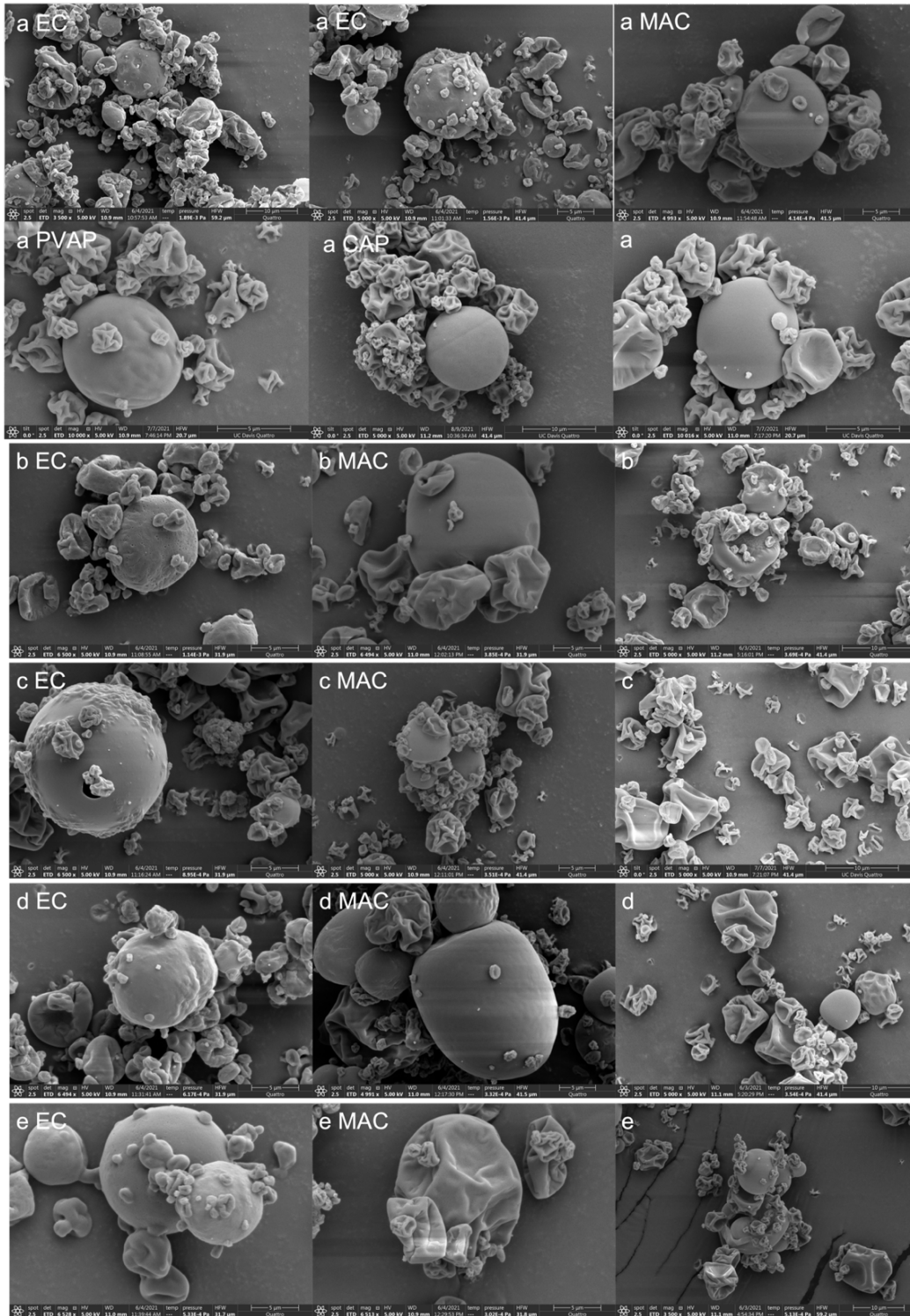


Figure 5–3. SEM of peptides loaded CoCo powders with/without the latex polymer where the Latex polymer is labelled: semaglutide (a); liraglutide (b); GLP-1(c); gonadorelin acetate (d); oxytocin acetate (e).

There is no clear correlation between powder surface structure and the release behavior. Semaglutide and liraglutide loaded EC CoCo powder with the prevalence of submicron-sized dimples along the surface resulted in the least peptide release in SGF. Semaglutide loaded CoCo powder with and without CAP shared similar surface structure while demonstrating different release behavior in SGF. It indicated that the matrix structure in the aqueous environment might be relevant to functional attributes of the powder (e.g. release behavior), but not the surface features of the dry powder.

5.4.4 Particle size of the peptides loaded CoCo microcapsules

Figure 5-4 shows the size distribution of peptide loaded microcapsules and **supplementary Table 5-1** shows the particle size of peptides microcapsules with the volume weighted mean diameter ($D_{4,3}$), the 10th percentile diameter ($D(0.1)$), median diameter ($D(0.5)$), and the 90th percentile diameter ($D(0.9)$). All the microcapsules showed a monomodal distribution. The $D_{4,3}$ for semaglutide powder was from 7.6 ± 0.0 to 15.0 ± 0.7 μm , where the EC, MAC and PVAP CoCo powders shared very similar size, the CoCo powder with slightly larger size of 9.7 ± 0.2 μm and the CAP CoCo with the largest size of 15.0 ± 0.7 μm . The increased size of the CAP CoCo powder may be relevant to the inclusion of CAP in the formulation, whereas the increased size did not lead to significant change of release behavior. The $D_{4,3}$ was from 6.4 ± 0.0 to 7.4 ± 0.0 μm , 8.6 ± 0.1 to 9.1 ± 0.1 μm , 8.4 ± 0.0 to 11.1 ± 0.4 μm , 7.5 ± 0.1 to 9.0 ± 0.1 μm for liraglutide, GLP-1, gonadorelin acetate and oxytocin acetate loaded powder.

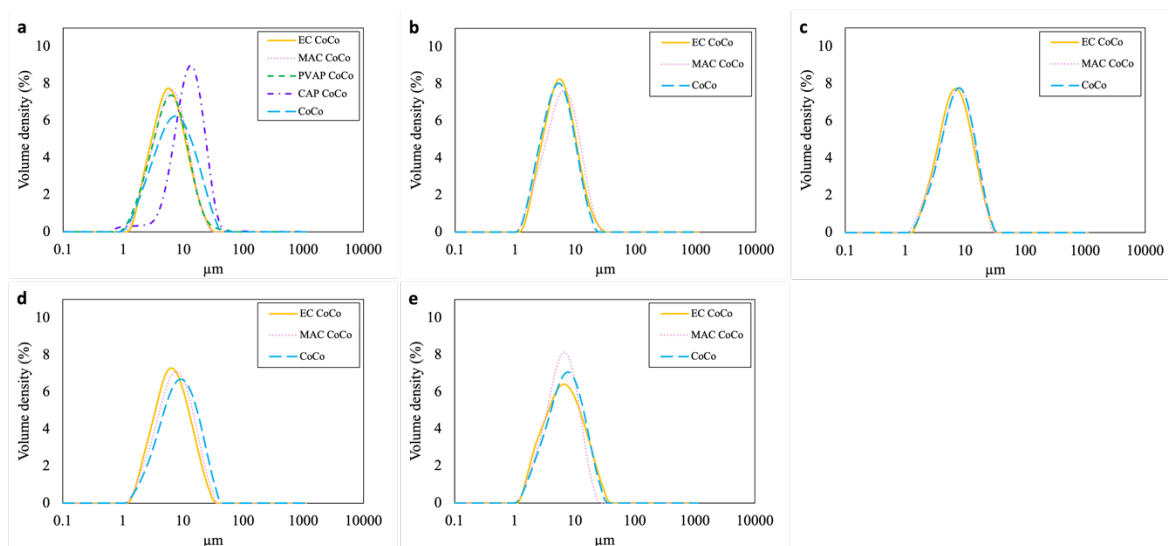


Figure 5–4. Particle size distribution of peptide-loaded CoCo microcapsules with/without the latex polymer: semaglutide (a); liraglutide (b); GLP-1(c); gonadorelin acetate (d); oxytocin acetate (e).

There is no clear connection between particle size to the release behavior based on the results. However, particle size is an important character that should be considered for formulation development for oral peptide delivery as the particles may influence the release kinetics (e.g erosion, dissolution) (Bækdal et al., 2021).

5.4.5 Powder yield and peptide loading of CoCo microcapsules

Table 5–2 shows the peptide loading and powder yield of the microcapsules from each formulation. The targeted loading of peptide for the CoCo formulation and the latex CoCo formulation was 20.00%, 15.24% (EC and MAC), 14.90% (PVAP) and 14.29% (CAP). Most of the peptide content in the powder was close to targeted content, suggesting the efficiency of the encapsulation. In some cases, the powder content was higher than the targeted value (e.g. semaglutide CoCo, gonadorelina acetate CoCo), which could be an indication of the lack of peptide homogeneity in the microcapsules.

The powder yield for each formulation was listed in **Table 5–2** as well. The powder yield was quite low for most of the formulations. This was related to the small spray drying size and low solid content of the feed. The solid content of the feed was below 1.5% for all the formulations and the spray size was only 25g for CoCo formulation and 50g for the latex CoCo formulation. A certain amount of spray dried powder was attached to evaporation chamber. Increase the solid content and spray size in the feed in the future work may improve the powder yield.

Table 5–2. Peptide loading and powder yield of the CoCo microcapsules with/without the latex polymer.

	Latex polymer	Semaglutide	Liraglutide	GLP-1	Gonadorelin acetate	Oxytocin acetate
Peptide in powder (%)	CoCo	21.23±0.24	18.48±0.71	21.18±0.24	22.12±0.10	17.98±0.13
	EC CoCo	17.65±0.29	16.55±0.16	14.78±0.10	15.83±0.03	15.52±0.17
	MAC CoCo	16.01±0.15	15.35±0.09	15.93±0.60	15.67±0.14	14.20±0.12
	PVAP CoCo	14.49±0.24	N/A			
	CAP CoCO	13.95±0.46				
Powder yield (%)	CoCo	56.08	42.28	57.68	50.08	50.48
	EC CoCo	56.23	47.54	50.29	59.08	50.29
	MAC CoCo	62.48	56.38	59.42	60.65	63.09
	PVAP CoCo	56.61	N/A			
	CAP CoCO	68.57				

N/A: Not applicable

5.5 Discussion

5.5.1 Peptide differences lead to various release profile of peptides from microcapsules in aqueous media

The differences in peptides have substantial effects on the release profile of peptides from microcapsules in SGF and SIF. It is likely that the extent to which the peptide interacts with the matrix is linked to the physicochemical properties of the peptide, resulting in difference in release.

First, the charges of the peptides can influence the interactions. The structure of the peptides is shown **Figure 5–5** with the charge sites circled. Semaglutide, liraglutide and GLP-1 carry charges along the chain, possibly enabling more interactions with the matrix. Gonadorelin acetate and oxytocin acetate only carry a few charges possibly with limited sites for interactions, resulting in overwhelming release in SGF and water. Second, the interactions could be relevant to structure of peptide. The presence of fatty acid side chain in liraglutide and semaglutide may impact the lipophilicity and polar surface area of the peptide, resulting in different interactions with the matrix. The lack of side chain makes GLP-1 much easier to be released compared to semaglutide and liraglutide. Cyclization strategies have been explored to enhance the bioactivity of oral peptide by removing the exposed N and C terminal that are particularly susceptible to enzyme cleavage (Nielsen et al., 2017). This suggests how the structure of the peptide affects the bioactivity of peptide through oral delivery. Third, the size and molecular size of the peptides are important to evaluate the interactions of peptides with the matrix. Semglutide of 4223.6 g/mol, liraglutide of 3751.2g/mol, GLP-1 of 3355.7 g/mol are larger than gonadorelin acetate of 1067.2 g/mol and oxytocin acetate of 1163.3 g/mol. The smaller gonadorelin acetate and oxytocin acetate are more prone to release out from the porous matrix.

5.5.2 The influence of latex polymer on release profile of peptides from microcapsules in aqueous media

The inclusion of latex polymer could provide better protection for some of the peptides (e.g. semaglutide, liraglutide and GLP-1) in SGF, as less peptide was released in SGF from the CoCo powder with latex polymer relative to the CoCo powder without latex. In SGF, the CoCo matrix alone was not effective enough at protecting peptide, possibly due to the less robust CoCo matrix related to possible weaker interactions of polymers under low pH as the undissolved (coacervated) fraction of gelatin was highest in water and less in the SGF and lowest in SIF (0%) as in Chapter 3, **Figure 3–7a**.

Latex polymers could enable protection for peptides in different ways: (1) latex polymer like EC, acting as moisture barrier, slows down the penetration of the media into the matrix and maintains the integrity of the matrix; (2) enteric polymer like PVAP and MAC enables resistance in low pH and dissolve at high pH.

Different latex polymer could impact release of peptides differently. For example, as shown in **Figure 5–1a**, the incorporation of EC in the CoCo microcapsules exhibited the strongest protection for semaglutide in SGF. It indicates that the moisture barrier layer formed by EC was more effective at retaining semaglutide compared to the protective layer formed by enteric polymers like PVAP, CAP and MAC. In addition, with current process and formulation condition, the EC CoCo formulation may be more effective at film forming compared to formulations with PVAP, CAP and MAC. The glass transition temperature, T_g of EC related to the degree of substitution was 140°C (Rekhi & Jambhekar, 1995).

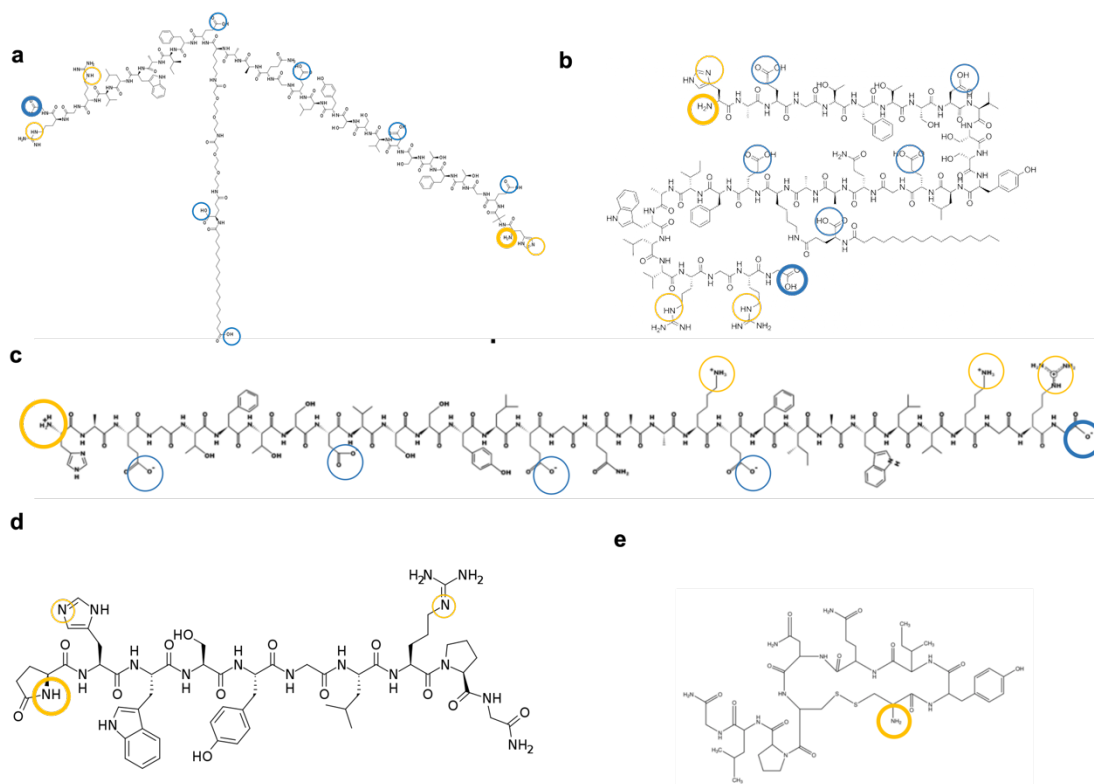


Figure 5–5. Structure of peptides: semaglutide (a); liraglutide (b); GLP-1 (c); gonadorelin acetate (d); oxytocin acetate (e). The positively and negatively charged groups are indicated by orange and blue circles, respectively. The bolded circles indicate charged ends.

The T_g of CAP has been reported as 160-170 °C (Sakellariou et al., 1985). The T_g of neat PVAP was determined to be 115 °C (Monschke et al., 2020). The MAC T_g was listed >100 °C (Ahmed et al., 2020). T_g is critical for the film formation. The polymer at temperatures above the T_g is in a viscous or rubbery state with more polymer segment mobility, facilitating the deformation and fusion of the colloidal particles and leading to film formation (Keddie, 1997). Plasticizer is widely used to lower the T_g to facilitate film formation if the T_g of the latex polymer is higher than the desired operating temperature. However, the extent to which the film formation of latex polymer may influence the release profile remains unclear in this work. Future work on formulation development focusing on optimizing latex polymer concentration, plasticizer type and

concentration could lead to more effective film formation and better protection for peptides in aqueous environments. Future work can also include the release test of peptide loaded microcapsules with the presence enzyme in SGF and SIF, since the pepsin, pancreatic enzymes are capable of degrading peptides. There have been efforts to enhance the bioactivity of oral salmon calcitonin by reducing the activity of local tryptic enzymes, resulting from co-administration of citric acid together with salmon calcitonin (Lee et al., 2000).

Although the inclusion of latex polymer showed no improvement for the release of gonadorelin acetate and oxytocin in SGF, latex CoCo microcapsules enabled retaining more of gonadorelin acetate. It indicates that the inclusion of latex as water barrier to CoCo system supports the protection for peptides. Oxytocin acetate, which is a small, hydrophilic, and barely charged peptide, was able to release easily from the matrix, suggesting that the protective matrix could still be very porous in water.

5.6 Conclusions

Promising enteric release of therapeutic peptides was achieved with 0.25 parts latex polymers -1.0 part CoCo polymers. The electrostatic attractive interactions of the matrix, the protective layer formed by latex polymer and interaction of peptide with the matrix appear to be the three main factors determining the release profile of peptide in different media. The electrostatic interactions of alginate and gelatin in the matrix were stronger in water than SGF and adding latex polymer could effectively strengthen the matrix in SGF, thereby protecting peptides from releasing. The interactions of peptide with matrix may play a vital role, as semaglutide and liraglutide carry more charges and side chain, enabling more interactions with the matrix and facilitating the enteric release. The most successful formulation was semaglutide loaded EC CoCo, where only $12.3 \pm 0.7\%$

of semaglutide released in SGF after 2h incubation and more 88% of semaglutide was released in SIF. A tailored approach for each peptide is needed to facilitate the oral delivery of peptide.

5.7 Abbreviations

CoCo: complex coacervated/complex coacervation; EC: ethylcellulose; MAC: methacrylic acid and ethyl acrylate copolymer; PVAP: polyvinyl acetate phthalate; CAP: cellulose acetate phthalate; SGF: simulated gastric fluid; SIF: simulated intestinal fluid.

5.8 Supplementary information

Supplementary Table 5–1. Particle size distribution of peptide loaded CoCo microcapsules with/without the latex polymer.

Peptide	Formulation	D _{4,3} , μm	D(0.1), μm	D(0.5), μm	D(0.9), μm
Semaglutide	EC CoCo	7.9±0.0	2.7±0.0	6.1±0.0	14.0±0.1
	MAC CoCo	7.6±0.0	2.7±0.0	6.4±0.0	14.1±0.1
	PVAP CoCo	7.8±0.1	2.5±0.0	6.3±0.0	14.5±0.1
	CAP CoCo	15.0±0.7	5.8±0.1	13.1±0.2	25.6±0.1
	CoCo	9.7±0.2	2.7±0.0	7.6±0.1	19.9±0.3
Liraglutide	EC CoCo	6.9±0.1	2.7±0.0	5.8±0.0	12.6±0.1
	MAC CoCo	7.4±0.0	2.6±0.0	6.4±0.0	13.9±0.0
	CoCo	6.4±0.0	2.5±0.0	5.4±0.0	11.7±0.1
GLP-1	EC CoCo	8.6±0.1	3.1±0.1	7.2±0.2	16.1±0.1
	MAC CoCo	8.7±0.1	3.0±0.0	7.5±0.1	16.1±0.2
	CoCo	9.1±0.1	3.2±0.1	7.8±0.1	16.9±0.1
Gonadorelin	EC CoCo	8.4±0.0	2.9±0.0	6.9±0.0	16.3±0.1
	MAC CoCo	9.4±0.1	3.0±0.0	7.8±0.1	18.2±0.1
	CoCo	11.1±0.4	3.4±0.1	9.1±0.3	21.9±0.9
Oxytocin	EC CoCo	8.8±0.0	2.6±0.0	6.9±0.0	18.0±0.0

	MAC CoCo	7.5±0.1	2.8±0.0	6.6±0.1	13.6±0.2
	CoCo	9.0±0.1	2.9±0.0	7.5±0.1	17.3±0.2
Control (containing no peptide)	EC CoCo	12.1±0.1	4.6±0.0	11.0±0.1	21.6±0.1
	MAC CoCo	7.7±0.1	2.8±0.0	6.6±0.0	14.2±0.2
	PVAP CoCo	13.0±1.9	3.9±0.0	10.0±0.0	21.2±0.2
	CAP CoCo	18.0±0.1	6.9±0.1	16.7±0.1	31.2±0.1
	CoCo	14.3±0.1	5.4±0.1	13.2±0.1	25.0±0.2

5.9 References

- Abeer, M. M., Rewatkar, P., Qu, Z., Talekar, M., Kleitz, F., Schmid, R., Lindén, M., Kumeria, T., & Popat, A. (2020). Silica nanoparticles: A promising platform for enhanced oral delivery of macromolecules. *Journal of Controlled Release*, 326, 544–555. <https://doi.org/https://doi.org/10.1016/j.jconrel.2020.07.021>
- Ahmed, A. R., Mota, J. P., Shahba, A. A.-W., & Irfan, M. (2020). Chapter 3 - Aqueous polymeric coatings: New opportunities in drug delivery systems (R. B. T.-D. D. A. Shegokar (ed.); pp. 33–56). Elsevier. <https://doi.org/https://doi.org/10.1016/B978-0-12-821222-6.00003-8>
- Bækdal, T. A., Donsmark, M., Hartoft-Nielsen, M.-L., Søndergaard, F. L., & Connor, A. (2021). Relationship Between Oral Semaglutide Tablet Erosion and Pharmacokinetics: A Pharmacoscintigraphic Study. *Clinical Pharmacology in Drug Development*, 10(5), 453–462. <https://doi.org/https://doi.org/10.1002/cpdd.938>
- Brayden, D. J., Hill, T. A., Fairlie, D. P., Maher, S., & Mrsny, R. J. (2020). Systemic delivery of peptides by the oral route: Formulation and medicinal chemistry approaches. *Advanced Drug Delivery Reviews*, 157, 2–36. <https://doi.org/https://doi.org/10.1016/j.addr.2020.05.007>
- Buckley, S. T., Bækdal, T. A., Vegge, A., Maarbjerg, S. J., Pyke, C., Ahnfelt-Rønne, J., Madsen, K. G., Schéele, S. G., Alanentalo, T., Kirk, R. K., Pedersen, B. L., Skyggebjerg, R. B., Benie, A. J., Strauss, H. M., Wahlund, P.-O., Bjerregaard, S., Farkas, E., Fekete, C., Søndergaard, F. L., ... Knudsen, L. B. (2018). Transcellular stomach absorption of a derivatized glucagon-like peptide-1 receptor agonist. *Science Translational Medicine*, 10(467), eaar7047. <https://doi.org/10.1126/scitranslmed.aar7047>
- Dong, Z., Ma, Y., Hayat, K., Jia, C., Xia, S., & Zhang, X. (2011). Morphology and release profile of microcapsules encapsulating peppermint oil by complex coacervation. *Journal of Food Engineering*, 104(3), 455–460. <https://doi.org/https://doi.org/10.1016/j.jfoodeng.2011.01.011>
- Drucker, D. J. (2020). Advances in oral peptide therapeutics. *Nature Reviews Drug Discovery*, 19(4), 277–289. <https://doi.org/10.1038/s41573-019-0053-0>
- Elias, R. J., Kellerby, S. S., & Decker, E. A. (2008). Antioxidant Activity of Proteins and Peptides. *Critical Reviews in Food Science and Nutrition*, 48(5), 430–441. <https://doi.org/10.1080/10408390701425615>
- Gombotz, W. R., & Wee, S. F. (2012). Protein release from alginate matrices. *Advanced Drug*

- Delivery Reviews*, 64, 194–205. <https://doi.org/https://doi.org/10.1016/j.addr.2012.09.007>
- Gouin, S. (2004). Microencapsulation: industrial appraisal of existing technologies and trends. *Trends in Food Science & Technology*, 15(7), 330–347. <https://doi.org/https://doi.org/10.1016/j.tifs.2003.10.005>
- Hawe, A., Poole, R., Romeijn, S., Kasper, P., van der Heijden, R., & Jiskoot, W. (2009). Towards Heat-stable Oxytocin Formulations: Analysis of Degradation Kinetics and Identification of Degradation Products. *Pharmaceutical Research*, 26(7), 1679–1688. <https://doi.org/10.1007/s11095-009-9878-2>
- Hristov, D., McCartney, F., Beirne, J., Mahon, E., Reid, S., Bhattacharjee, S., Penarier, G., Werner, U., Bazile, D., & Brayden, D. J. (2020). Silica-Coated Nanoparticles with a Core of Zinc, L-Arginine, and a Peptide Designed for Oral Delivery. *ACS Applied Materials & Interfaces*, 12(1), 1257–1269. <https://doi.org/10.1021/acsami.9b16104>
- Keddie, J. L. (1997). Film formation of latex. *Materials Science and Engineering: R: Reports*, 21(3), 101–170. [https://doi.org/https://doi.org/10.1016/S0927-796X\(97\)00011-9](https://doi.org/https://doi.org/10.1016/S0927-796X(97)00011-9)
- Keddie, J. L., & Routh, A. F. (2010). *An Introduction to Latex and the Principles of Colloidal Stability BT - Fundamentals of Latex Film Formation: Processes and Properties* (J. L. Keddie & A. F. Routh (eds.); pp. 1–26). Springer Netherlands. https://doi.org/10.1007/978-90-481-2845-7_1
- Knudsen, L. B., & Lau, J. (2019). The Discovery and Development of Liraglutide and Semaglutide. *Frontiers in Endocrinology*, 10, 155. <https://doi.org/10.3389/fendo.2019.00155>
- Lau, J. L., & Dunn, M. K. (2018). Therapeutic peptides: Historical perspectives, current development trends, and future directions. *Bioorganic & Medicinal Chemistry*, 26(10), 2700–2707. <https://doi.org/https://doi.org/10.1016/j.bmc.2017.06.052>
- Lecomte, F., Siepmann, J., Walther, M., MacRae, R. J., & Bodmeier, R. (2004). Polymer blends used for the aqueous coating of solid dosage forms: importance of the type of plasticizer. *Journal of Controlled Release*, 99(1), 1–13. <https://doi.org/https://doi.org/10.1016/j.jconrel.2004.05.011>
- Lee, Y.-H., Perry, B. A., Sutyak, J. P., Stern, W., & Sinko, P. J. (2000). Regional Differences in Intestinal Spreading and pH Recovery and the Impact on Salmon Calcitonin Absorption in Dogs. *Pharmaceutical Research*, 17(3), 284–290. <https://doi.org/10.1023/A:1007596821702>
- McClements, D. J. (2018). Encapsulation, protection, and delivery of bioactive proteins and peptides using nanoparticle and microparticle systems: A review. *Advances in Colloid and Interface Science*, 253, 1–22. <https://doi.org/https://doi.org/10.1016/j.cis.2018.02.002>
- Monschke, M., Kayser, K., & Wagner, K. G. (2020). Processing of Polyvinyl Acetate Phthalate in Hot-Melt Extrusion—Preparation of Amorphous Solid Dispersions. In *Pharmaceutics* (Vol. 12, Issue 4). <https://doi.org/10.3390/pharmaceutics12040337>
- Nielsen, D. S., Shepherd, N. E., Xu, W., Lucke, A. J., Stoermer, M. J., & Fairlie, D. P. (2017). Orally Absorbed Cyclic Peptides. *Chemical Reviews*, 117(12), 8094–8128. <https://doi.org/10.1021/acs.chemrev.6b00838>
- Petereit, H.-U., & Weisbrod, W. (1999). Formulation and process considerations affecting the stability of solid dosage forms formulated with methacrylate copolymers. *European Journal of Pharmaceutics and Biopharmaceutics*, 47(1), 15–25. [https://doi.org/https://doi.org/10.1016/S0939-6411\(98\)00083-6](https://doi.org/https://doi.org/10.1016/S0939-6411(98)00083-6)
- Rastogi, S., Shukla, S., Kalaivani, M., & Singh, G. N. (2019). Peptide-based therapeutics: quality specifications, regulatory considerations, and prospects. *Drug Discovery Today*, 24(1), 148–162. <https://doi.org/https://doi.org/10.1016/j.drudis.2018.10.002>

- Rekhi, G. S., & Jambhekar, S. S. (1995). Ethylcellulose - A Polymer Review. *Drug Development and Industrial Pharmacy*, 21(1), 61–77. <https://doi.org/10.3109/03639049509048096>
- Sakellariou, P., Rowe, R. C., & White, E. F. T. (1985). The thermomechanical properties and glass transition temperatures of some cellulose derivatives used in film coating. *International Journal of Pharmaceutics*, 27(2), 267–277. [https://doi.org/https://doi.org/10.1016/0378-5173\(85\)90075-4](https://doi.org/https://doi.org/10.1016/0378-5173(85)90075-4)
- Sarabandi, K., Gharehbeqlou, P., & Jafari, S. M. (2020). Spray-drying encapsulation of protein hydrolysates and bioactive peptides: Opportunities and challenges. *Drying Technology*, 38(5–6), 577–595. <https://doi.org/10.1080/07373937.2019.1689399>
- Saravanan, M., & Rao, K. P. (2010). Pectin–gelatin and alginate–gelatin complex coacervation for controlled drug delivery: Influence of anionic polysaccharides and drugs being encapsulated on physicochemical properties of microcapsules. *Carbohydrate Polymers*, 80(3), 808–816. <https://doi.org/https://doi.org/10.1016/j.carbpol.2009.12.036>
- Tang, Y., Scher, H. B., & Jeoh, T. (2020). Industrially scalable complex coacervation process to microencapsulate food ingredients. *Innovative Food Science & Emerging Technologies*, 59, 102257. <https://doi.org/https://doi.org/10.1016/j.ifset.2019.102257>
- Tang, Y., Scher, H., & Jeoh, T. (2021). *Microencapsulation of chemicals and bioactives by in situ complex coacervation during spray drying*. U.S. Patent Application No. 17/178,866, Publication No. US20210316265A1.
- Twarog, C., Fattah, S., Heade, J., Maher, S., Fattal, E., & Brayden, D. J. (2019). Intestinal Permeation Enhancers for Oral Delivery of Macromolecules: A Comparison between Salcaprozate Sodium (SNAC) and Sodium Caprate (C(10)). *Pharmaceutics*, 11(2), 78. <https://doi.org/10.3390/pharmaceutics11020078>
- Udenigwe, C. C. (2014). Bioinformatics approaches, prospects and challenges of food bioactive peptide research. *Trends in Food Science & Technology*, 36(2), 137–143. <https://doi.org/https://doi.org/10.1016/j.tifs.2014.02.004>
- Wang, Y., Lomakin, A., Kanai, S., Alex, R., & Benedek, G. B. (2015). Transformation of Oligomers of Lipidated Peptide Induced by Change in pH. *Molecular Pharmaceutics*, 12(2), 411–419. <https://doi.org/10.1021/mp500519s>
- Wasilewska, K., & Winnicka, K. (2019). Ethylcellulose–A Pharmaceutical Excipient with Multidirectional Application in Drug Dosage Forms Development. In *Materials* (Vol. 12, Issue 20). <https://doi.org/10.3390/ma12203386>
- Yang, Z., Peng, Z., Li, J., Li, S., Kong, L., Li, P., & Wang, Q. (2014). Development and evaluation of novel flavour microcapsules containing vanilla oil using complex coacervation approach. *Food Chemistry*, 145, 272–277. <https://doi.org/https://doi.org/10.1016/j.foodchem.2013.08.074>
- Zu, Y., Luo, Y., & Ahmed, S. U. (2007). Effect of Neutralization of Poly(Methacrylic Acid-co-ethyl Acrylate) on Drug Release From Enteric-coated Pellets Upon Accelerated Storage. *Drug Development and Industrial Pharmacy*, 33(4), 457–473. <https://doi.org/10.1080/03639040601085383>

Chapter 6 Microencapsulation of bromelain by industrially scalable complex coacervation process

6.1 Introduction

Bromelain derived from stems and fruits of the pineapple plant belongs to a group of proteolytic enzymes (da Silva, 2017; M6ty6n et al., 2013). Bromelain finds application in many areas including food, pharmaceutical, tenderization, detergents, and the textile because of its strong proteolytic activity (Arshad et al., 2014). Bromelain can also provide therapeutic benefits including oral treatment of inflammatory, blood coagulation related diseases, modulation of tumor growth etc. due to its anti-inflammatory, anti-thrombotic, anti-edematous and fibrinolytic activities (Maurer, 2001). The anti-inflammatory activity of bromelain is related to the proteolytic activity as the bromelain proteolytically removes certain cell surface molecules that could impact lymphocyte migration and activation (Hale et al., 2005). Maintaining the proteolytic activity of bromelain is crucial for its application. Study has demonstrated that bromelain, especially stem bromelain that is predominantly in commercially available bromelain, shows activity over a wide range of pH. However, bromelain is susceptible to self-hydrolysis over time and stress conditions such as elevated temperature, high acidity, gastric proteases, limit its activity and hence its application (Caraglia et al., 2011). One challenge of the application of bromelain in the food industry is to maintain bromelain activity during product processing and shelf storage.

Microencapsulation of bromelain can facilitate the application of bromelain by providing a protective barrier to help bromelain maintain activity over stress conditions such as heat treatment. Bernela et al. (Bernela et al., 2016) showed that bromelain encapsulated in katira gum nanoparticles can enhance its anti-inflammatory activity. Nanoencapsulation of bromelain with chitosan offered prolonged release of bromelain in vitro antioxidant and antiproliferative test

(Ataide et al., 2021). However, studies have also shown that the encapsulation process resulted in bromelain activity loss (e.g. 76% of activity remained in polyacrylic acid nanoparticles) depending on the process condition (Wei et al., 2017).

In this work, the CoCo process was applied to microencapsulate pineapple extract (Tang et al., 2020, 2021b, 2021a). Unlike conventional complex coacervation, the CoCo process consolidates multiple steps into one step to form dry complex coacervated microcapsules by spray drying. The objective of this work was to explore the capability of the CoCo process to maintain bromelain activity by having bromelain as the matrix component as well as protecting it as a cargo and thus evaluate the commercial potential of the CoCo process to incorporate encapsulated bromelain into various food product.

6.2 Materials and methods

6.2.1 Materials

Pineapple extract powder was provided by Treasure8, LLC (San Francisco, CA). High viscosity sodium alginate (GRINDSTED Alginate FD 155) was purchased from DuPont Nutrition and Health. Succinic acid, ammonium hydroxide, sodium hydroxide and hydrochloric acid were purchased from Fisher Scientific. The Bio-Rad protein assay reagent containing Coomassie® Brilliant Blue G-250 dye, phosphoric acid and methanol was purchased from Bio-Rad. Albumin standard (2mg/ml) and EnzChek™ Protease Assay Kit, red fluorescence (catalog number E6639) was purchased from Thermo Fisher Scientific.

6.2.2 Methods

6.2.2.1 Measurement of isoelectric point (pI) of protein in pineapple extract powder

The pI of protein in pineapple extract powder was determined by acid/base titration. The pH values of 0.2% (w/v) pineapple extract powder solution was measured as a function of titrant (0.1 M NaOH) volume at room temperature. The equivalent point on titration curve determined from the first derivative was corresponding to pI of protein in pineapple extract powder.

6.2.2.2 Measurement of the protein content in pineapple extract powder

The protein concentration in pineapple extract powder was measured by the Bio-Rad protein assay (Bio-Rad, Hercules, CA) based on the Bradford dye-binding method following manufacturer recommended protocols for the microplate standard assay (Bradford, 1976). Microplate standard Bio-Rad protein assay was used by mixing 10 μ l standard or sample and 200 μ l dye reagent. Albumin standard (2mg/ml) was used to make the standard curve in the range of 50–400 μ g/ml. 1mg/ml of pineapple extract powder was made by dissolving pineapple extract powder in water and then diluted in the range of 200-800 μ g/ml.

6.2.2.3 Formation of bromelain CoCo powder

To form Bromelain-CoCo powder, two formulations were used as shown in **Table 6–1**. For formulation 1, the spray drying feed was made up by 0.75% (w/w) alginate, 0.5% (w/w) succinic acid and 3% (w/w) pineapple extract with pH adjusted to 7.8 using ammonium hydroxide. For formulation 2, the spray drying feed was made up by 1% (w/w) alginate, 0.5% (w/w) succinic acid and 3% (w/w) pineapple extract with pH adjusted to 6.8 using ammonium hydroxide. The feed was spray dried by a Buchi B290 laboratory spray dryer at an inlet air temperature of 130 °C,

maximum aspirator airflow rate (35 m³/h), 45% of maximum feed peristaltic pump flow rate (~14 mL/min), and 50 mm nozzle pressure. The outlet temperature was 54~60 °C during spray drying.

Table 6–1. Formulations used in the formation of bromelain CoCo microcapsules.

Formulation ID ¹	Pineapple extract concentration (w/w, % w.b.)	Succinic acid concentration (w/w, % w.b.)	Alginate concentration (w/w, % w.b.)	Feed pH
0.75A-CoCo	3.00	0.50	0.75	7.8
1A-CoCo	3.00	1.00	1.00	6.8

¹The formulation ID were coded to indicate the alginate (A) wet basis loading in the feed. (e.g. 0.75A indicates a wet basis loading of 0.75% w/w alginate).

6.2.2.4 Determination of the percent of coacervated protein of the total protein

The percent of coacervated protein of the total protein was calculated by this equation:

$$\% \text{ coacervated protein} = 1 - \frac{\text{soluble(uncoacervated) protein}}{\text{total protein}}$$

To measure the soluble protein, 1% (w/v) of bromelain-CoCo powder was dispersed in water with continuous agitation for 2h. The pH of the suspension was measured, followed by centrifugation at 10,000g for 2 min. The supernatant was analyzed for dissolved protein by microplate standard Bio-Rad protein assay as described in 6.2.2.2.

To measure the total protein in bromelain-CoCo powder, 1% (w/v) of the bromelain-CoCo powder was dispersed in water, and sodium hydroxide was added to bring the pH to 9, where the suspension pH was higher than the pI of protein. The suspension was agitated until the powders were fully dissolved (~2h). The solution was analyzed for total protein by microplate standard Bio-Rad protein assay as described in 6.2.2.2.

6.2.2.5 Bromelain proteolytic activity measurement

The bromelain activity in pineapple extract powder and bromelain-CoCo powder was measured by EnzChek™ Protease Assay (E 6639, red fluorescence). The Kit contains casein derivatives that are labeled with the pH-insensitive red-fluorescent BODIPY® TR-X (E6639) dyes. Proteolytic activity releases fluorescent BODIPY TR-X dye-labeled peptides with excitation/emission maxima of 589/617 nm. The accompanying increase in fluorescence is proportional to protease activity.

To measure the bromelain activity in pineapple extract powder, 10 µg/ml of BODIPY TR-X casein substrate was made using 20 mM Tris-HCl with pH 7.8 as the supplier suggested. The bromelain-CoCo powder was dispersed in water (1mg/mL) with continuous agitation for 1h. Pineapple extract powder dispersed in water (1mg/mL) with continuous agitation for 1h and pH was adjusted to match with the pH of bromelain-CoCo sample. The sample (pineapple extract sample or bromelain-CoCo sample) was diluted using 20 mM Tris-HCl with pH 7.8 to the protein concentration of the sample in the range of 0-10 µg/ml. An aliquot of 100 µl diluted sample was mixed with 100 µl 10 µg/ml BODIPY TR-X casein in 96-well fluorescence microplate. The sample was incubated for one hour and protected from light. The fluorescence was read after one-hour incubation using plate reader at excitation/emission of 589/617 nm.

Bromelain activity recovery was calculated by the following equation:

% bromelain activity recovery

$$= \frac{\text{fluorescence change per unit bromelain in CoCo sample}}{\text{fluorescence change per unit bromelain in pineapple extract sample}}$$

6.2.2.6 Statistical analysis

Data were reported as mean \pm standard deviation. ANOVA and Tukey's post hoc multiple comparison test were used to determine differences between groups. Statistical analysis was performed using JMP (SAS Institute Inc., Cary, NC, USA). P-values less than 0.05 were considered significant.

6.3 Results and discussion

6.3.1 *pI* of protein in pineapple extract powder

The isoelectric point of the protein in the pineapple extract powder, estimated at the maximum of the first derivative of the acid/base titration curve, was $pI = 5.92 \pm 0.03$ (Figure 6–1). The isoelectric point of stem bromelain and fruit bromelain was >10 and 4.8 respectively reported in the literature (Maurer, 2001). Knowing the *pI* of the protein in the extract powder is important to formulate the spray drying feed. The pH of feed was adjusted above the isoelectric point of the protein to minimize the interactions between protein and alginate in the feed.

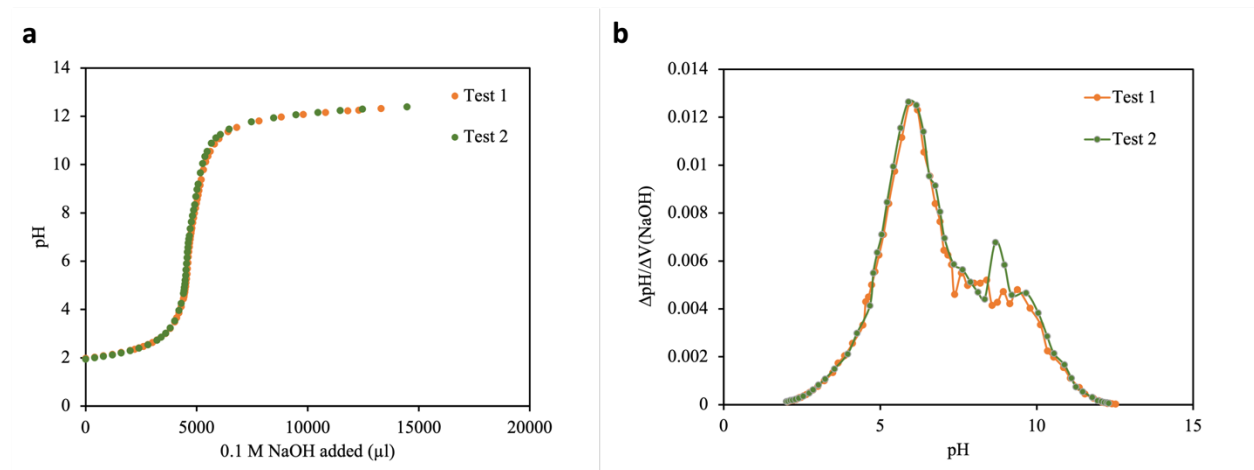


Figure 6–1. Titration curve of 0.2% (w/v) pineapple extract solution (a); First derivative of the titration curve of 0.2% (w/v) pineapple extract solution (b).

6.3.2 The protein content in pineapple extract powder

The concentration of protein in the pineapple extract solution was determined by Bradford assay and the content of protein in pineapple extract powder was $25.2 \pm 1.0\%$. Studies have shown that the pineapple extract contains bromelain and other components such as reducing sugars and soluble fibers (Huang et al., 2021). Purification followed by bromelain extraction has been widely used to achieve the desirable level of bromelain purity depending on its intended use. Purification technologies include precipitation, ultrafiltration, chromatography steps with ion exchange, affinity, and gel filtration and some novel purification technologies such as reverse micellar extraction, aqueous two-phase systems, and adsorption (Arshad et al., 2014).

6.3.3 Percent of coacervated protein of the total protein in the CoCo powder

The bromelain protein loading in the CoCo powder generated using the 0.75A-CoCo was 19.5% on a mass basis, of which 50.7% was coacervated with alginate. The bromelain protein loading of the CoCo powder generated using the 1A-CoCo powder was 18.6%, with 40.4% of the protein coacervated with alginate as shown in **Table 6–2**, significantly less than that of 50.7% in the 0.75A CoCo powder. Higher concentration of alginate resulted in slightly less coacervated protein in the CoCo microcapsules. Higher concentration of alginate led to higher viscosity in the feed and might influence the atomization process and the mobility of the alginate, resulting in different interactions with protein during spray drying.

Table 6–2. Percent of coacervated protein in bromelain-CoCo powders on a mass basis. Each sample was measured in triplicate.

Sample	0.75A-CoCo	1A-CoCo
% protein of CoCo powder	19.5% ± 0.7%	18.6%±0.4%
% uncoacervated protein of CoCo powder	9.6% ± 0.7%	11.1% ± 0.6%
% coacervated protein of total protein	50.7±3.0%	40.4±3.8%

6.3.4 Bromelain activity recovery of CoCo microcapsules after spray drying

The bromelain activity recovery of the bromelain CoCo powder after spray drying determined from EnzChek protease assay E6639 was calculated as described in 6.2.2.5. As shown in **Figure 6–2**, the bromelain activity recovery of the 1A-CoCo powder at pH 5.4 was up to 102.0±3.1% compared to 73.7±3.8% in the 0.75A-CoCo powder. The bromelain activity recovery of 0.75A-CoCo powder at pH 7.7 was not significantly different from that at pH 5.4.

The bromelain activity was well maintained during spray drying by increasing the alginate concentration in the formulation. The presence of alginate could serve as a barrier to protect bromelain from the heat stress during spray drying. More coacervated protein may not be necessary to maintain the bromelain activity but it may influence the release of bromelain in aqueous environment that needs to be further explored.

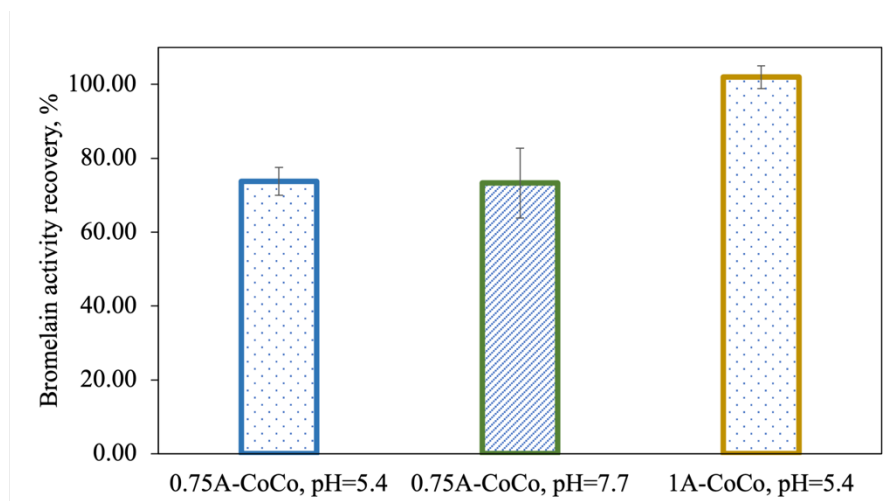


Figure 6–2. Bromelain activity recovery of the 0.75A-CoCo and 1A-CoCo powders dispersed in water with/without pH adjustment. Error bars represent standard deviation of triplicates.

In a scale-up trial, 1000g spray feed was prepared using the 1A-CoCo formulation to generate a larger amount of sample. Bromelain activity recovery of the CoCo powder was measured to investigate the influence of long retention time of the CoCo powder in the collection chamber (at elevated temperatures) on the enzyme activity. **Table 6–3** shows the bromelain activity recovery of various bromelain CoCo powders. The longer retention time in the collection chamber with elevated temperature could be detrimental to the bromelain activity but the bromelain activity was still up to 83.2%.

Table 6–3. Bromelain activity recovery of bromelain CoCo powders after spray drying.

Sample	Bromelain activity recovery	Powder yield ³	Outlet temperature and time in Collection chamber
0.75A-CoCo	73.7±3.8%	53.41%	54°C, 7.5min
1A-CoCo ¹	102.0±3.1%	50.66%	58°C, 8.5min
1A-CoCo ²	83.2±3.0%	52.44%	56~60°C, 80min

¹The powder was made from formulation 1A-CoCo with spray feed of 100g described in 6.2.2.4.

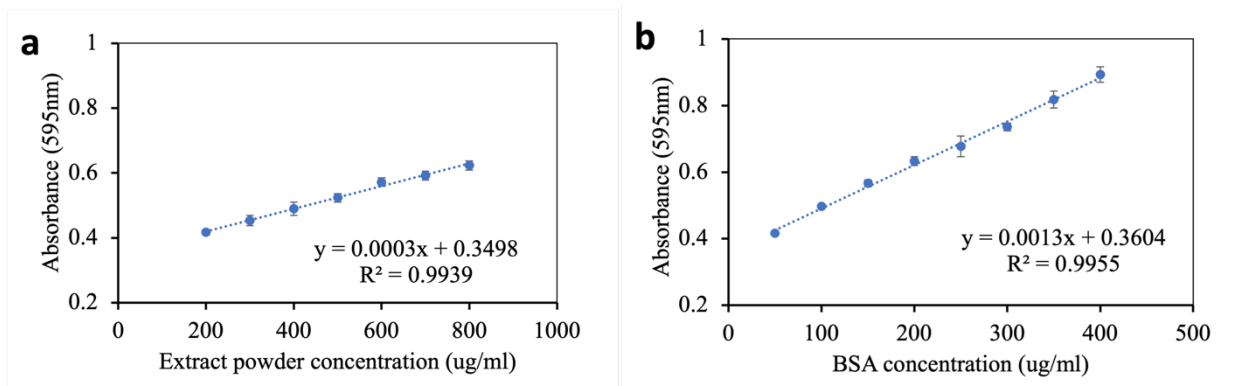
²The powder was made from formulation 1A-CoCo with spray feed of 1000g described in 6.2.2.4.

³Small portion of the powder was in cyclone and was not collected.

6.4 Conclusions

The bromelain activity during spray drying was well maintained during spray drying using the CoCo process where bromelain was both the cargo as well as the matrix component. With approximately 40.4% protein coacervated with alginate, the bromelain activity recovery of the bromelain 1A-CoCo powder was up to $102.0 \pm 3.1\%$. This study demonstrated the capability of the CoCo process to maintain maximum bromelain activity and could facilitate the incorporation of bromelain into food products in a cost-effective way. Further optimization of spray drying process parameters can be done to increase the powder yield during spray drying. In addition, future work (e.g. release work, shelf life study) related to the targeted application of bromelain can be explored to understand how the bromelain in the matrix responds to the stress conditions such as heat.

6.5 Supplementary information



Supplementary Figure 6–1. Absorbance of pineapple extract powder (a); Standard curve for Bio-Rad Protein microplate standard assay, bovine serum albumin (BSA) (b). Error bars represent standard deviation of triplicates.

6.6 References

- Arshad, Z. I. M., Amid, A., Yusof, F., Jaswir, I., Ahmad, K., & Loke, S. P. (2014). Bromelain: an overview of industrial application and purification strategies. *Applied Microbiology and Biotechnology*, *98*(17), 7283–7297. <https://doi.org/10.1007/s00253-014-5889-y>
- Ataide, J. A., Cefali, L. C., Figueiredo, M. C., Braga, L. E. de O., Ruiz, A. L. T. G., Foglio, M. A., Oliveira-Nascimento, L., & Mazzola, P. G. (2021). In vitro performance of free and

- encapsulated bromelain. *Scientific Reports*, 11(1), 10195. <https://doi.org/10.1038/s41598-021-89376-0>
- Bernela, M., Ahuja, M., & Thakur, R. (2016). Enhancement of anti-inflammatory activity of bromelain by its encapsulation in katira gum nanoparticles. *Carbohydrate Polymers*, 143, 18–24. <https://doi.org/https://doi.org/10.1016/j.carbpol.2016.01.055>
- Bradford, M. M. (1976). A rapid and sensitive method for the quantitation of microgram quantities of protein utilizing the principle of protein-dye binding. *Analytical Biochemistry*, 72(1), 248–254. [https://doi.org/https://doi.org/10.1016/0003-2697\(76\)90527-3](https://doi.org/https://doi.org/10.1016/0003-2697(76)90527-3)
- Caraglia, M., Rosa, G. D., Abbruzzese, A., & Leonetti, C. (2011). Nanotechnologies: new opportunities for old drugs. The case of Aminobisphosphonates. *J. Nanomed. Biother. Discov*, 1, 1–2.
- da Silva, R. R. (2017). Bacterial and Fungal Proteolytic Enzymes: Production, Catalysis and Potential Applications. *Applied Biochemistry and Biotechnology*, 183(1), 1–19. <https://doi.org/10.1007/s12010-017-2427-2>
- Hale, L. P., Greer, P. K., Trinh, C. T., & James, C. L. (2005). Proteinase activity and stability of natural bromelain preparations. *International Immunopharmacology*, 5(4), 783–793. <https://doi.org/https://doi.org/10.1016/j.intimp.2004.12.007>
- Huang, C. W., Lin, I. J., Liu, Y. M., & Mau, J. L. (2021). Composition, enzyme and antioxidant activities of pineapple. *International Journal of Food Properties*, 24(1), 1244–1251. <https://doi.org/10.1080/10942912.2021.1958840>
- Maurer, H. R. (2001). Bromelain: biochemistry, pharmacology and medical use. *Cellular and Molecular Life Sciences CMLS*, 58(9), 1234–1245.
- Mótyán, J. A., Tóth, F., & Tózsér, J. (2013). Research Applications of Proteolytic Enzymes in Molecular Biology. *Biomolecules*, 3(4), 923–942. <https://doi.org/10.3390/biom3040923>
- Tang, Y., Scher, H. B., & Jeoh, T. (2020). Industrially scalable complex coacervation process to microencapsulate food ingredients. *Innovative Food Science & Emerging Technologies*, 59, 102257. <https://doi.org/https://doi.org/10.1016/j.ifset.2019.102257>
- Tang, Y., Scher, H. B., & Jeoh, T. (2021a). Volatile Retention and Enteric Release of d-Limonene by Encapsulation in Complex Coacervated Powders Formed by Spray Drying. *ACS Food Science & Technology*, 1(11), 2086–2095. <https://doi.org/10.1021/acsfoodscitech.1c00308>
- Tang, Y., Scher, H., & Jeoh, T. (2021b). *Microencapsulation of chemicals and bioactives by in situ complex coacervation during spray drying*. U.S. Patent Application No. 17/178,866, Publication No. US20210316265A1.
- Wei, B., He, L., Wang, X., Yan, G. Q., Wang, J., & Tang, R. (2017). Bromelain-decorated hybrid nanoparticles based on lactobionic acid-conjugated chitosan for in vitro anti-tumor study. *Journal of Biomaterials Applications*, 32(2), 206–218.

Chapter 7 Conclusions and future work

7.1 Summary

There is unmet need for an effective and inexpensive delivery matrix for the application of bioactive component in food and pharmaceutical industries. To address the problem, I developed a novel industrially scalable complex coacervation process (the CoCo process). This work investigated how to control the barrier properties of complex coacervated matrix formed by the CoCo process to offer desirable functional attributes for different types of bioactive compounds. Specially, the influence of formulation variables on the physicochemical properties of the matrix was investigated and the relation of extent of complex coacervation and the stability of the cargo and release profile was explored, where the extent of complex coacervation was defined as the fraction of polymers that do not solubilize from the CoCo particles when the spray dried powders are suspended in water and it was defined to assess the extent to which all polymers within the particles participate in complex coacervation.

First, for encapsulation of D-limonene, a volatile oil, formulation variables including succinic acid and gelatin concentration influenced the extent of complex coacervation and the barrier properties such as release profile of D-limonene. The CoCo powders formulated with 4% gelatin, 0.5% alginate, either 0.5% or 0.75% succinic acid exhibited excellent barrier property to retain up to 78% of D-limonene, during spray drying with only 2-8 % loss during 4-months of storage, and provide promising enteric release of D-limonene. The extent of complex coacervation was crucial to control the release of D-limonene in aqueous environment. For volatile retention of D-limonene in the dry microcapsules, controlling the extent of complex coacervation was not important. The emulsifier that impacts the emulsion size, emulsion stability and the formation of complex coacervates at the interface could impact the volatile retention of D-limonene.

Second, latex polymer was incorporated to the CoCo formulation. The addition of ethylcellulose in the CoCo microcapsules accelerated D-limonene loss and oxidation in spray dried powders, accelerated the release of D-limonene from microcapsules in water and SGF, and slowed the initial release of D-limonene from microcapsules in SIF. Promising enteric release of semaglutide and liraglutide was achieved with 0.25 parts latex polymers - 1.0 part CoCo polymers made by gelatin, alginate and succinic acid. Specifically, only $12.3\pm 0.7\%$ of semaglutide and $24.0\pm 0.5\%$ of liraglutide were released in simulated gastric fluid in 2h from complex coacervation microcapsules with the inclusion of ethylcellulose, while more than 88% of peptides was released in simulated intestinal fluid.

Third, the proteolytic activity of bromelain was well preserved by the CoCo process. With approximately 40% protein coacervated with alginate, the bromelain activity recovery in bromelain CoCo powder was up to $102.0\pm 3.1\%$. Bromelain was not only the cargo but also incorporated as wall material to interact with alginate to form complex coacervated microcapsules, demonstrating the potential of the CoCo process to encapsulate active enzyme.

7.2 Future work

7.2.1 Physicochemical and structural properties of the CoCo matrix

Future work is needed for better understanding of the formation of complex coacervates by investigating the physicochemical and structural properties of the CoCo matrix and followed by understanding how the physicochemical and structural properties of the CoCo matrix can influence the barrier properties of the CoCo matrix related to targeted functional attributes like prolonged shelf life and desirable release kinetics.

So far, no experimental evidence has shown how the distribution of complex coacervates along the matrix affects the barrier properties. For example, it is not clear if the complex coacervates more concentrated around the cargo will provide better protection for cargo against volatilization or oxidation compared to complex coacervates more evenly distributed along the matrix. Understanding the effects of the distribution of complex coacervates on barrier properties of the microcapsules can lead to a better understanding of the significance of the protein at the interface in complex coacervation.

Scattering-type scanning near-field optical microscopy can be used to obtain the nano-Fourier transform infrared (FTIR) spectra and topography. FTIR spectroscopy is a widely used tool to determine functional group in chemicals by absorption spectra, but the spatial resolution is limited to a few micrometers. Scanning near-field optical microscopy can be regarded as an extended atomic force microscopy that can analyze the backscattered light with a specially designed Fourier Transform spectrometer. It enables optical imaging and spectroscopy at the nanoscale. The nano-FTIR spectra and topography obtained by scanning near-field optical microscopy can help locate the position of complex coacervates along the microcapsules by identifying the characteristic peaks of complex coacervates in nanoscale.

Third, future efforts can be made to investigate the microstructure of the CoCo powders such as the porosity measurement of the dry powder, cross-section SEM, and the microstructure change in different release media. For microstructure change in different release mediums, the matrix building components like alginate and gelatin can be stained for microstructural analysis of the CoCo powders. For example, Alexa Fluor 488 reactive dye contains a tetrafluorophenyl (TFP) ester and can react efficiently with primary amines of proteins to form stable dye-protein conjugates, which can be used for staining gelatin. Alexa Fluor 555 cadaverine is an amine-

containing and carboxylic acid-reactive reagent. Alexa Fluor 555 cadaverine coupling with reagent such a carbodiimide (EDC), N-hydroxysuccinimide (NHS)/EDC or sulfo-NHS/EDC can react with carboxylic acid for staining alginate. The confocal micrographs may show the change of the distribution of the polymer after the exposure of the CoCo powder to specific conditions, providing information about the microstructure change of the matrix. For example, study has shown that the microstructure of oil loaded alginate-casein complex coacervated microcapsules was analyzed using confocal microscopy by having the oil phase stained with Nile red while the protein phase stained with fluorescein isothiocyanate (FITC).

7.2.2 Influence of formation and process parameters on barrier properties of CoCo microcapsules

Further investigation of formulation and process parameters should be explored to modulate the barrier properties of the CoCo matrix. The extent of complex coacervation can be modulated by polymer pair, polymer concentration in the formulation, acid type and concentration. For example, a wide range of pH can be achieved by modulating the type and concentration of the acid. Process development can be tailored based on the type of cargo. A wide range of process parameters (such as inlet temperature) can be investigated in the future work of D-limonene encapsulation by the CoCo process. Further application of the CoCo technology in other scalable drying processes such as fluidized bed coating also has the potential to energize the development of innovative products for targeted fields.

7.2.3 Modeling the kinetic release of bioactive compound

In chapter 3, the correlation of the percent of D-limonene release and the extent of complex coacervation in each medium indicated that the dissolution was the release mechanism. In future work, mathematical modeling can be developed to describe the release kinetics of bioactive compound release from microcapsules in aqueous environments. The model can be used for understanding the release mechanism (e.g. whether it is dissolution related diffusion), identifying key parameters affecting release behavior and empowering microcapsule design such as selection of appropriate biodegradable materials.

The model can be developed based on two key assumptions: (i) The release D-limonene from microcapsule is by diffusion through the matrix and can be expressed by Fick's second law. (ii) Effective diffusion coefficient of bioactive compound (D_e) through the matrix taking account of matrix dissolution. Independent experiments will be conducted to determine a correlation between apparent bioactive diffusivity and the extent of complex coacervation that has dependency of matrix dissolution. Then, an equation of D_e related to the extent of complex coacervation will be developed and input parameters will be obtained. The output of model will be the release kinetics of D-limonene from microcapsule. Agreement of the model simulation and experimental measurements will imply that the model's description about dissolution related diffusion is correct and the model will be validated.

7.3 Conclusions

A novel industrially scalable complex coacervation process was developed and the successful application of the CoCo process to encapsulate different type of bioactives has been demonstrated. The barrier properties of the CoCo matrix were tunable by modulating the formulation variables

to offer desirable functional attributes for different type of cargo. For food applications, the CoCo microcapsules formulated with gelatin, alginate and succinic acid exhibited excellent barrier property to retain volatile oil-D-limonene in dry powder and control the release of D-limonene in aqueous environments. Demonstrating the potential of the CoCo process to encapsulate active enzymes, full bromelain proteolytic activity during spray drying was achieved, where bromelain was both the cargo as well as the matrix component. For pharmaceutical applications, peptide therapeutics, semaglutide and liraglutide, were successfully encapsulated by the CoCo process with enteric release when the formulation was amended with a latex polymer. Overall, the industrially-scalable CoCo process has been shown to be effective for cargo protection and controlled release for applications in food and pharmaceutical industries.